



AFRL-AFOSR-UK-TR-2019-0060

Towards Improved Understanding of Damage and Fracture of High-Performance Cementitious Materials by Development of Mesoscale Analysis Capabilities: 3-D microstructure reconstruction and FE Simulations

Jose Luis Alves
UNIVERSIDADE DO MINHO
LARGO PACO
BRAGA, 4704-553
PT

11/25/2019
Final Report

DISTRIBUTION A: Distribution approved for public release.

Air Force Research Laboratory
Air Force Office of Scientific Research
European Office of Aerospace Research and Development
Unit 4515 Box 14, APO AE 09421

REPORT DOCUMENTATION PAGE			<i>Form Approved</i> <i>OMB No. 0704-0188</i>		
<p>The public reporting burden for this collection of information is estimated to average 1 hour per response, including the time for reviewing instructions, searching existing data sources, gathering and maintaining the data needed, and completing and reviewing the collection of information. Send comments regarding this burden estimate or any other aspect of this collection of information, including suggestions for reducing the burden, to Department of Defense, Executive Services, Directorate (0704-0188). Respondents should be aware that notwithstanding any other provision of law, no person shall be subject to any penalty for failing to comply with a collection of information if it does not display a currently valid OMB control number.</p> <p>PLEASE DO NOT RETURN YOUR FORM TO THE ABOVE ORGANIZATION.</p>					
1. REPORT DATE (DD-MM-YYYY) 25-11-2019		2. REPORT TYPE Final		3. DATES COVERED (From - To) 30 Sep 2015 to 29 Sep 2018	
4. TITLE AND SUBTITLE Towards Improved Understanding of Damage and Fracture of High-Performance Cementitious Materials by Development of Mesoscale Analysis Capabilities: 3-D microstructure reconstruction and FE Simulations				5a. CONTRACT NUMBER	
				5b. GRANT NUMBER FA9550-15-1-0486	
				5c. PROGRAM ELEMENT NUMBER 61102F	
6. AUTHOR(S) Jose Luis Alves				5d. PROJECT NUMBER	
				5e. TASK NUMBER	
				5f. WORK UNIT NUMBER	
7. PERFORMING ORGANIZATION NAME(S) AND ADDRESS(ES) UNIVERSIDADE DO MINHO LARGO PACO BRAGA, 4704-553 PT				8. PERFORMING ORGANIZATION REPORT NUMBER	
9. SPONSORING/MONITORING AGENCY NAME(S) AND ADDRESS(ES) EOARD Unit 4515 APO AE 09421-4515				10. SPONSOR/MONITOR'S ACRONYM(S) AFRL/AFOSR IOE	
				11. SPONSOR/MONITOR'S REPORT NUMBER(S) AFRL-AFOSR-UK-TR-2019-0060	
12. DISTRIBUTION/AVAILABILITY STATEMENT A DISTRIBUTION UNLIMITED: PB Public Release					
13. SUPPLEMENTARY NOTES					
14. ABSTRACT Starting from a set of images obtained from micro-computer tomography of a sample of concrete, several numerical tools were developed in order to implement the following steps in image processing: denoising, smoothing and segmentation, in order to obtain a 3D segmentation with separated phases, i.e. to distinguish between matrix, aggregated and voids. This segmented information was then used to generate geometrically accurate finite elements (FE) meshes of the whole domain and of some pre-selected representative volume elements (RVE) to be used in the numerical simulations of concrete loading tests. A new constitutive and damage coupled model is proposed and implemented in a finite element solver and, with an initial set of constitutive and damage parameters identified based on literature data, RVEs were used to run numerical simulations of well-known tests (HC, UXC, TXC) commonly used to characterize cementitious materials.					
15. SUBJECT TERMS EOARD, Cementitious, mesoscale modeling					
16. SECURITY CLASSIFICATION OF:			17. LIMITATION OF ABSTRACT SAR	18. NUMBER OF PAGES	19a. NAME OF RESPONSIBLE PERSON FOLEY, JASON
a. REPORT Unclassified	b. ABSTRACT Unclassified	c. THIS PAGE Unclassified			19b. TELEPHONE NUMBER (Include area code) 011-44-1895-616036

UNIVERSITY OF MINHO
SCHOOL OF ENGINEERING

Final Report on # Grant FA9550-15-1-0486

Towards Improved Understanding of
Damage and Fracture of High-Performance Cementitious Materials
by Development of **Mesoscale Analysis** Capabilities:
3-D microstructure reconstruction and FE Simulations

José Luis de Carvalho Martins Alves

November 17th, 2019

Summary

In what follows is briefly summarized the work developed and main achievements under the Grant #FA9550-15-1-0486, entitled “Towards Improved Understanding of Damage and Fracture of High-Performance Cementitious Materials by Development of Mesoscale Analysis Capabilities: 3-D microstructure reconstruction and FE Simulations”.

Starting from a set of images obtained from micro-computer tomography of a sample of concrete, several numerical tools were developed in order to implement the following steps in image processing: denoising, smoothing and segmentation, in order to obtain a 3D segmentation with separated phases, i.e. to distinguish between matrix, aggregated and voids. This segmented information was then used to generate geometrically accurate finite elements (FE) meshes of the whole domain and of some pre-selected representative volume elements (RVE) to be used in the numerical simulations of concrete loading tests.

A new constitutive and damage coupled model is proposed and implemented in a finite element solver and, with an initial set of constitutive and damage parameters identified based on literature data, RVEs were used to run numerical simulations of well-known tests (HC, UXC, TXC) commonly used to characterize cementitious materials.

In summary,

- Developed numerical algorithms and tools proved to be able to generate accurate FE meshed of the studied concrete sample;
- First order attribute, i.e. porosity, is the main features determining the mechanical behavior of concrete materials;
- Macroporosity determined from segmentation analysis, i.e. measuring of void contents is not a good measure of the total porosity of the material
- Macroscopic and homogeneous models must take into account both macroporosity (the one that we can see and measure from identified voids in voxel data of μ CT images) and microporosity (i.e. very small porosity finely dispersed and undetectable in the matrix, undetectable from μ CT);
- A new constitutive and damage coupled model is proposed to model and describe the mechanical behavior of cementitious materials;
- Finally, if macroporosity is taken into account by voids and microporosity is taken into account as a homogeneous and isotropic porous matrix, the numerical simulations of well-known loading tests (HC, UXC and TXC) display a very good agreement with experimental data taken from literature.

Document Content:

Chapter 1	4
3D reconstruction procedure and images analysis	
Chapter 2	12
3D FE meshes and examples of snapshots taken from the 3D tetrahedral FE meshes of the whole domain and RVEs	
Chapter 3	29
new constitutive and damage coupled model for cementitious materials	
Chapter 4	49
Comparison numerical vs experimental results	

Initial task description and Scheduling:

Task 1: Development of 3-D Voxel-based Microstructure Reconstruction Algorithms and Data Processing Software

Task 2: Development of Capabilities for Features Identification, Clustering and Metrics

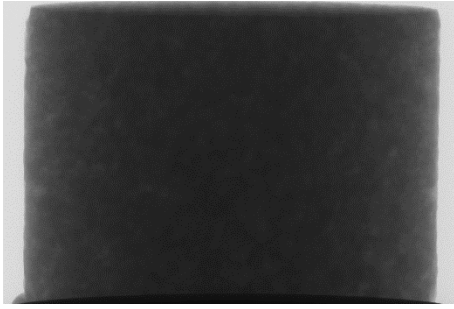
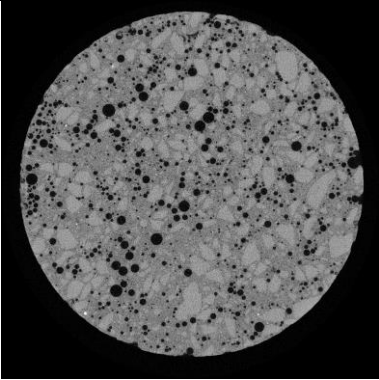
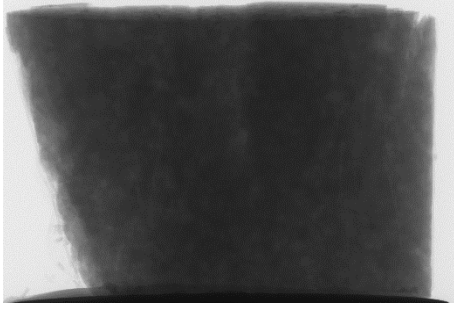
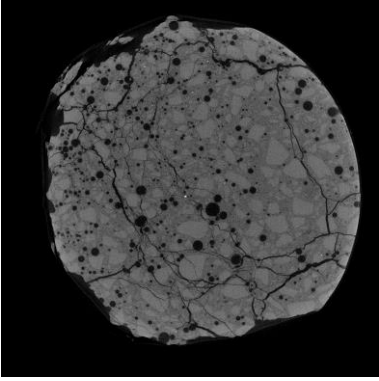
Task 3: Development of an advanced high quality multi-material and morphologies-oriented tetrahedral finite element mesh generation software

Task 4: constitutive and Damage modelling

Chapter 1

Two fine aggregate concrete samples were characterized by micro-CT, and the two sets of images provides for analysis.

The two samples can be identified as follows:

	External view	Example of a layer
Pristine		
Fractured		

Initial set of images:

Pristine sample:

4000 x4000 pixels x 2590 layers [82,2671] = **41.4 GVoxels (!!!)**

Voxel size = $4.95 \mu\text{m}^3$.

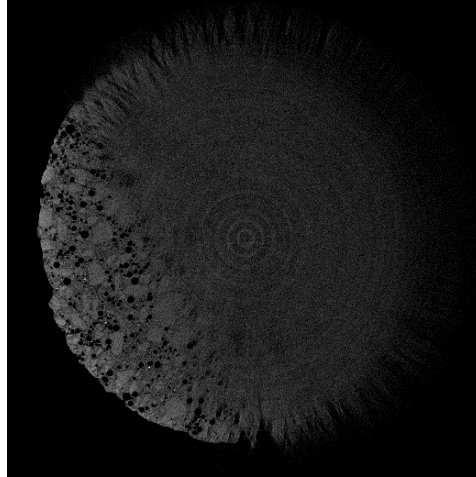
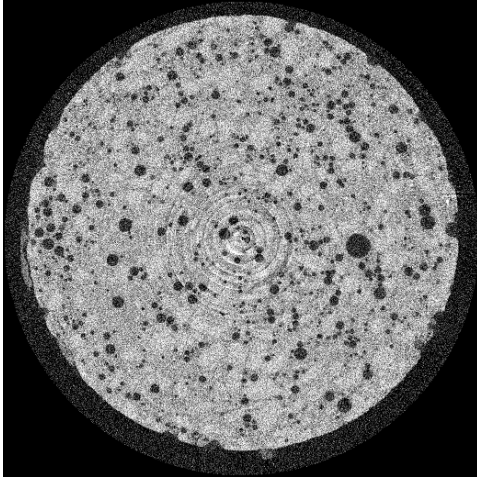
Fractured sample:

4000 x4000 pixels x 2590 layers [118,2661] = **40.7 GVoxels (!!!)**

Voxel size = $4.95 \mu\text{m}^3$.

a) Pristine sample, top and bottom

A preliminary look at the layers of the pristine samples allowed to observe that, at the axial top and bottom of the cylindrical sample, several specific features related with sample preparation and/or data acquisition, as shown in following figures,



should be eliminated from the analysis. Therefore, in order to eliminate such effects, several layers of the initial set of images, namely layers [82,149] and [2501,2671] were not taken into account in the following analysis.

So, for image segmentation and 3D reconstruction, the following set of images was considered:

$$4000 \times 4000 \text{ pixels} \times 2351 \text{ layers [150,2500]} = \mathbf{37.6 \text{ GVoxels (!!!)}}$$

$$\text{Voxel size} = 4.95 \mu\text{m}^3.$$

b) Images decimation (by 2)

The original set of images corresponds to a massive data of around 37.6 GigaVoxels. Such amount of data is, in practice, computationally untreatable. Besides, the voxel size of $4.95 \mu\text{m}^3$, i.e. pixel size of $4.95 \mu\text{m} \times 4.95 \mu\text{m}$ and layer spacing of $4.95 \mu\text{m}$ can also be considered too small with respect to the geometrical features within the sample. Having this in mind, the original data was decimated by 2, i.e. new size of data will be of:

$$\mathbf{2000 \times 2000 \text{ pixels} \times 1295 \text{ layers} = 4.7 \text{ GVoxels}}$$

$$\text{corresponding to a voxel size of } 9.9 \mu\text{m}^3.$$

The following procedure was implemented:

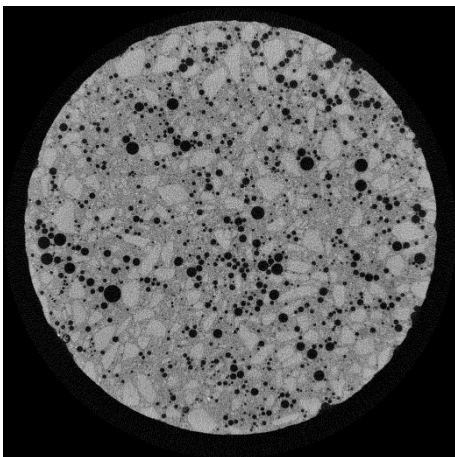
- 1) Gaussian smoothing: Images are very noisy; in order to minimize its role, a Gaussian smoothing was applied to each pixel (standard deviation of 2 pixels);
- 2) After smoothing, image is decimated by 2, in order to obtain a numerically more treatable problem (too much memory required...);
- 3) Pixel's gray scale values is scaled to the range of [0,127]

c) Image analysis

In order to achieve a 3D reconstruction of the geometrical features (voids, concrete, aggregates,...) within the concrete samples, one must develop an algorithm able to segment the full set of images in order to distinguish the following domains:

- Outside world, id0, color: white
- matrix, id1, color black
- aggregates, id2, color: blue
- voids/porosity id3, color: blue

For the sake of exemplification, in the following figure it is shown the image in gray scale correspondent to one of the layers:



The following points must be highlighted:

- Images are very noisy, i.e. the amplitude of noise has a similar magnitude to the gray scale values between the two main domains, matrix and aggregates;
- Contrast between voids (and outside world) and matrix/aggregates can be clearly seen
- Low contrast between matrix and aggregates at the pixel level;
- It was also found that image intensity (average gray scale value) diminishes radially;

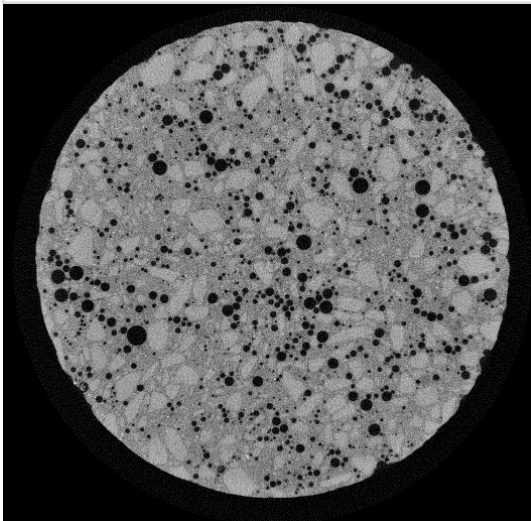
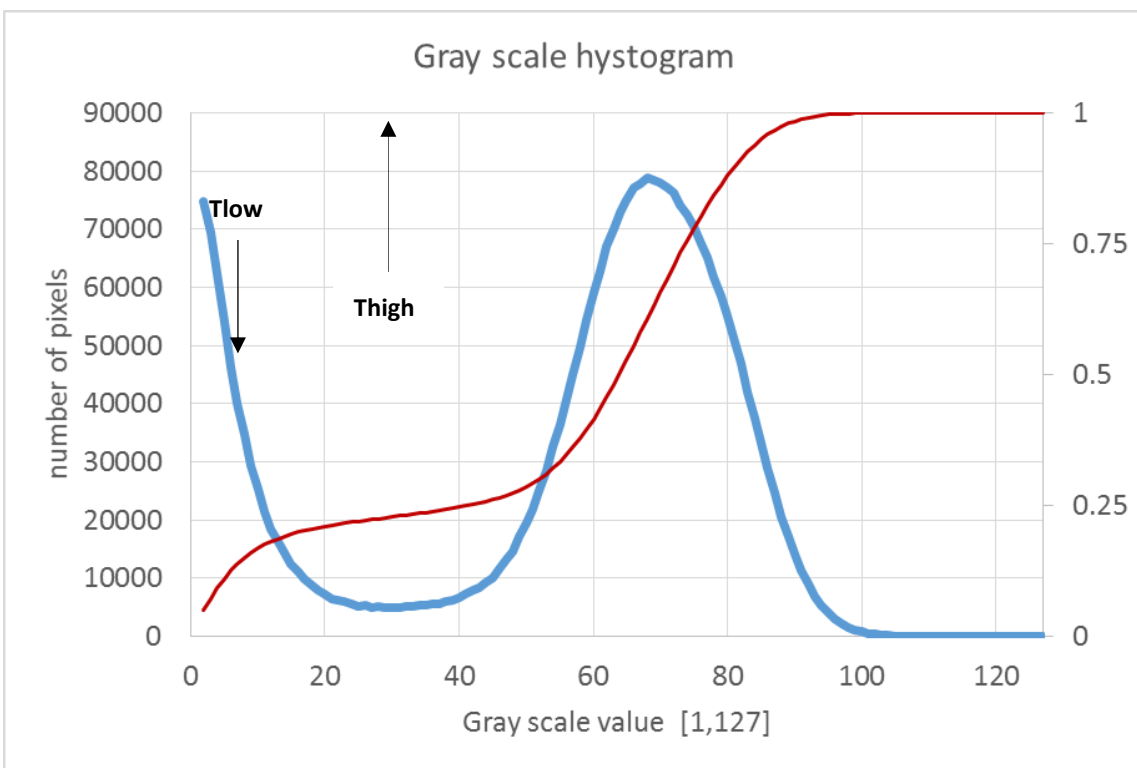
- Average gray scale intensity of the image layers evolves along sample axial axis.

d) Image Segmentation

The goal is to identify the several phases (outside world, matrix/concrete, aggregates and internal voids).

As aforesaid, the main difficulty is the lack of contrast between aggregates and matrix, i.e. the gray scale values of these two phases are too close to allow a clear identification of the two subdomains.

The following figure depicts the frequency histogram of one layer,



There are clearly two main domains

- The left side (darker pixels), i.e. gray scale values up to around 30, which represents pixels belonging to both outside world and voids/porosity;
- The right side, i.e. gray scale values from around 30, which can be roughly decomposed into two sub-domain (left and right side with respect to the maximum value: these two subdomains will be hereafter interpreted as matrix (the darker area, i.e. lower values of the gray scale), and aggregates (the lighter area, i.e. higher values of the gray scale)

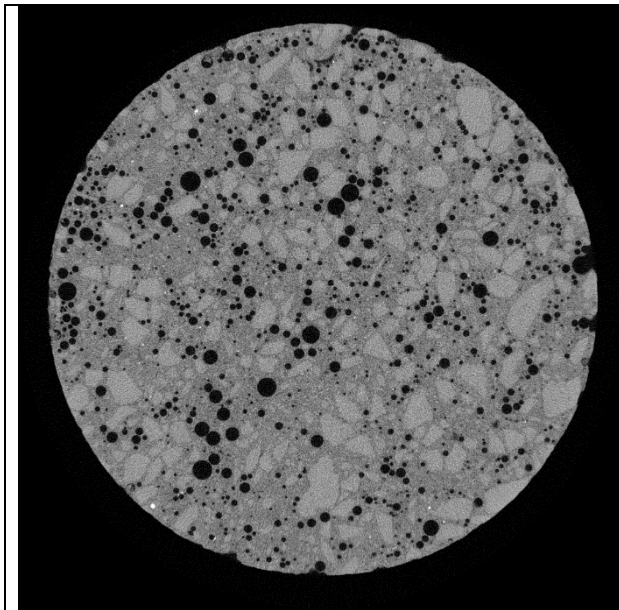
There is, however, an additional issue. Because the gray scale values of matrix and aggregate subdomains are too close, these two regions cannot be evaluated simple by the gray scale value at each pixel. Instead, the strategy adopted was to mimic the eye, which evaluates/classifies each pixel by evaluating the neighborhood domain.

So, based on the above shown histogram and discussion, two threshold values are identified:

- Tlow: defined as the **first** change of slope of the histogram curve
- Thigh: defined as the **second** change of slope of the histogram curve

Then, a so called Gray Neighborhood Value is determined for each pixel.

The following sequences of images are an example of application of the above described procedure:



Original image,
Gray scale,
after smoothing and decimation by
2.

Outside world and voids are
displayed with the darker pixels.

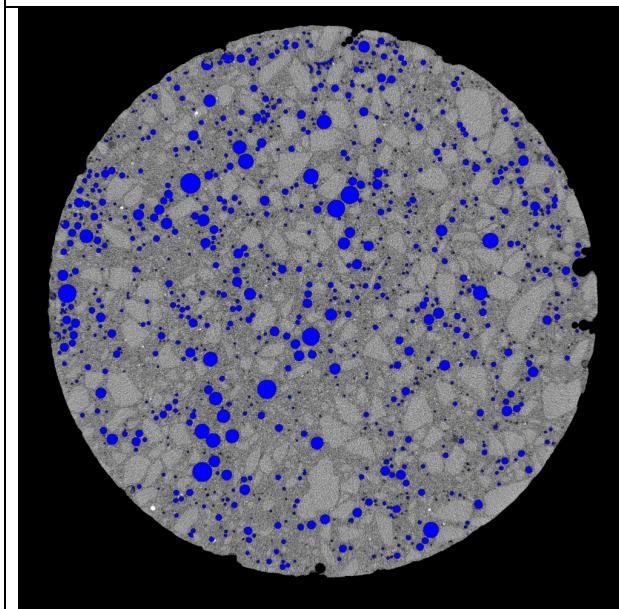
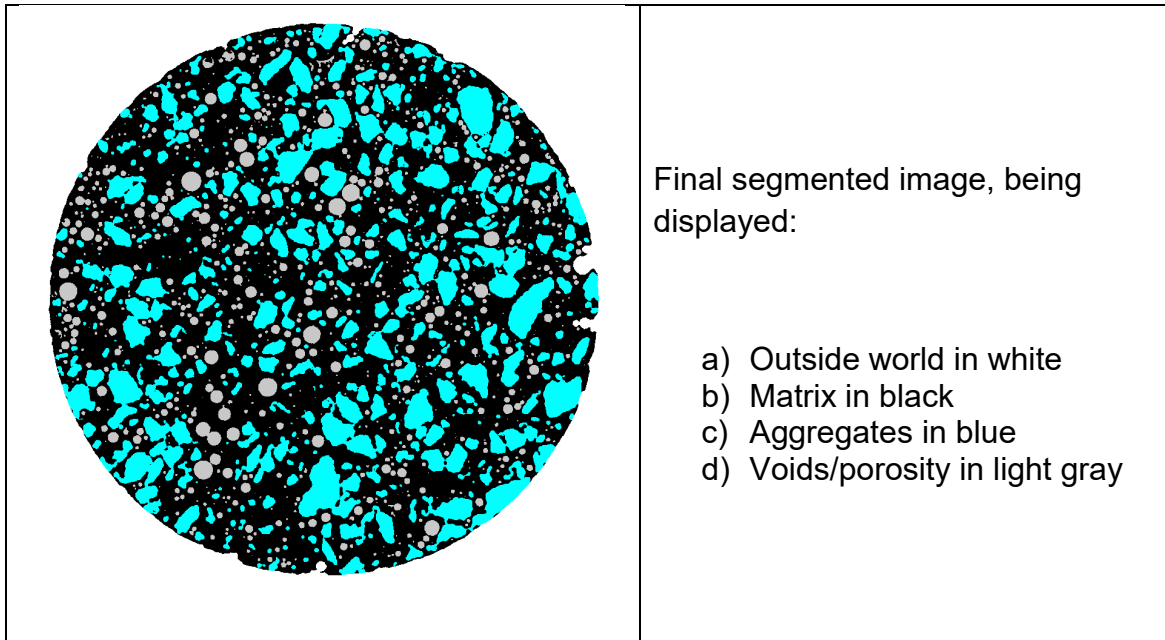
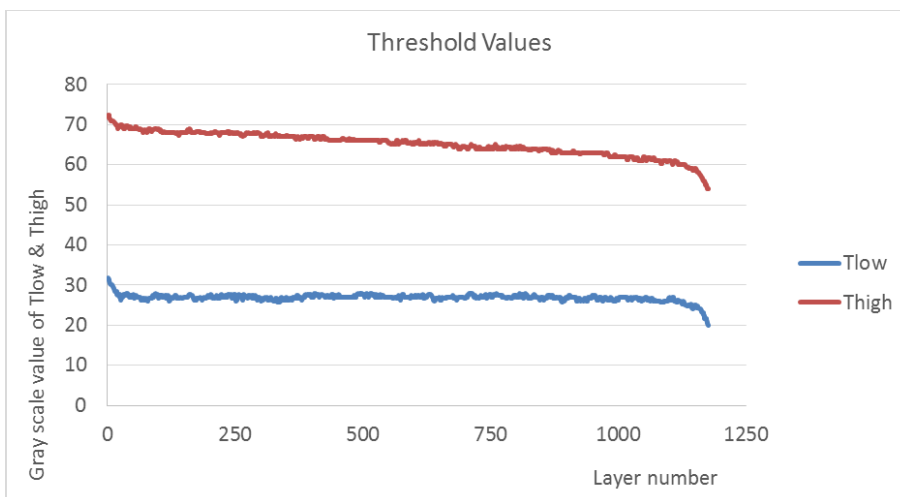


Image after identification of
threshold value T_{low} and
respective segmentation of outside
world (shown in black) and
voids/porosity (displayed in blue.
The remaining pixels keep their
original gray scale values



e) Basic statistical data

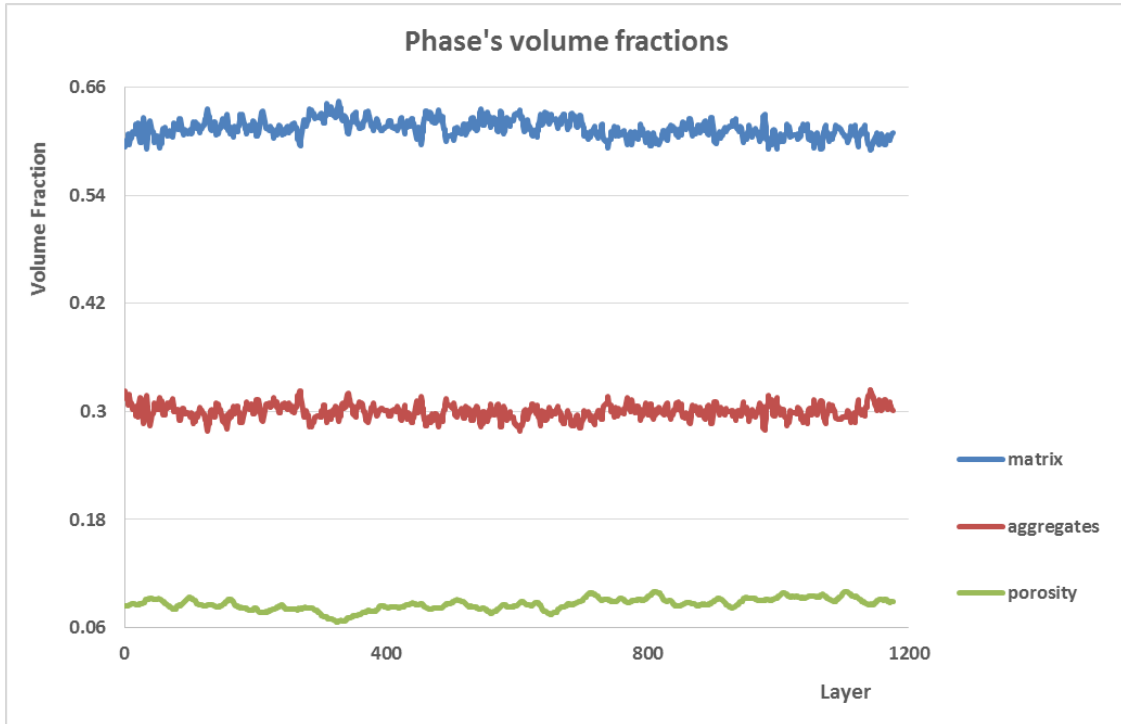
Next figure shows the evolution of the threshold values along the axial axis of the cylindrical sample (i.e. layer by layer). As previously mentioned, it can be seen that, in overall, images become darker from bottom to upper (from left to right on the figure).



Concerning phases' volume fractions, the average values are as follows:

- 61.6 % of matrix
- 29.5 % of aggregates
- 8.8 % of porosity

Minor variations can be seen between layers, as depicted on the next figure (material is rather isotropic and homogeneous in terms of heterogeneities (aggregates and pores) spatial distribution:

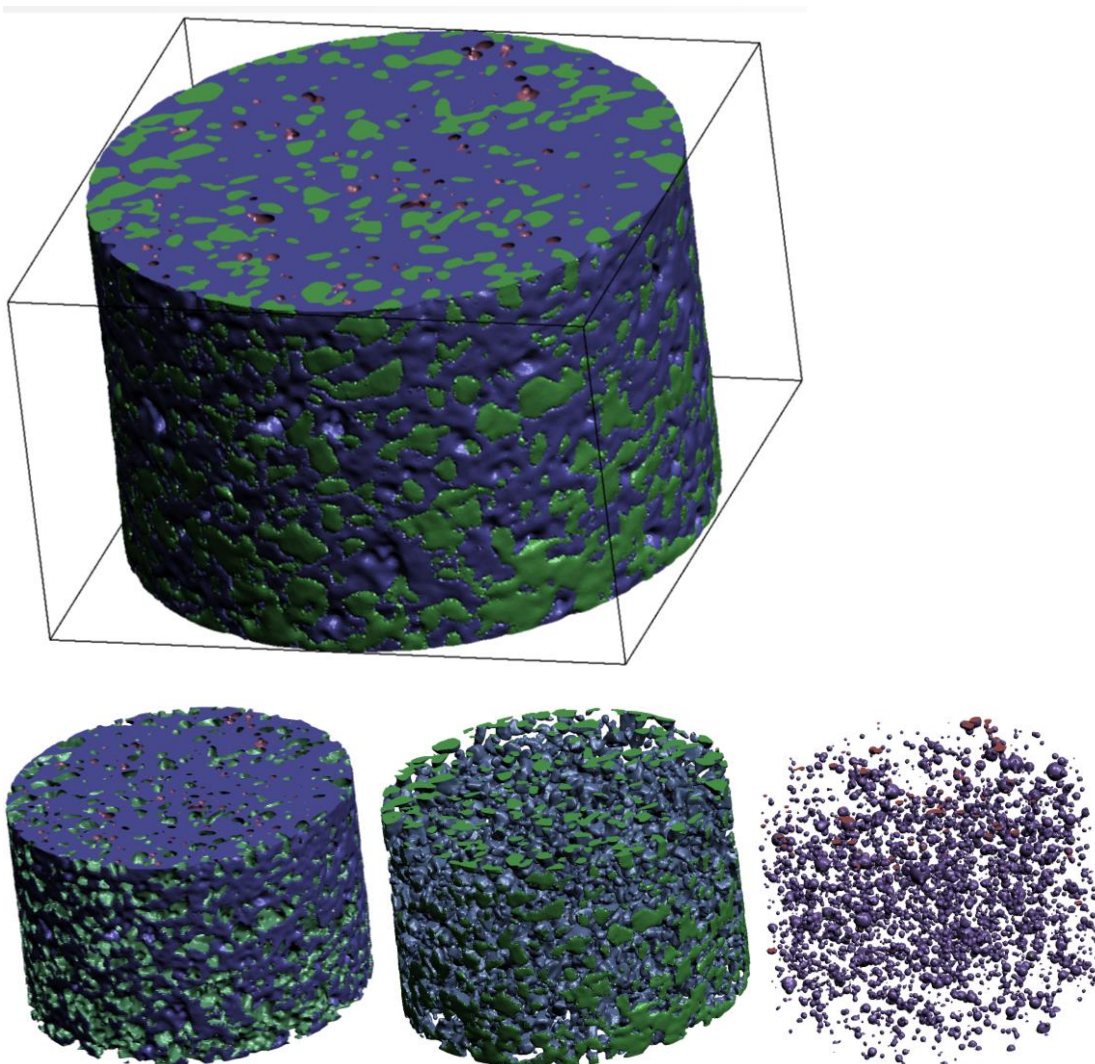


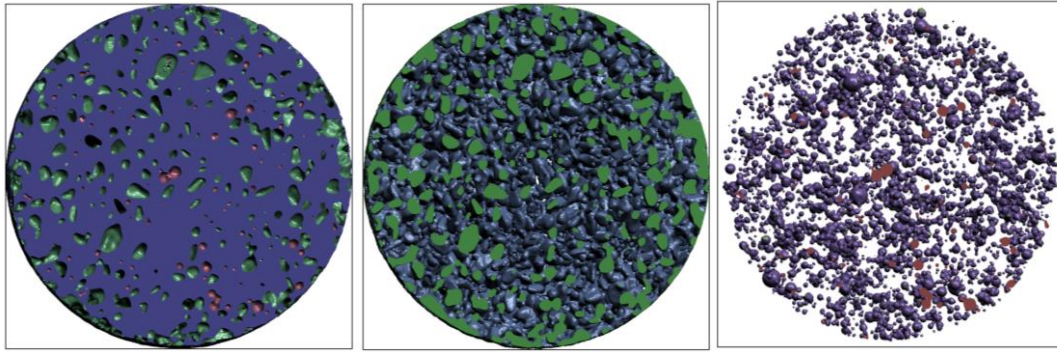
Chapter 2

3D reconstruction and FE meshing

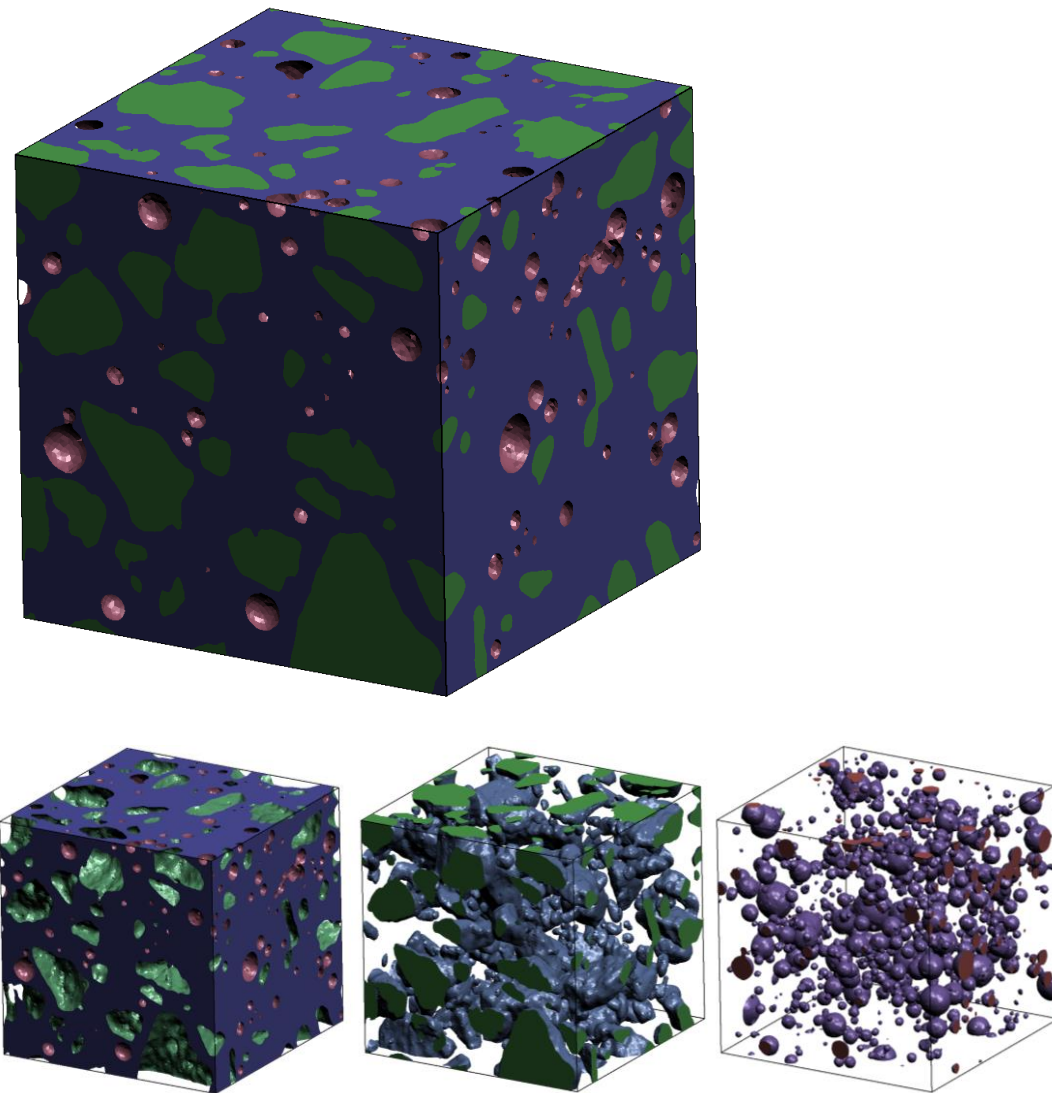
After image segmentation, the 3D reconstruction consists basically in the stacking of the 2D images into a 3D structure of voxels (a voxels is, basically, a 3D pixel, which height is assumed to be the distance between layers).

The 3D reconstruction of the full domain (**19.8 mm x 19.8 mm x 11.6 mm**), as shown in the next screenshots,





and an example of a so-called Representative Volume Element (RVE), with size of 3.96 mm x 3.96 mm x 3.96 mm, which will be later on used for numerical simulations.



Statistical Data

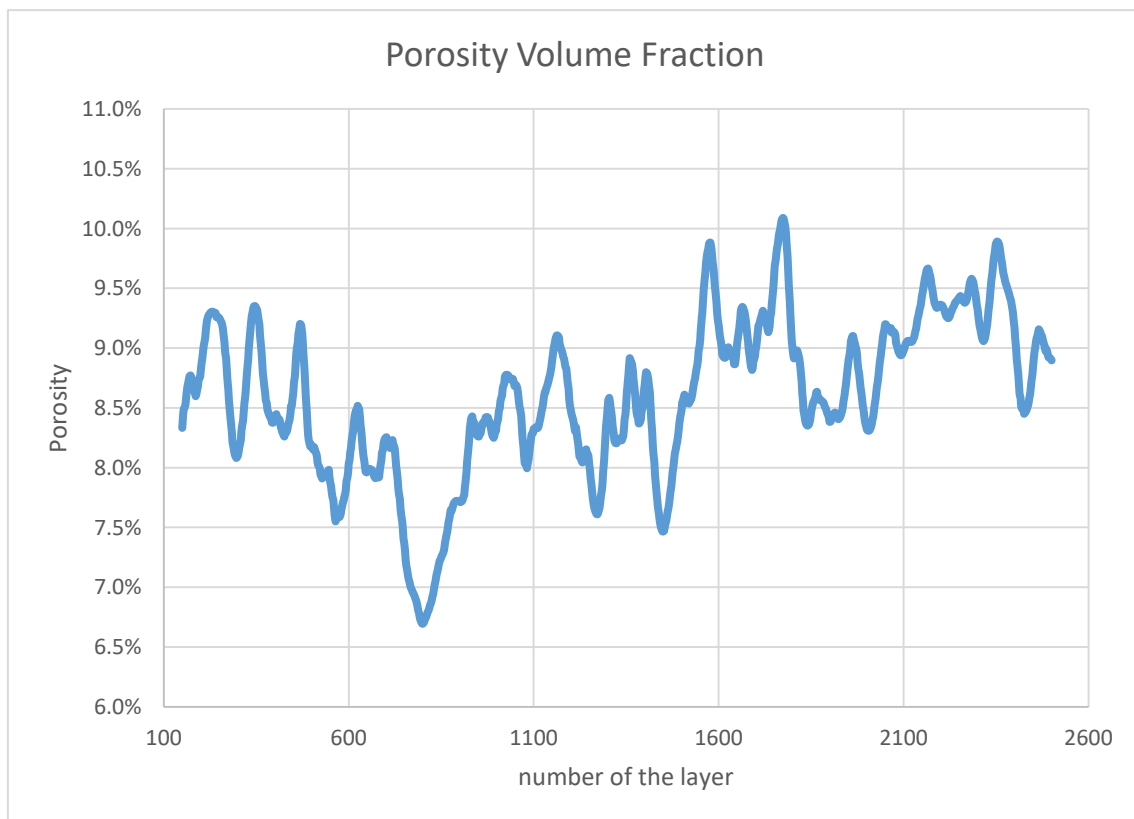
After segmentation, data was analyzed in order to determine the most relevant statistical data.

The average volume fractions of the full domain are as follows:

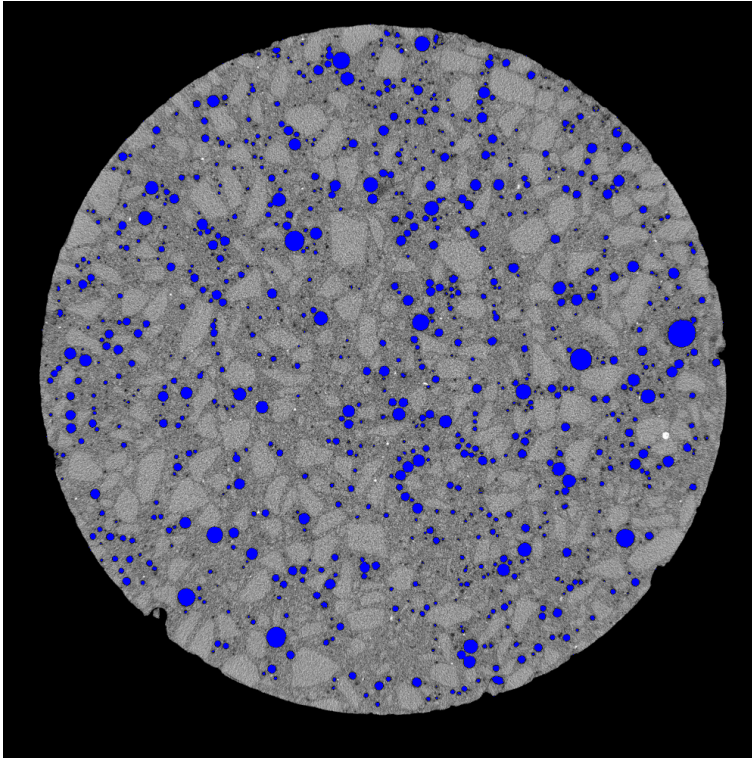
		Volume Fraction
Matrix		62.7%
Sand/aggregates		28.7%
Macro porosity		8.6%
Volume	[mm ³]	2952.9

Additionally, the distribution of matrix+sand and porosity is rather uniform along the axial axis of the sample. Next figure shows the evolution of porosity.

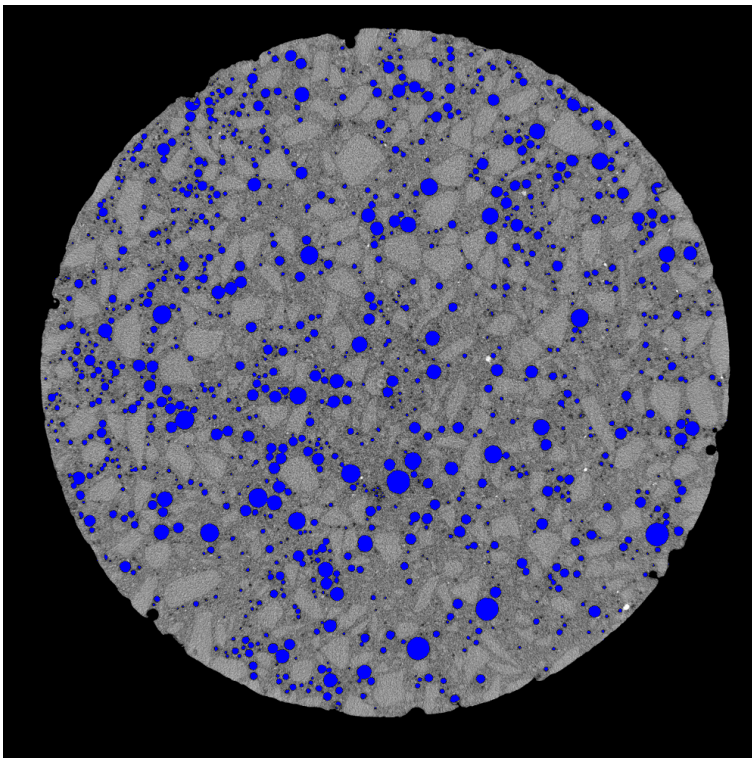
Porosity ranged between 6.7% and 10.1%:



Layers at which porosity was minimum and maximum are shown in the next figures:



Layer 798, Porosity = 6.7%



Layer 1772, Porosity = 10.1%

The total domain contains about 50k independent pores (50 028)!

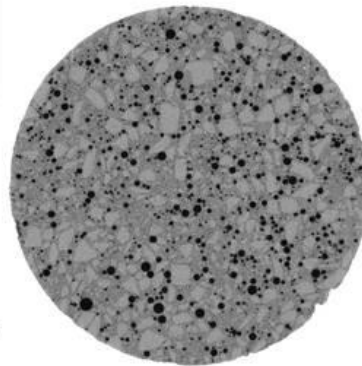
Examples of 3D FE tetrahedral meshes

→ 3D reconstruction of μ CT data



← external view

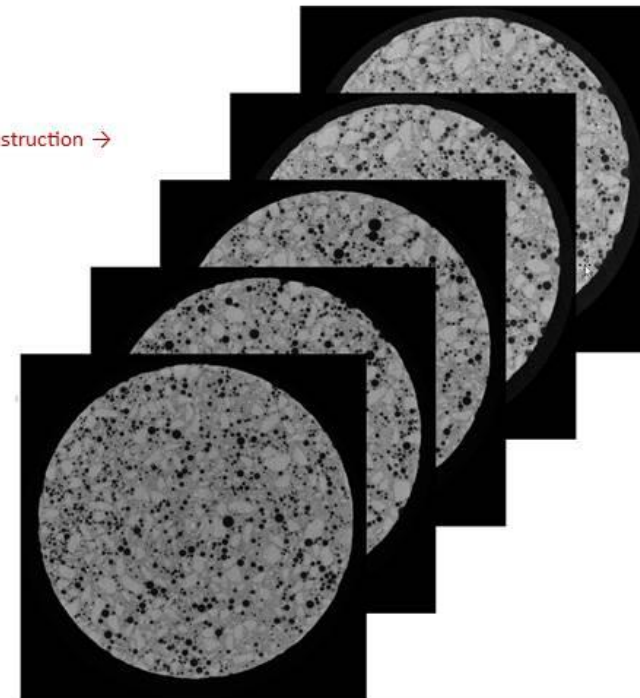
↓ 1 slice



2590 slices
4000 x 4000 pixels/slice
41.4 Giga Voxels

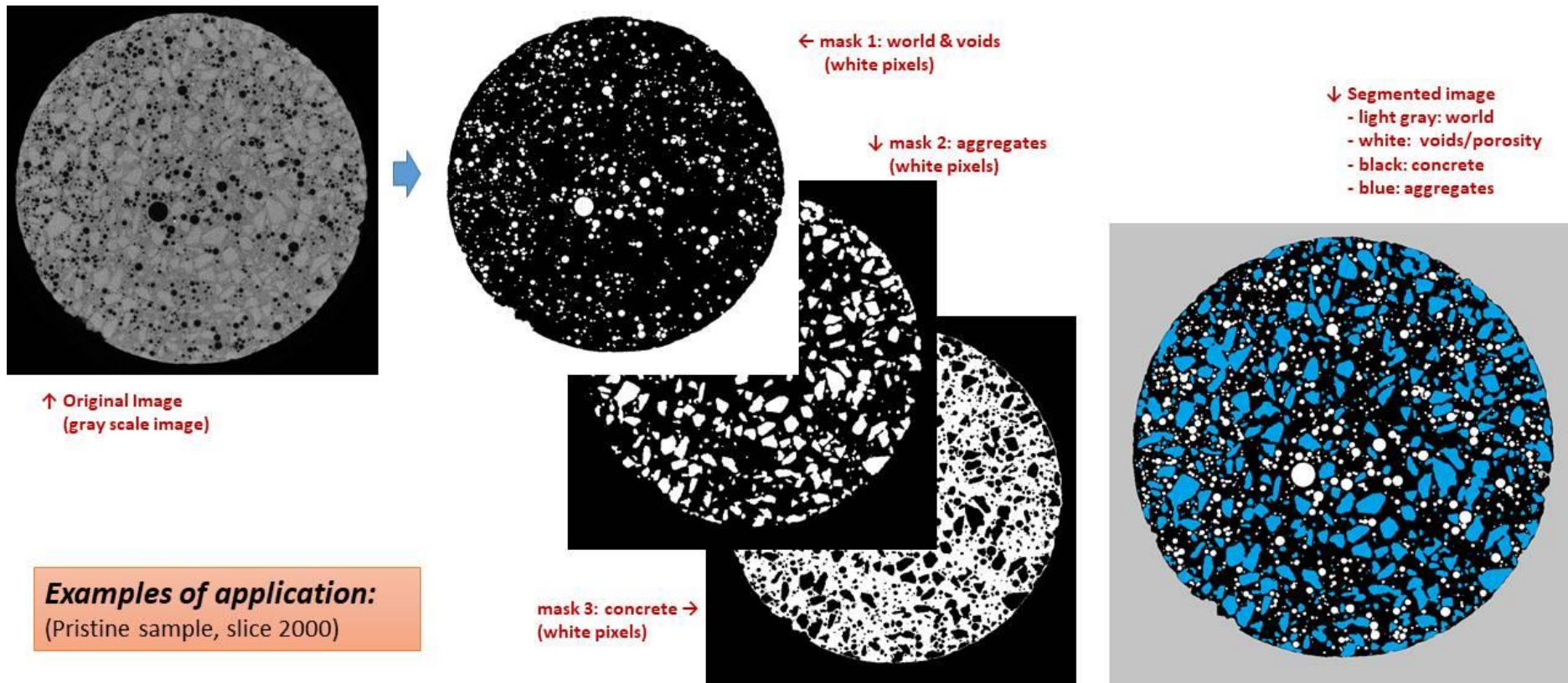
Voxel size: 4.95 μm x 4.95 μm x 4.94 μm
Sample size: 19.8mm x 19.8mm x 12.8mm

3D reconstruction →

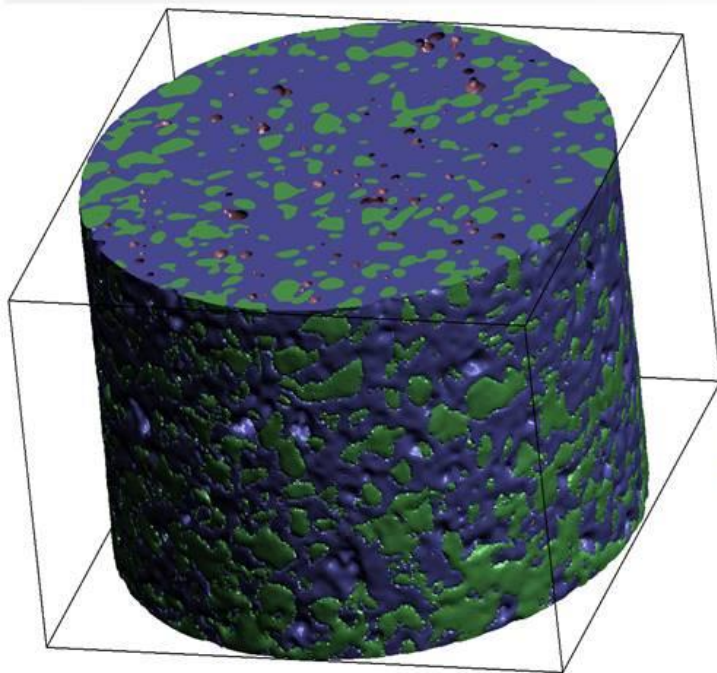


3D reconstruction of a multi-slice micro-CT of a pristine sample of a high performance concrete

→ 3D reconstruction of μ CT data

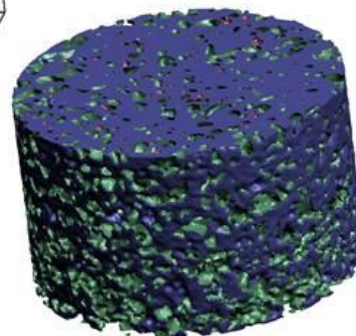


→ 3D FE meshing of the whole domain

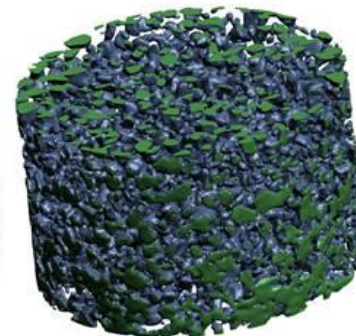


tetrahedral FE mesh :
Pristine sample, full volume!

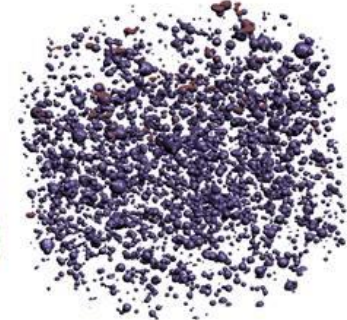
↓ matrix



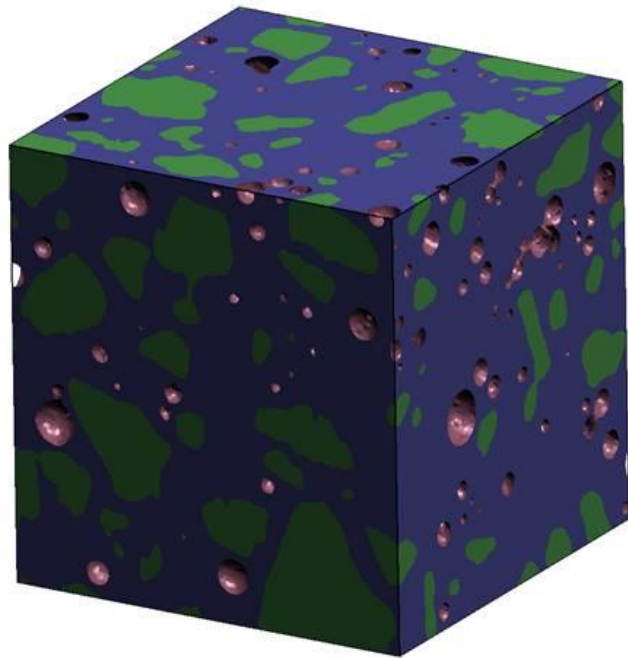
↓ aggregates



↓ voids

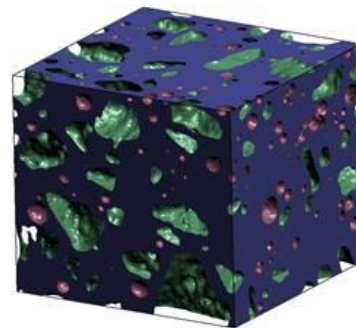


→ 3D FE meshing of a RVE

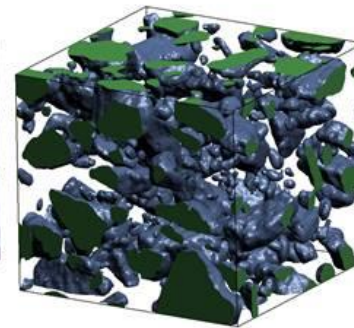


tetrahedral FE mesh :
RVE – Representative Volume Element

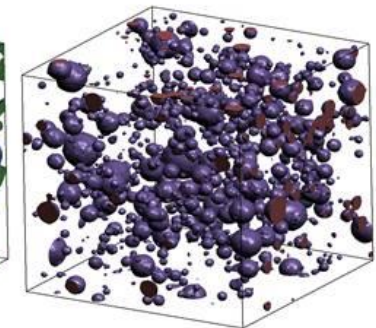
↓ matrix



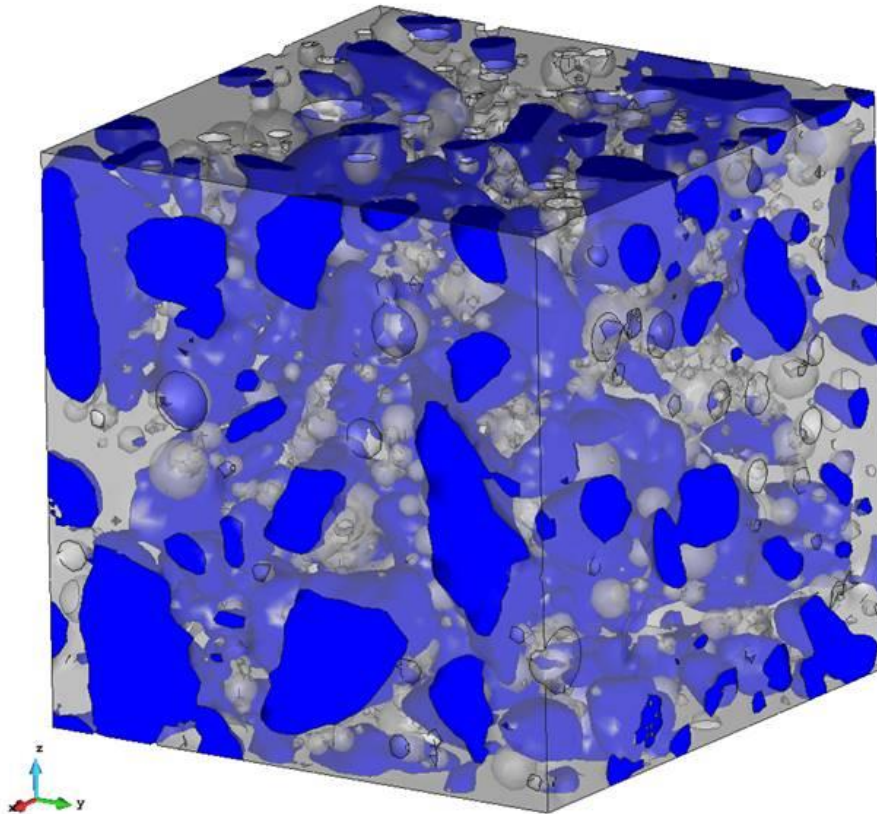
↓ aggregates



↓ voids



→ 3D FE RVE data

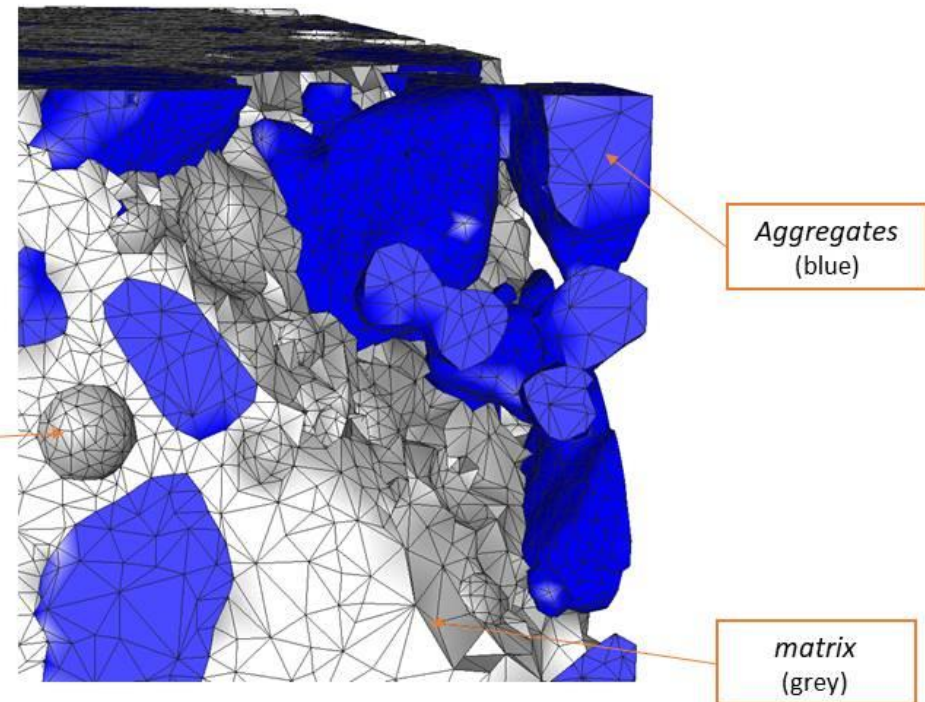
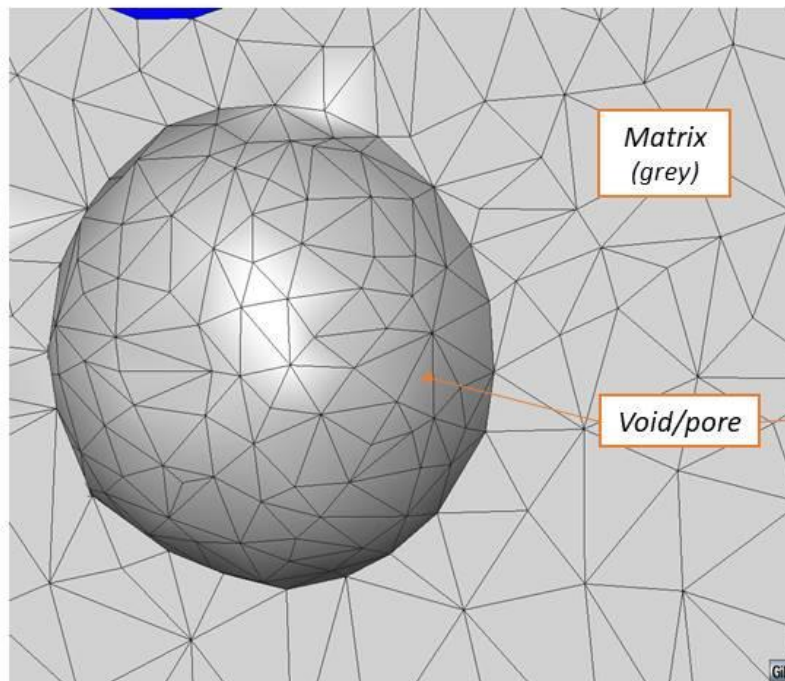


RVE	VFraction	NE*	NN
Matrix	71.81%	619 254	-x-
Aggregates	21.57%	234 012	-x-
Voids	6.62%	-x-	-x-
Total	100%	853 266	154 128

*4-node linear tetrahedral finite elements

(10-node quadratic will be tested, but NN = 1 203 210 !!!)

→ 3D FE RVE, mesh details

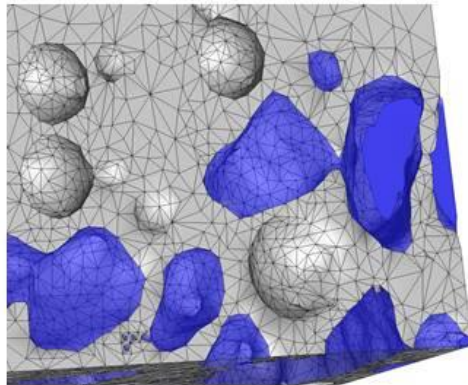


Exemplification of the accurate geometrical modelling of the geometrical specificities of pores and aggregates.

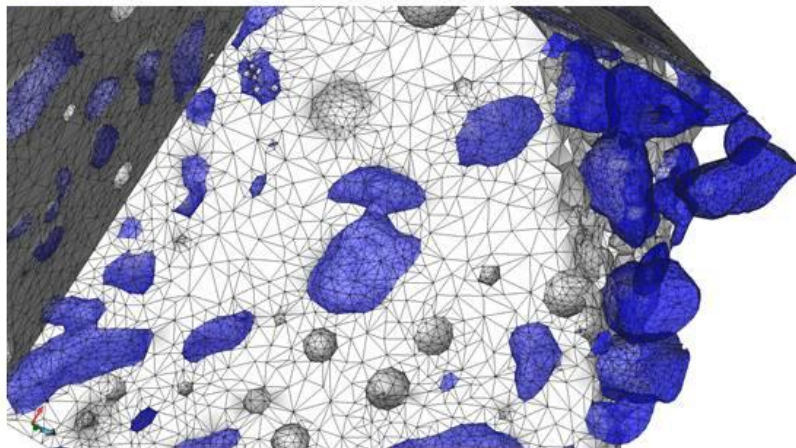
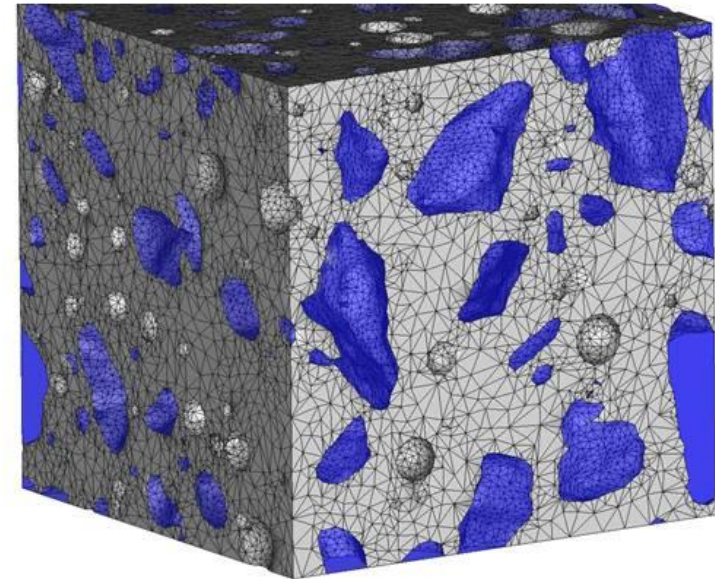
Left: example of the internal surface of one pore; this spherical shape is very well captured and described by the FE mesh

Right: example of the internal FE mesh and geometry of the aggregates (*matrix partially removed to allow an insight of the internal structure/geometry*)

→ 3D FE RVE, mesh details



RVE = Matrix (grey)
+ Aggregates (blue)
+ Voids



Different views of the RVE FE mesh:

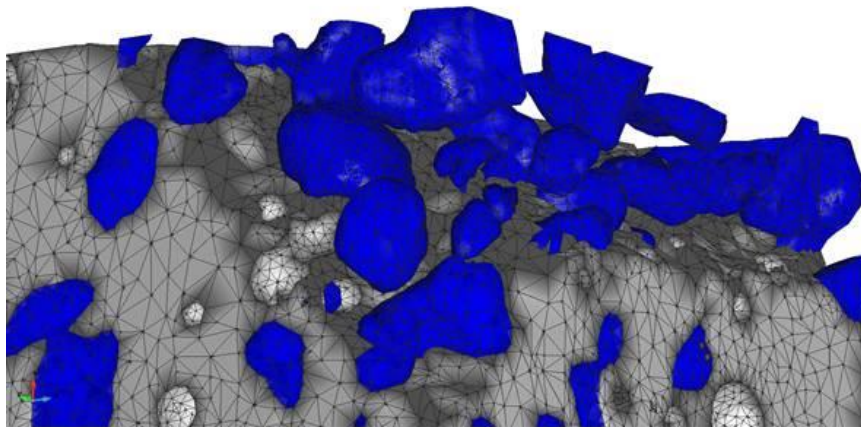
Right: external view of the RVE FE mesh

Left (Up): zoom of RVE FE mesh, with aggregates set transparent

Left (Down): example of the internal FE mesh and geometry of the aggregates

(matrix partially removed to allow an insight of the internal structure/geometry)

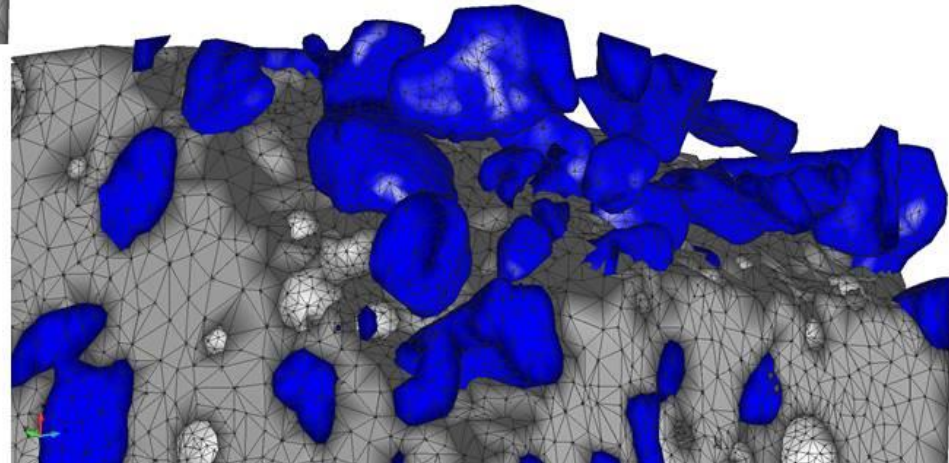
→ 3D FE RVE, mesh details



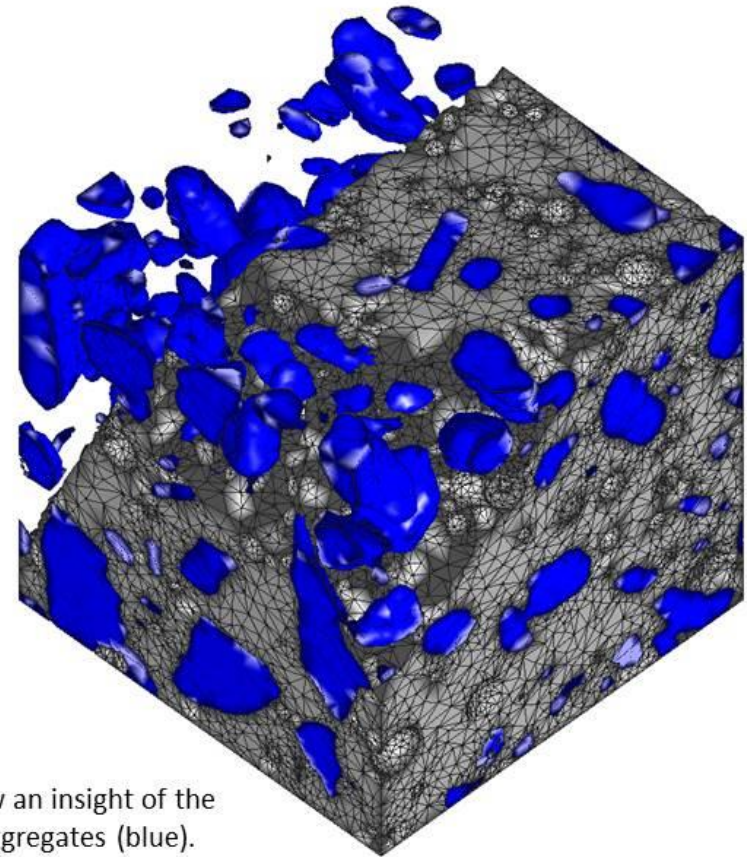
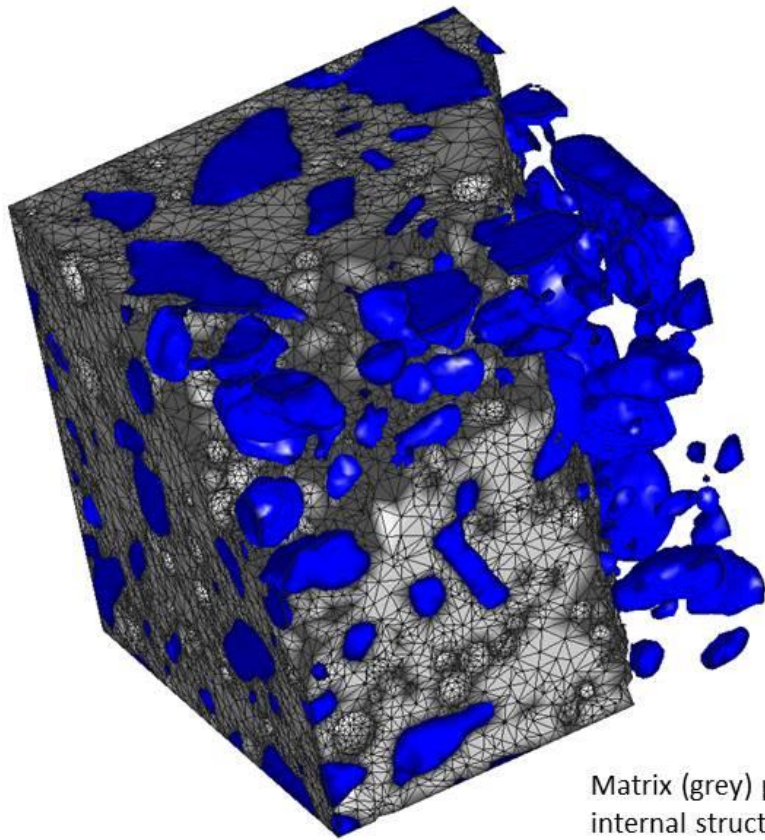
RVE = Matrix (grey)
+ Aggregates (blue)
+ Voids

Images showing the internal geometrical details of the RVE: matrix (grey) is partially removed to allow an insight of the internal structure/geometry of aggregates (blue).

The aggregates and internal pores are embedded in the matrix.

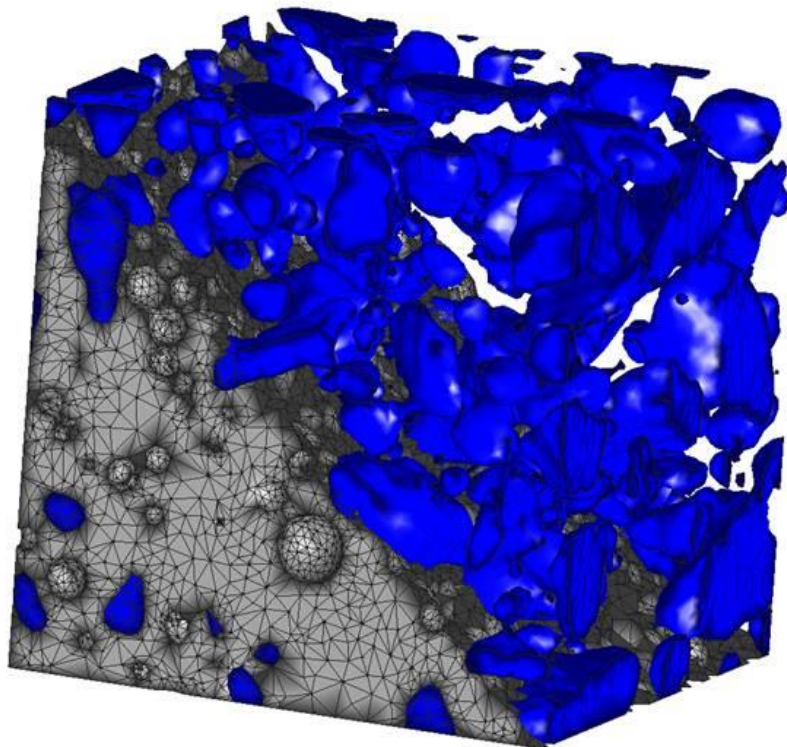


→ 3D FE RVE, mesh details

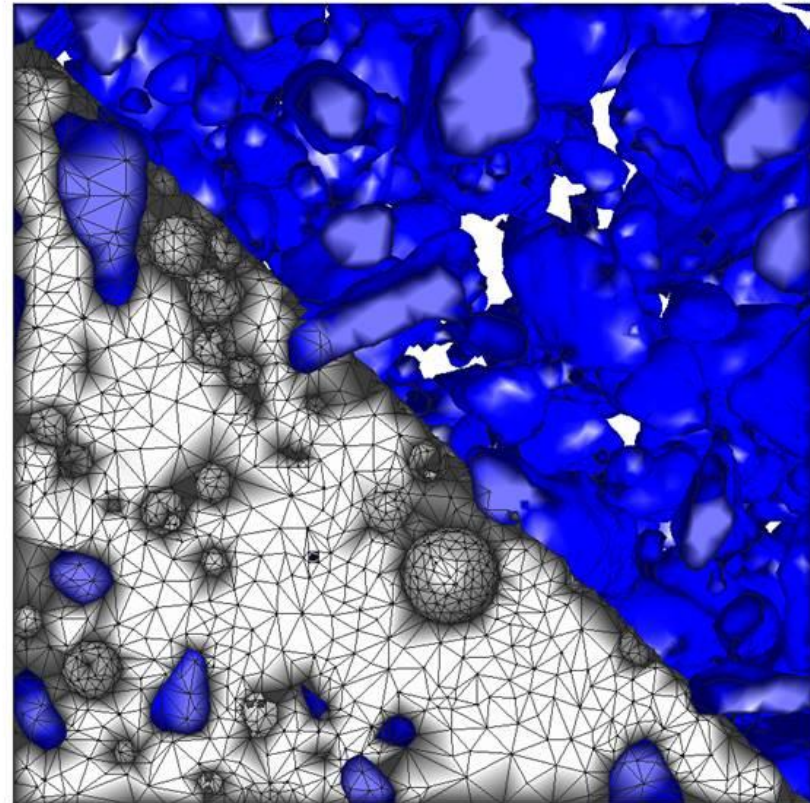


Matrix (grey) partially removed to allow an insight of the internal structure and distribution of aggregates (blue).

→ 3D FE RVE, mesh details



Matrix (grey) partially removed to allow an insight of the internal structure and distribution of aggregates (blue).



→ 3D FE RVE simulation

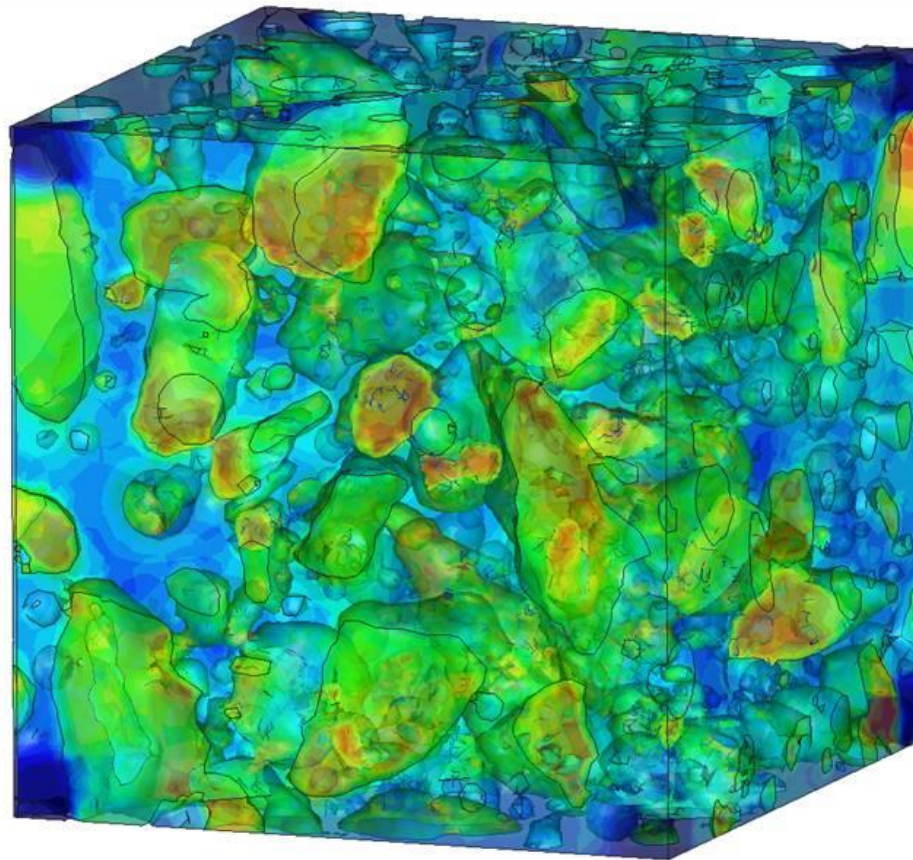
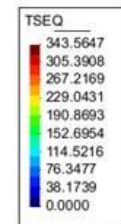
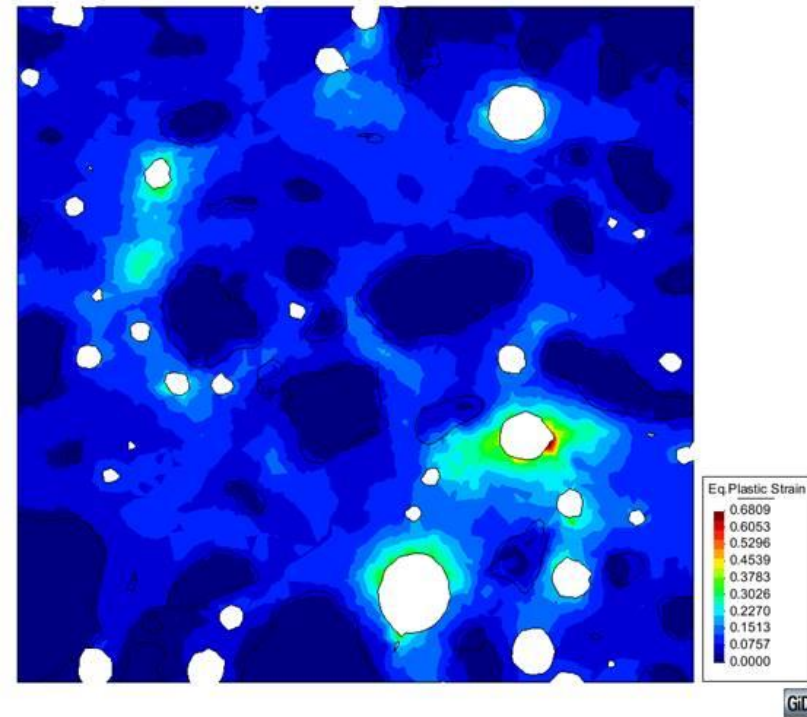
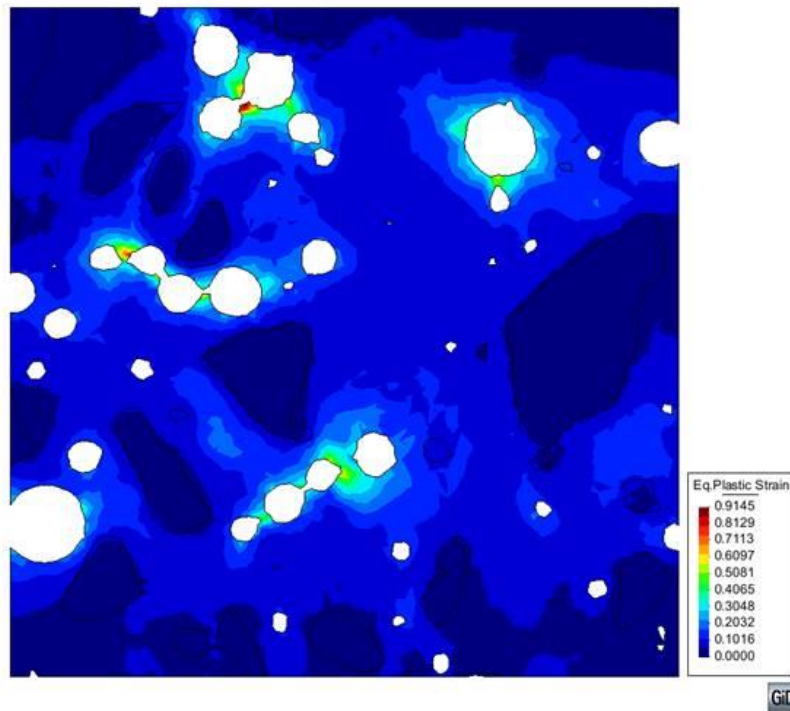


Figure showing the fields of the **Equivalent Stress** for **Hydrostatic Compression**

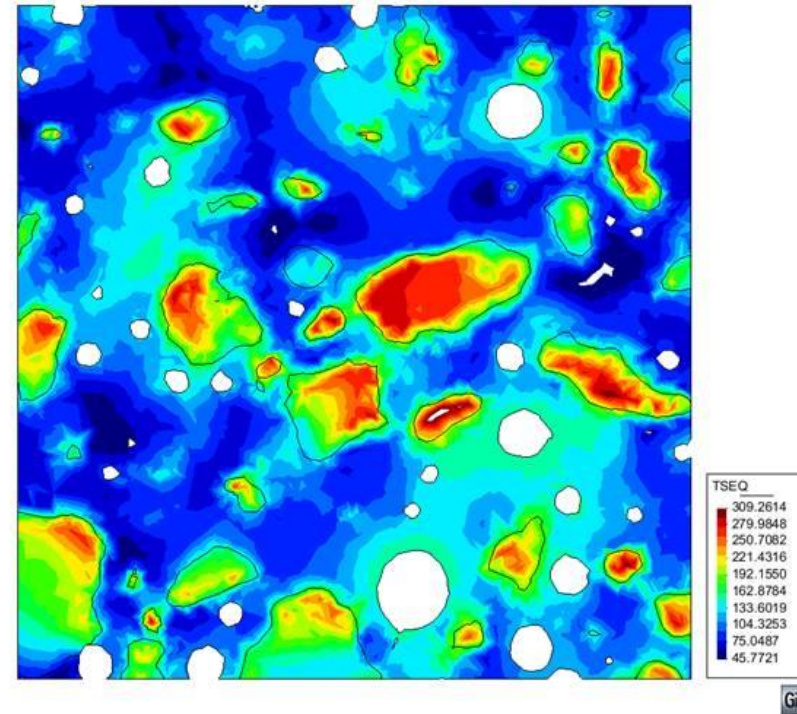
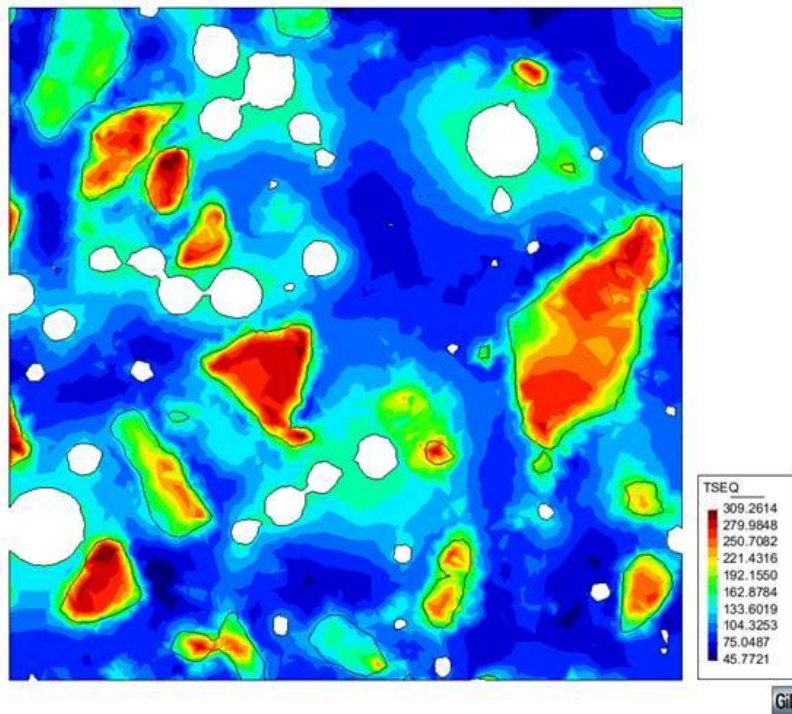


→ 3D FE RVE simulation



Examples of the distribution of the **equivalent plastic strain** in two sections of the RVE under **hydrostatic compression**: white regions correspond to pores; the dark blue regions to aggregates, which do not plastify due to their higher strength; on the contrary, the matrix plastifies, and higher plastification occurs in the vicinity of pores and ligaments between pores due to compaction.

→ 3D FE RVE simulation



Examples of the distribution of the **equivalent stress** in two sections of the RVE under **hydrostatic compression**: white regions correspond to pores; higher (red areas) equivalent stresses occur in aggregates due to the higher strength; Lower values of the equivalent stress (dark blue areas) are in the vicinity of voids' surfaces due to stress free conditions.

Chapter 3

In what follows a new damage model for concrete materials is proposed. A continuum model of a new plasticity-damage model for concrete materials is briefly formulated and described.

However, no mechanical data was available for the cementitious material for which μ CT was performed. In order to overcome such difficulty, mechanical data on which the model is being developed is that reported in W. Heard's PhD thesis, namely in what concerns with the following tests/loadings:

- HC,
- UXC,
- TXC,

as shown on the next figures (taken from W. Heard's PhD thesis) :

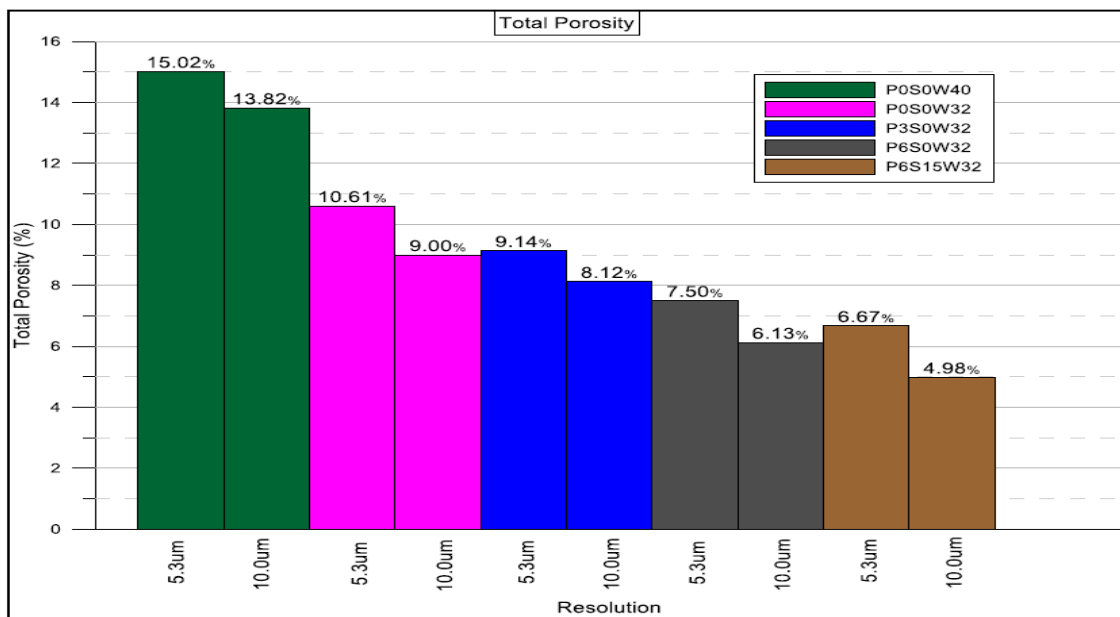


Figure 3.15 Total porosity for mix PxS0W32, P0S0W40 and P6SW32

Heard studied several materials.

Two of them, referred as P6S15W32 concrete samples, display a macroscopic porosity of around 6%, similar to the material studied in the present work.'

Next figures, also taken from W. Heard's PhD thesis, are the mechanical responses determined for the P6S15W32 samples under the abovementioned loadings, respectively HC, UXC and TXC.

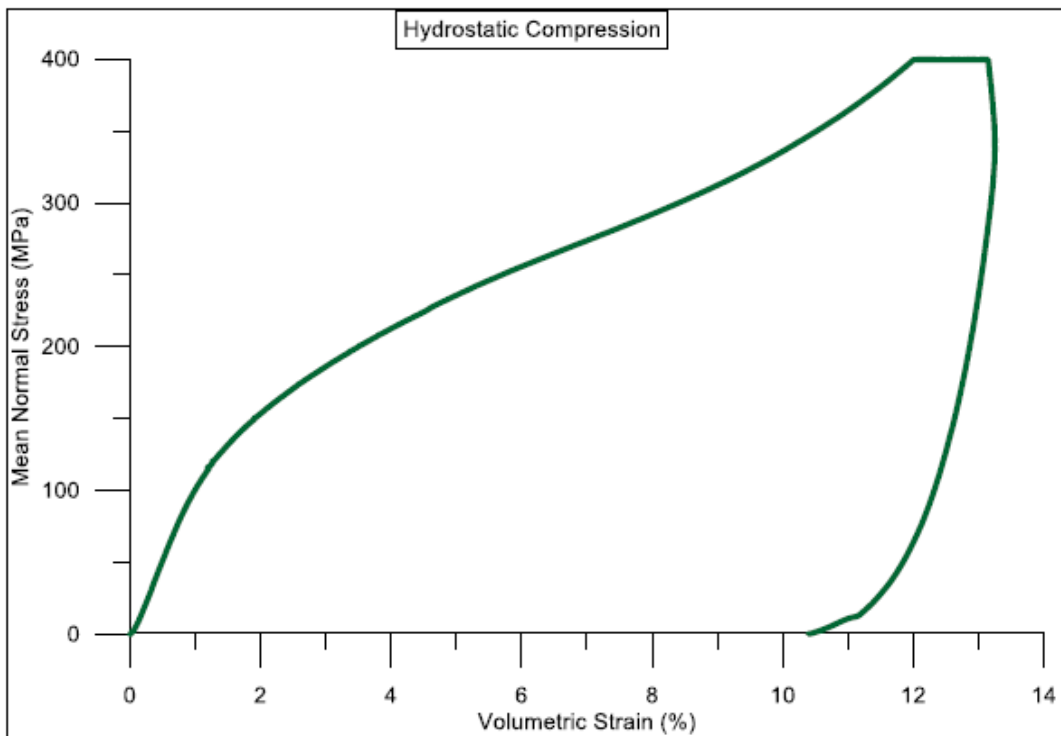


Figure 4.11 Pressure volume response

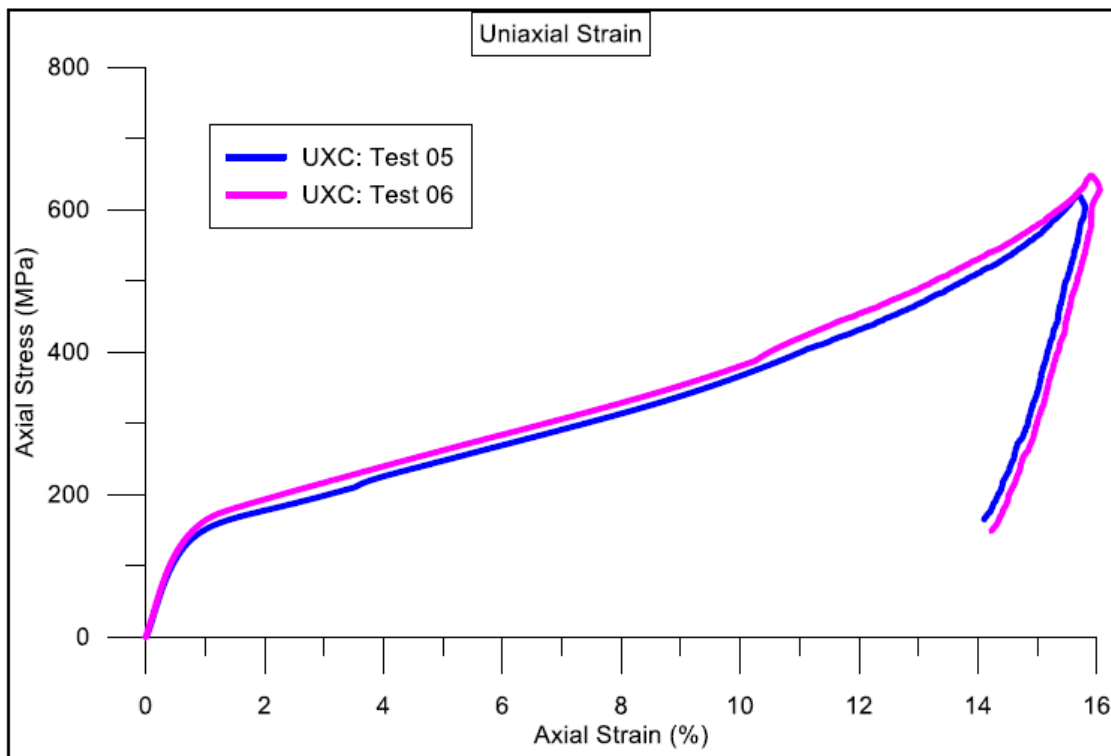


Figure 4.13 Stress versus strain response for two UXC experiments

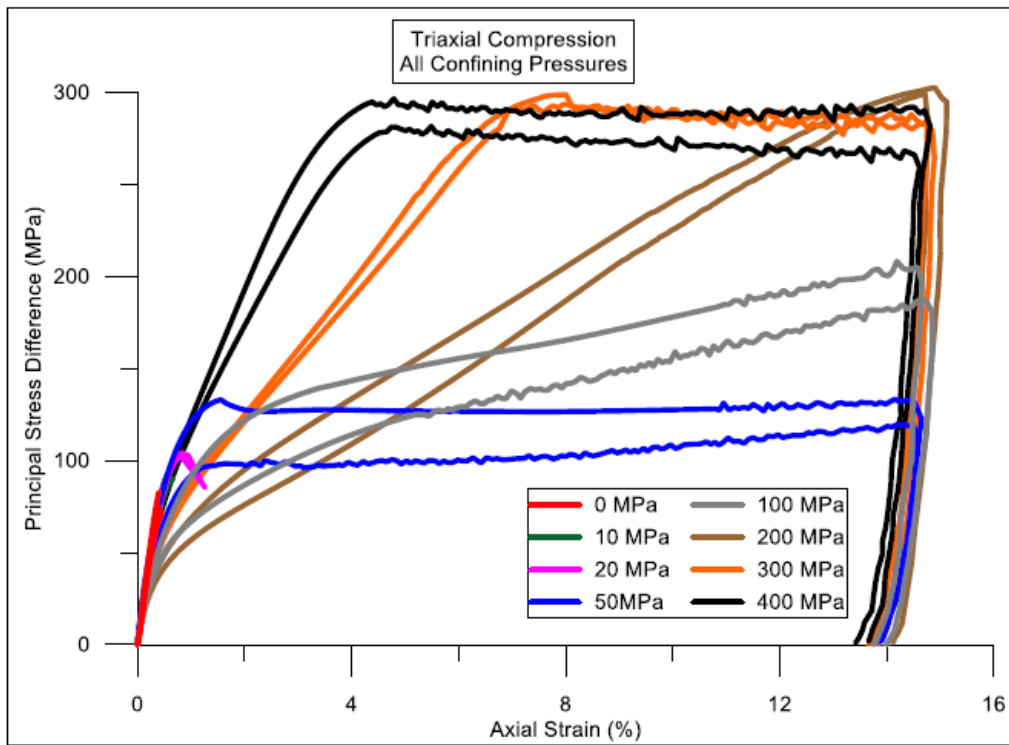


Figure 4.22 TxC: PSD vs axial strain for all confining pressures 0 MPa to 400 MPa

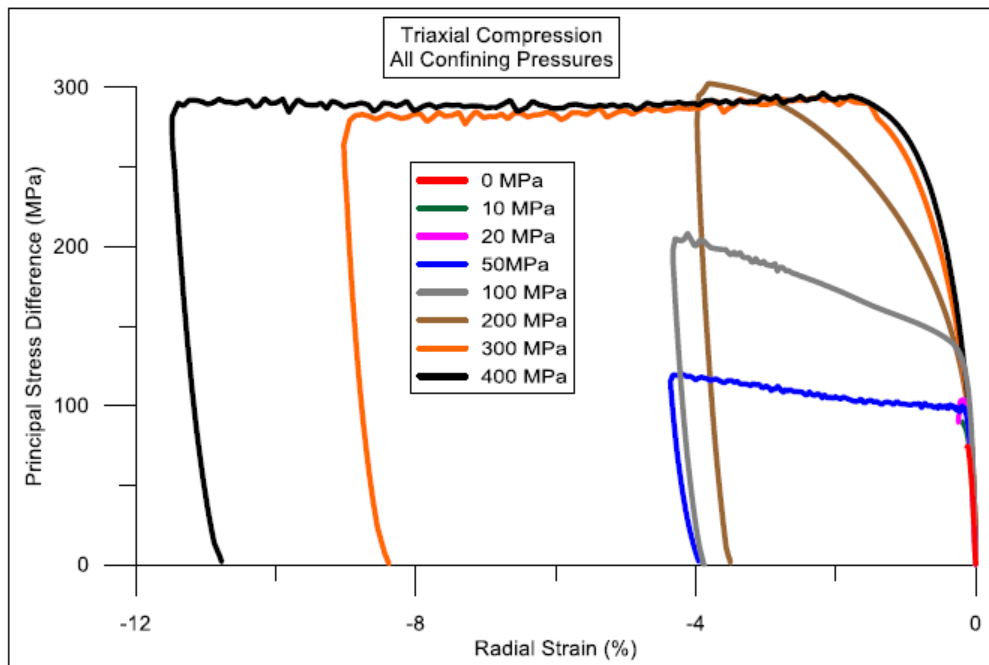


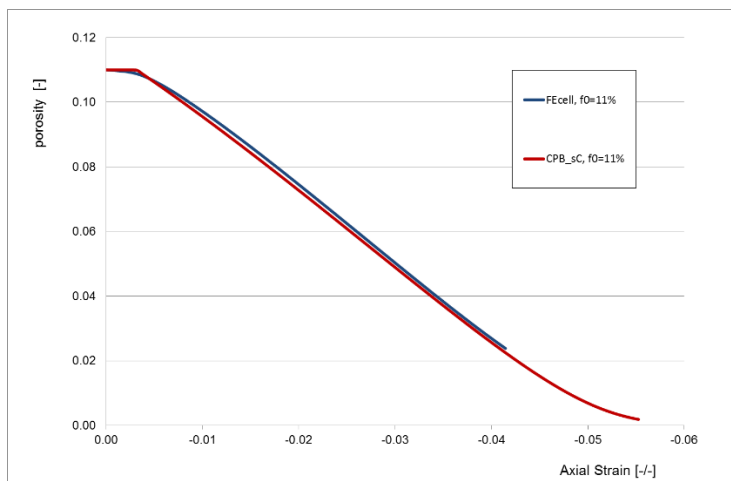
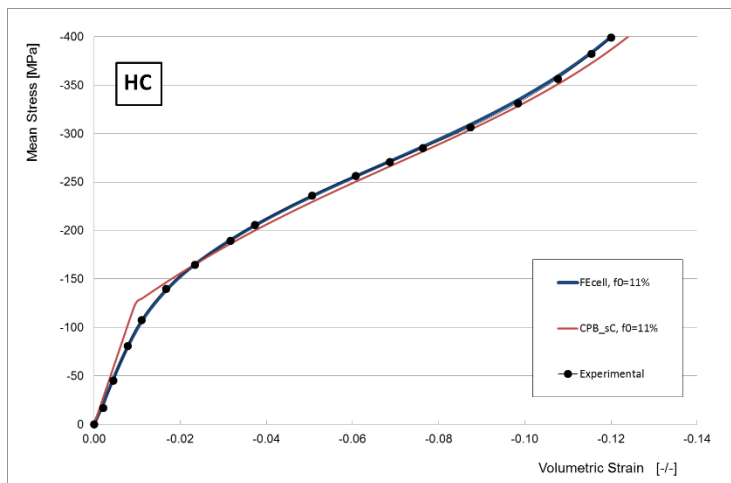
Figure 4.24 TxC: PSD vs radial strain for all confining pressures 0 MPa to 400 MPa

New constitutive and damage model for cementitious materials

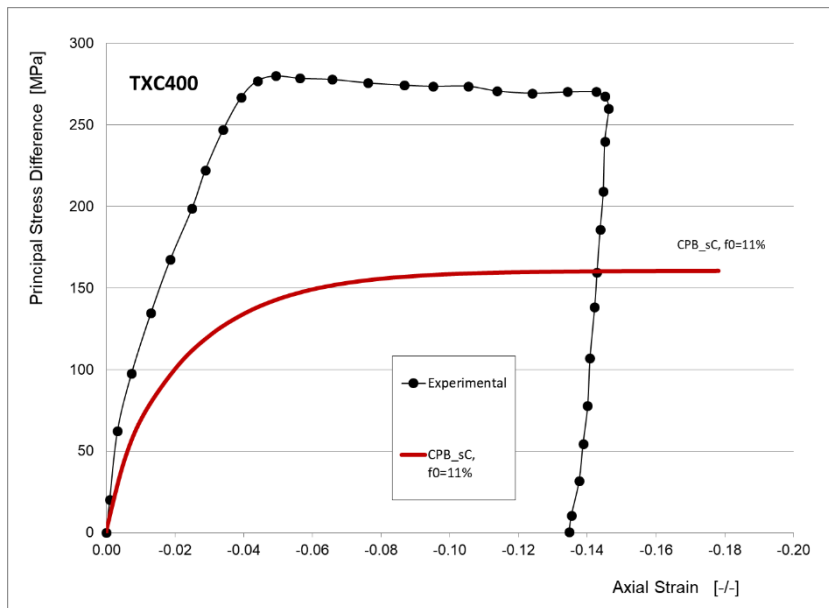
So-far, most state-of-the-art models does not take into account plasticity, and damage and fracture simulation of concrete are basically carried out in a purely elastic framework, with the pressure versus volumetric strain being described by a so-called equation of state (EOS).

First simulations of the hydrostatic compression test (HC) already allow validate the proposed approach, developed under an elasto-plastic framework. The EOS can indeed be replaced by a constitutive equation. However, further developments are yet required.

As example, in what follows is depicted a comparison between experimental results of the HC test with numerical results obtained by an incremental elasto-plastic code considering a porous medium with an asymmetric behavior (yielding in compression much higher than yielding in tension). Initial porosity was taken as 11%, which includes macro and micro porosity.



However, when comparing the experimental and numerical results for the TXC400 loading case, the discrepancy is too large, as shown:

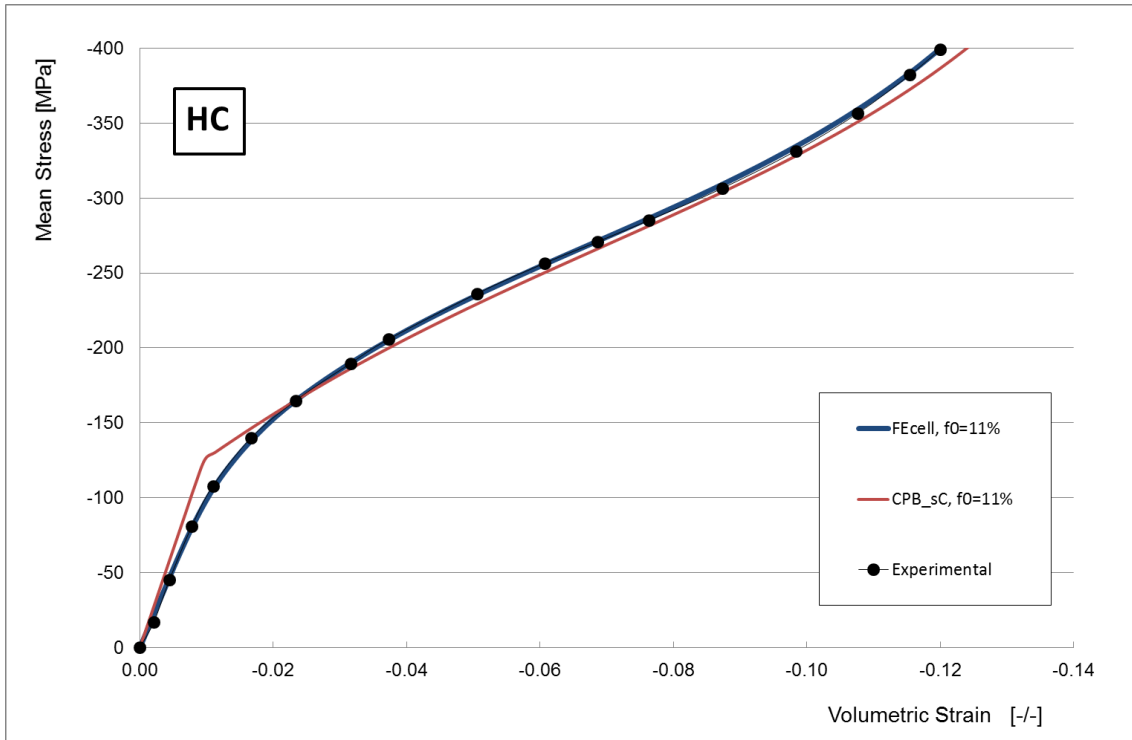


It means that the constitutive model need to be improved, and the accumulated damage taken into account using internal and experimentally meaningful variables.

The idea is thus the reproduction of the HC, TXC and UXC experimental tests, with a new modelling coupling plasticity and damage!

Most of the models published in the literature describe damage on concrete materials based on the definition of a threshold based on the total elastic energy associated with positive elastic strains. A total Lagrangean and purely elastic formulations are commonly adopted, in which the total strain tensor is always well formulated and known. Moreover, the usually seen evolution of the volumetric strain with the hydrostatic pressure is described by a so-called Equation Of State (EOS). However, such experimentally observable phenomenon (the evolution of an inelastic volumetric contraction with a compressive hydrostatic pressure) is clearly associated with the inelastic (plastic) behavior of the materials.

Using a porous model, setting the initial porosity to a value close to the one of the real material, and tuning the hardening parameters, one was able to describe very accurately the volumetric behavior of the concrete under hydrostatic compression, as show in the next figure.



So, assuming that a plasticity model works rather well to replace the EOS approach, remains the modelling of damage.

The mechanical behavior of concretes seems to be coupled by three simultaneous phenomena:

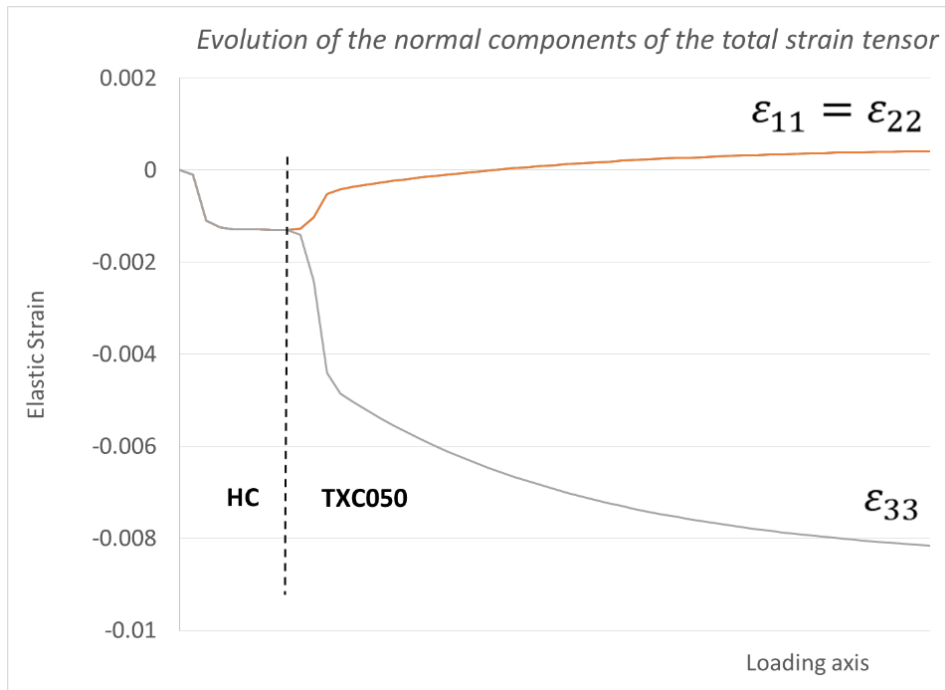
- A) The flow stress driven by the internal friction between particles during plastic deformation, i.e. a dependency of the flow stresses with the hydrostatic pressure;
- B) The damage by crushing; and
- C) The damage by tensile elastic strains.

The new model must address the three abovementioned phenomena / damage mechanisms.

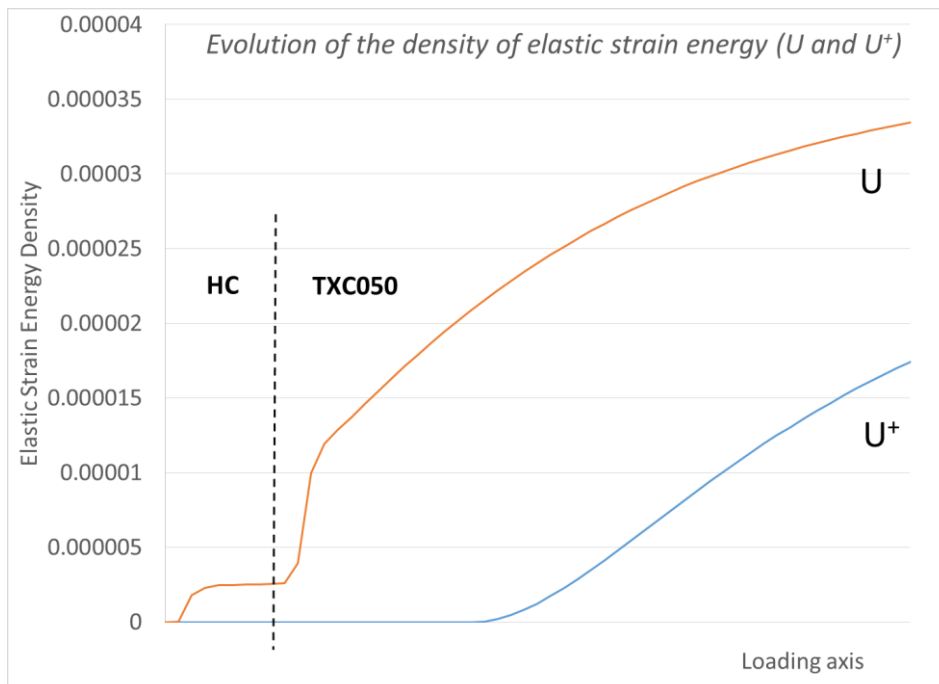
The first question that arises is that, in a plasticity model, due to the formulations in rates, the elastic part of the total strain rate tensor is known, but not the total elastic strain tensor, ϵ^e . To be known, it must be integrated in time, such that:

$$\epsilon^e = \int_t \dot{\epsilon}^e dt, \text{ with } \dot{\epsilon}^e = \dot{\epsilon} - \dot{\epsilon}^p.$$

The following figure shows the evolution of the normal components of the total strain tensor in case of the TXC050 test, i.e. hydrostatic compression up to 50 MPa and then uniaxial compression with a lateral pressure of 50 MPa.



Two other measures were analyzed, $U = \frac{1}{2} \boldsymbol{\epsilon}^e : \mathbf{C}^e : \boldsymbol{\epsilon}^e$ and $U^+ = \frac{1}{2} \langle \boldsymbol{\epsilon}^e \rangle_+ : \mathbf{C}^e : \langle \boldsymbol{\epsilon}^e \rangle_+$



Interestingly, one see that the elastic strain energy associated to the positive components of the total strain tensor becomes non-null at a given point of the loading. A similar behavior can be found in other experimental tests, such as Uniaxial compression (UC) and TXC010, but not in case of UXC and TXC100 and higher.

So, two main ideas will be followed in order to develop the damage model to be implemented

- a) A brittle fracture occurs due to positive magnitudes of the principal strains. Besides, following the work of Cui et al. 2018, the threshold value will be set on the energy, and not on the magnitude of the elastic strains. The stress levels are due to previous crushing-type damage:

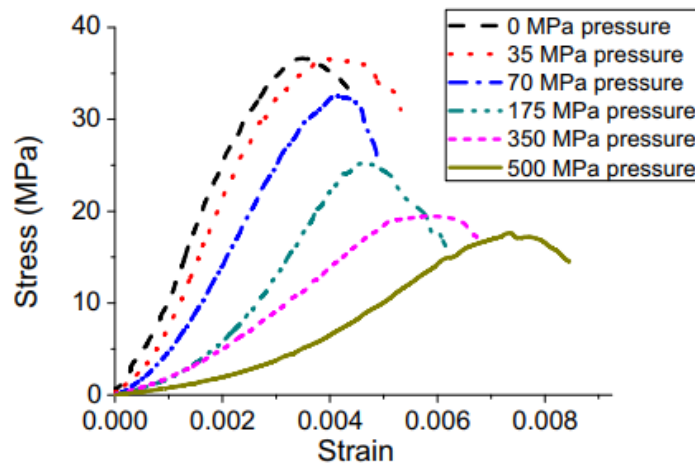


Fig. 2. Compressive stress-strain curve of the specimen after hydrostatic tests.

- b) Crushing-damage is introduced by the volumetric compression of the porous concrete. This damage shall not be taken into account in the compressive bulk modulus (or not?)
- c) Internal friction of the material determines the levels of the observable flow stress.

Damage Variables

D_H – Hydrostatic damage variable

Hydrostatic damage is observable, and can be described as the loss of integrity of the cementitious matrix during the hydrostatic compression.

During compaction, the porosity f decreases, negative (compression) volumetric strain increases, the material plasticizes and hydrostatic must increase, because after a strain path change (e.g. uniaxial compression after hydrostatic compression), the mechanical properties clearly evidence a deterioration.

However, during compaction such deterioration is not detectable, because the material is being mainly loaded in compression, and in this case the bulk modulus increases due to compaction without exhibiting any degradation.

The challenge now is, 1st how to model hydrostatic damage, and 2nd how to eliminate its effect from bulk modulus.

Let us start by decomposing the total strain tensor into volumetric and deviatoric parts,

$$\boldsymbol{\varepsilon}^e = \varepsilon_V^e \mathbf{I} + \boldsymbol{\varepsilon}^{e'}$$

and, associated to such decomposition, also the elastic energy can be decomposed into volumetric and deviatoric parts, such that

$$U = \frac{1}{2} \boldsymbol{\varepsilon}^e : \mathbf{C}^e : \boldsymbol{\varepsilon}^e$$

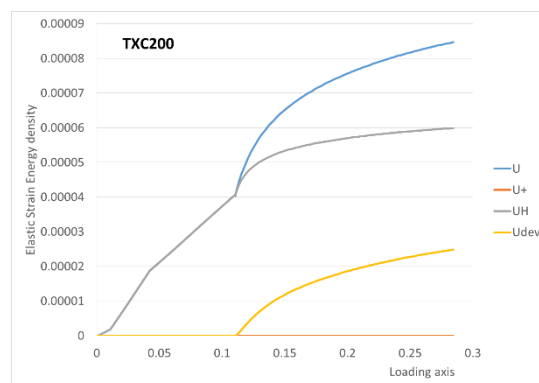
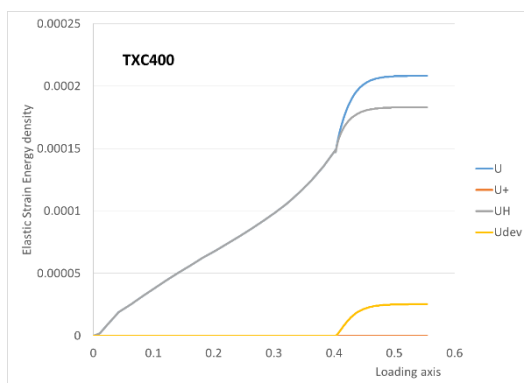
$$U^V = \frac{1}{2} \varepsilon_V^e \mathbf{I} : \mathbf{C}^e : \varepsilon_V^e \mathbf{I}$$

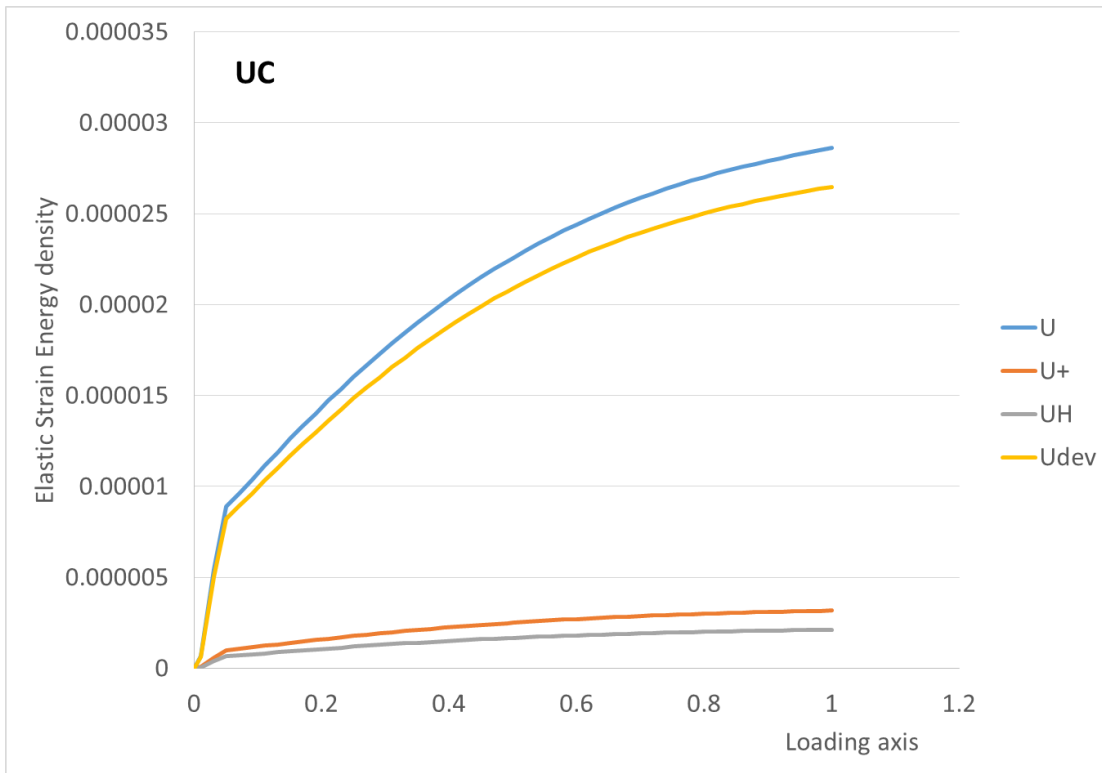
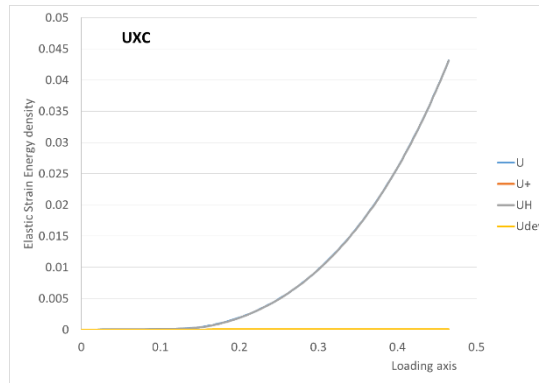
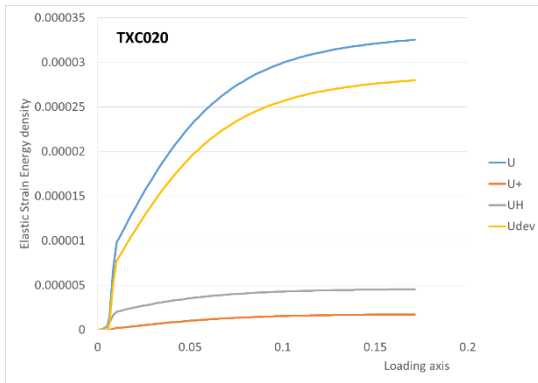
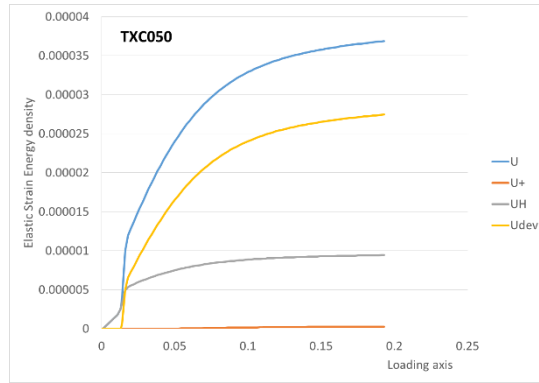
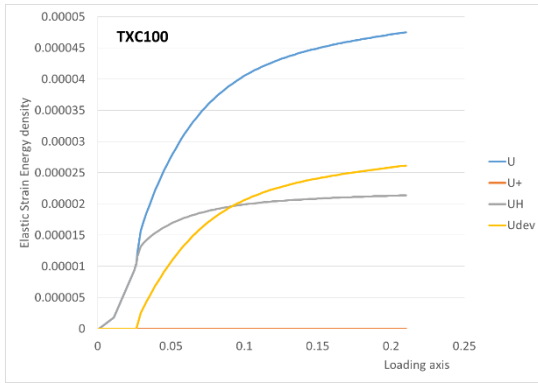
$$U^D = \frac{1}{2} \boldsymbol{\varepsilon}^{e'} : \mathbf{C}^e : \boldsymbol{\varepsilon}^{e'}$$

$$U^+ = \frac{1}{2} \langle \boldsymbol{\varepsilon}^e \rangle_+ : \mathbf{C}^e : \langle \boldsymbol{\varepsilon}^e \rangle_+$$

The volumetric elastic strain energy represents the “cohesive” part of the total elastic energy, while the deviatoric one represents the here called “non-cohesive” part. The larger of these two quantities will play the major role.

Some examples of application are shown in the next figures:





As can be observable, in some cases the deviatoric elastic strain energy becomes larger than the volumetric one, while in other loading can it never occurs.

The evolution of the hydrostatic damage evolves with the concrete crushing. Let us consider the following damage potential,

$$\Psi_H = \varepsilon_V - \varepsilon_V^c,$$

with

$$\Psi_H < 0 \Rightarrow \dot{D}_H = 0$$

$$\Psi_H = 0 \Rightarrow \dot{D}_H > 0$$

$\Psi_H = 0$ is the limit of the non-growing damage domain, and ε_V^c is the present current value for ε_V , that is, for a given material point is the maximum between ε_V ever reached during the loading and the threshold value ε_V^{c0} , i.e.

$$\varepsilon_V^c = \max(\varepsilon_V, \varepsilon_V^{c0}).$$

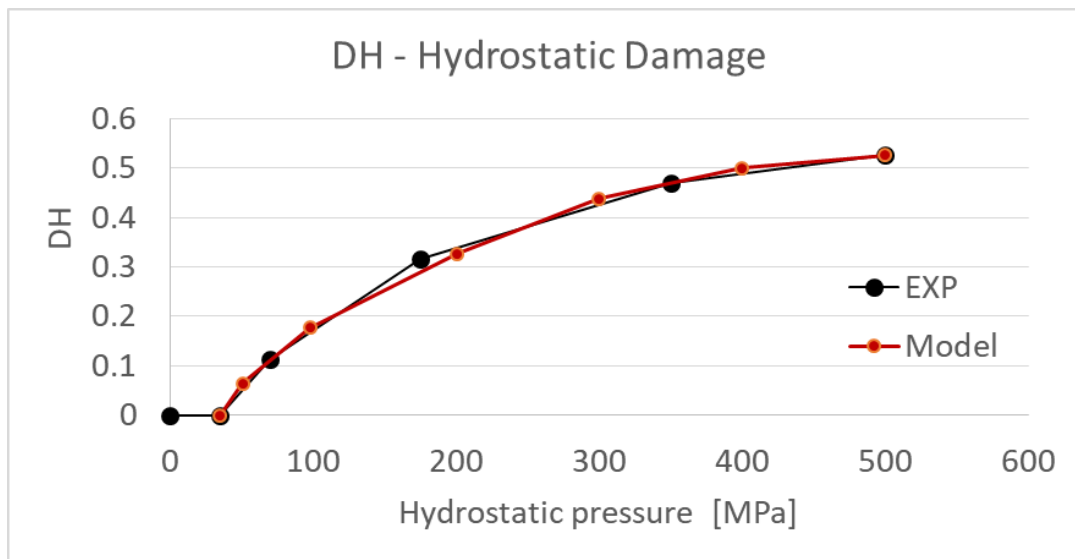
The point here is how the damage variable D_H evolves. The damage model proposed here is based on the following, integrated, equation of evolution of the hydrostatic damage,

$$D_H = f(\varepsilon_V), \quad \text{i.e.} \quad D_H = C_1 \cdot \left(\frac{|\varepsilon_V| - \varepsilon_V^c}{2 \cdot f_0} \right)^{C_2},$$

being ε_V the volumetric strain, f_0 the initial porosity and C_1, C_2 are model parameters. Based on the work of Cui et al. 2018, these parameters were determined taking into consideration the published experimental results, such that:

$$D_H = 0.6 \cdot \left(\frac{|\varepsilon_V| - 0.0038}{2 \cdot f_0} \right)^{0.3},$$

with the following graphical representation:



As depicted in the figure, the hydrostatic damage D_H increases with the volumetric compression due to the hydrostatic pressure.

Damage Variables

D_t – Tensile damage variable

The second damage variable is associated with tensile elastic strains.

The tensile damage potential is defined as

$$\Psi_t = U^+ - U_c^+,$$

being U^+ the elastic strain energy associated to the positive components of the total elastic strain tensor, and U_c^+ is a critical threshold value such that $U_c^+ = \max(U^+, U_{c0}^+)$. Tensile damage evolution law is

$$\Psi_t < 0 \Rightarrow \dot{D}_t = 0$$

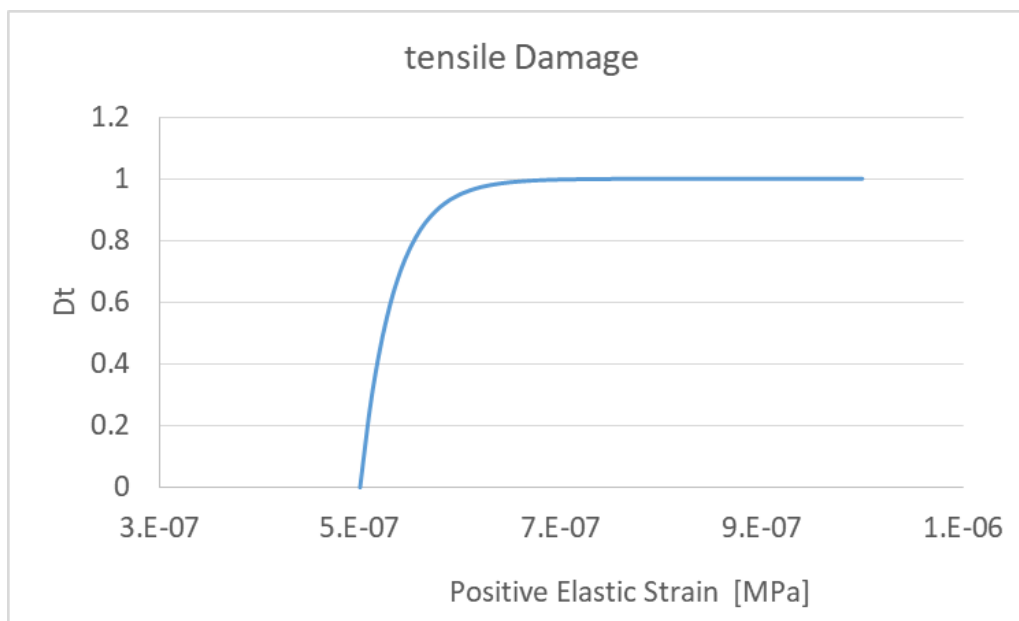
$$\Psi_t = 0 \Rightarrow \dot{D}_t > 0,$$

with the total tensile damage given by the expression, after integration,

$$D_t(U^+) = 1 - \frac{U_{c0}^+(1-A_1)}{U^+} - \frac{A_1}{\exp[B_1(U^+ - U_{c0}^+)]}$$

The following parameters are chosen,

$U_{c0}^+ = 5 \times 10^{-7} \text{ MPa}$, $A_1 = 3 \times 10^7$, $B_1 = 1$, with $D_t(U^+)$ defined as shown in the graphic:



Damage Variables

D – Total Damage

Given that the quantities D_H and D_t are now known, the total damage must be updated.

Let's consider that the total damage can be defined as

$$D = 1 - (1 - D_H)(1 - D_t)$$

As previously shown, depending on the stress loading path, the ratio between U_{vol} and U_{dev} is different.

Because the experimental observation that under a purely compaction loading the material stiffens, with an observable increase of the bulk modulus, we will consider that, if the loading path is predominately of the compaction type, the hydrostatic damage cannot be taken into account.

A loading path is considered ***predominately of the compaction type*** always that the volumetric part of the elastic strain energy density is larger than the deviatoric one, i.e.

$$\text{Compaction if } U^V > U^D.$$

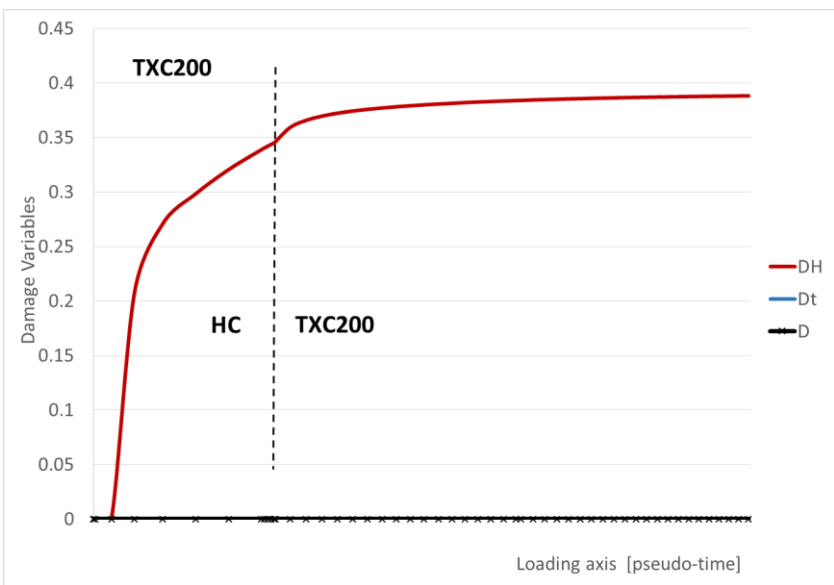
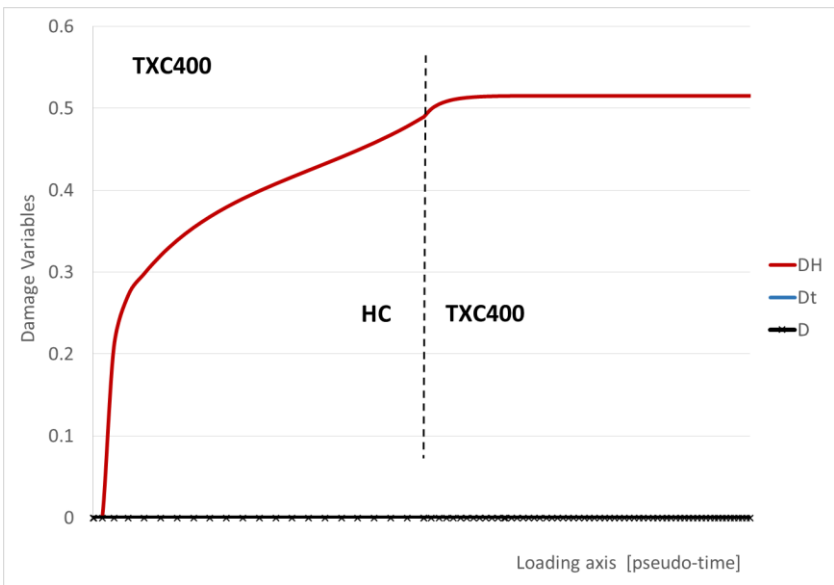
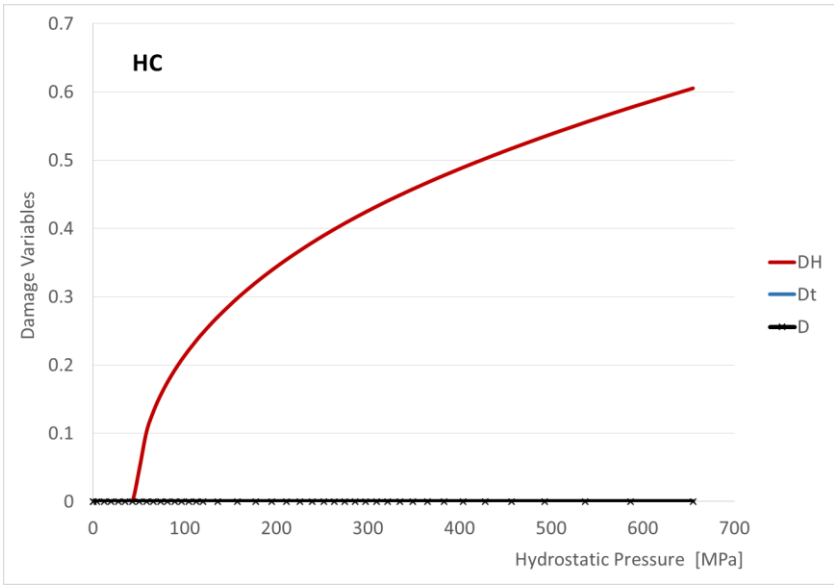
On the other hand, the role of the hydrostatic damage will progressively considered progressively as a function of the following ratio:

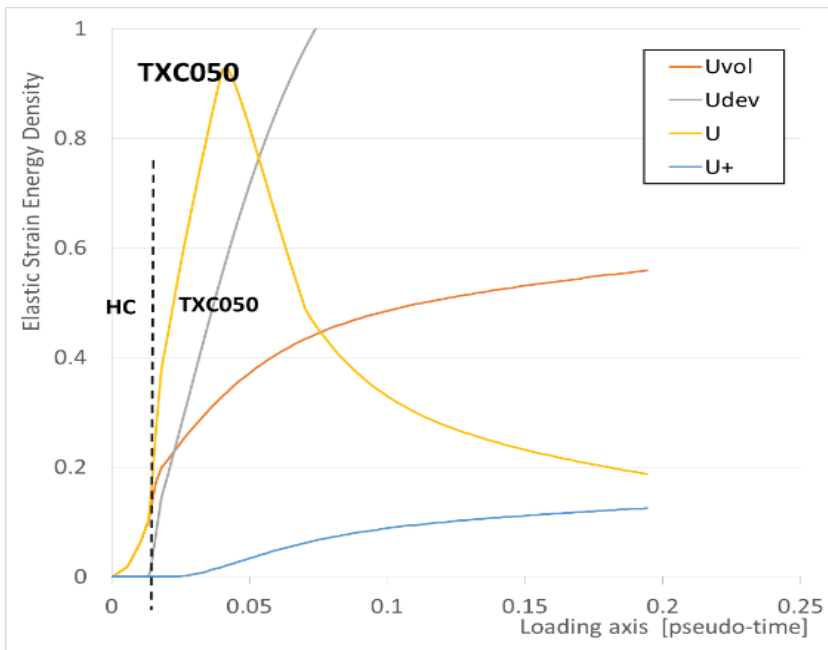
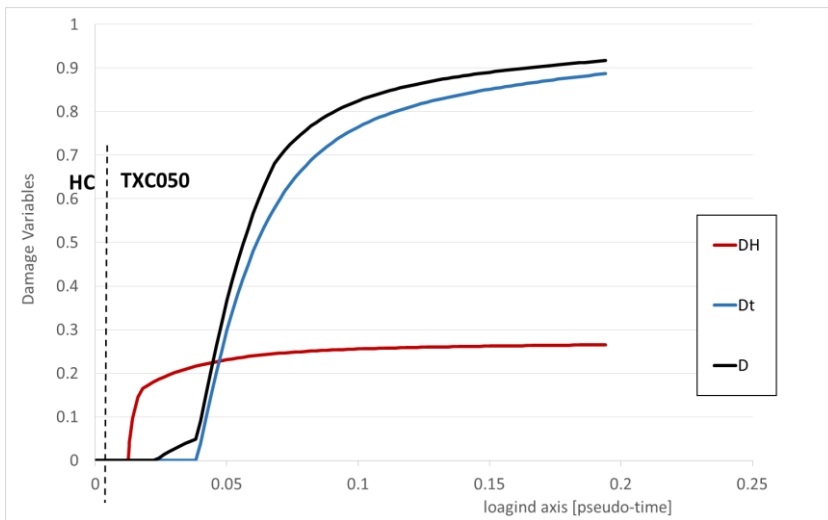
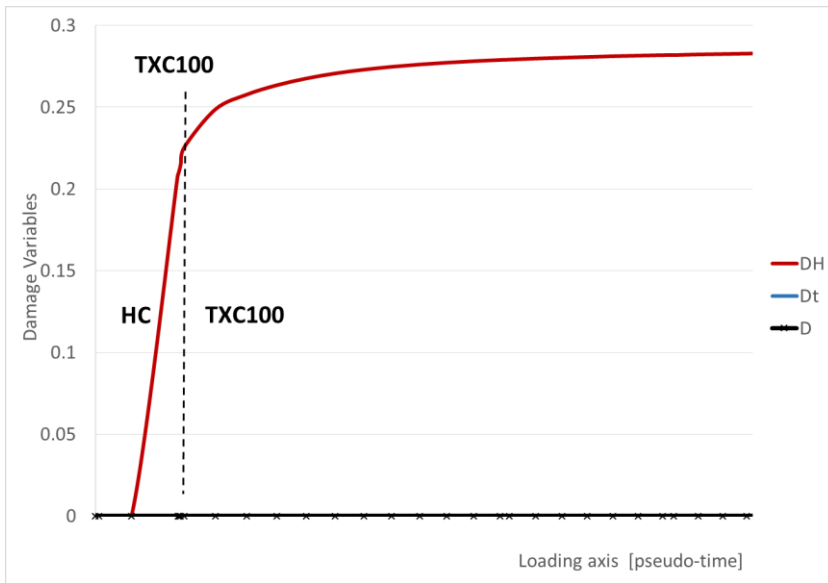
$$D_H = D_H \left\langle \frac{U^D - U^V}{U^T} \right\rangle_+$$

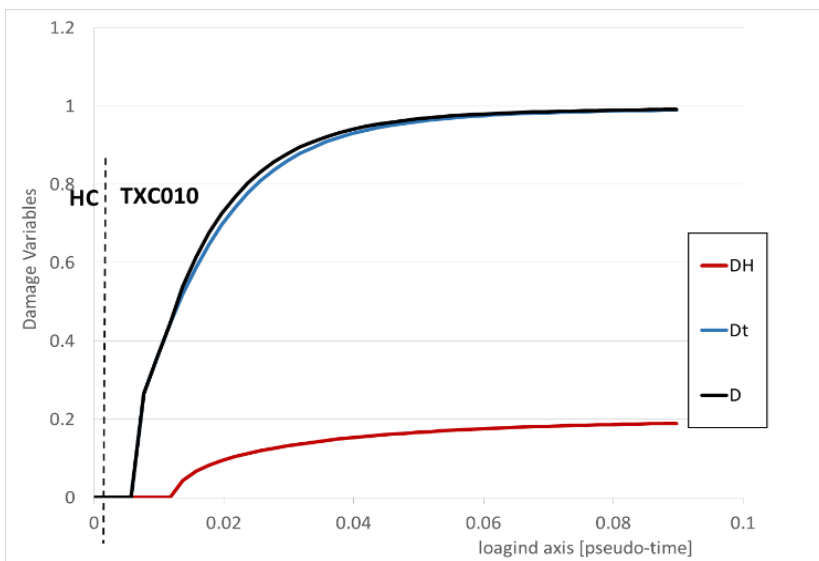
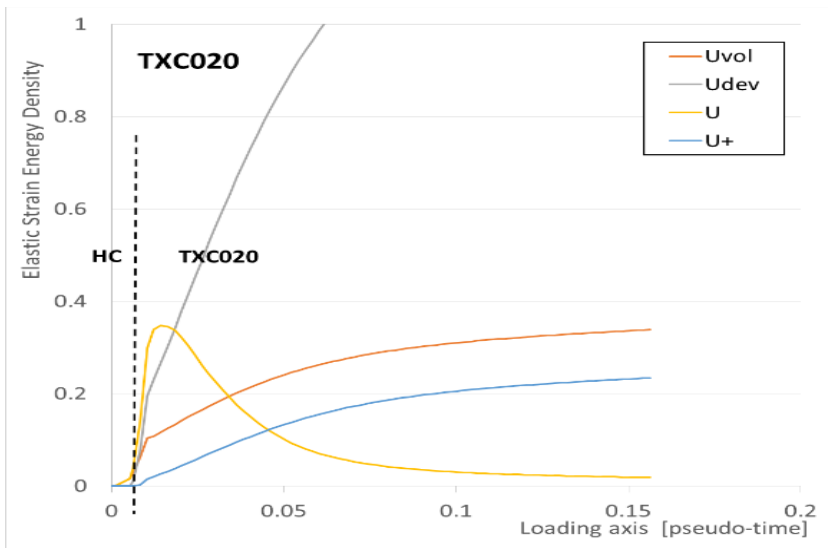
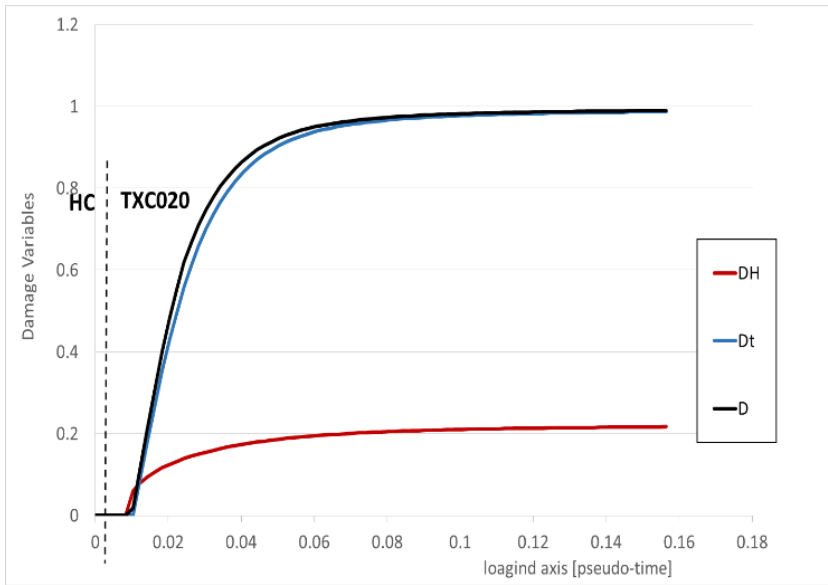
In wat concerns the tensile damage, it is considered directly, as shown in the final expression:

$$D = 1 - \left(1 - \left\langle \frac{U^D - U^V}{U^T} \right\rangle_+ D_H \right) (1 - D_t)$$

Some examples are given in the next figures:







Elastic Properties

Because f is a state variable quantifying the internal porosity, the effective elastic properties can be dependent on it.

So, let us consider that the average elastic properties of the bulk materials are, E_0 and ν_0 , respectively, Young modulus and Poisson ratio.

The effect elastic properties are as follows:

$$E = \left(1 - \frac{5}{3}f\right) E_0, \quad \text{and}$$

$$\nu = \nu_0.$$

This means that the increase of the elastic properties and in particular of the bulk modulus are automatically considered during concrete compaction.

Weakening of the mechanical properties due to damage

After damage accumulation, the (*elastic*) mechanical properties of the material must be decreased.

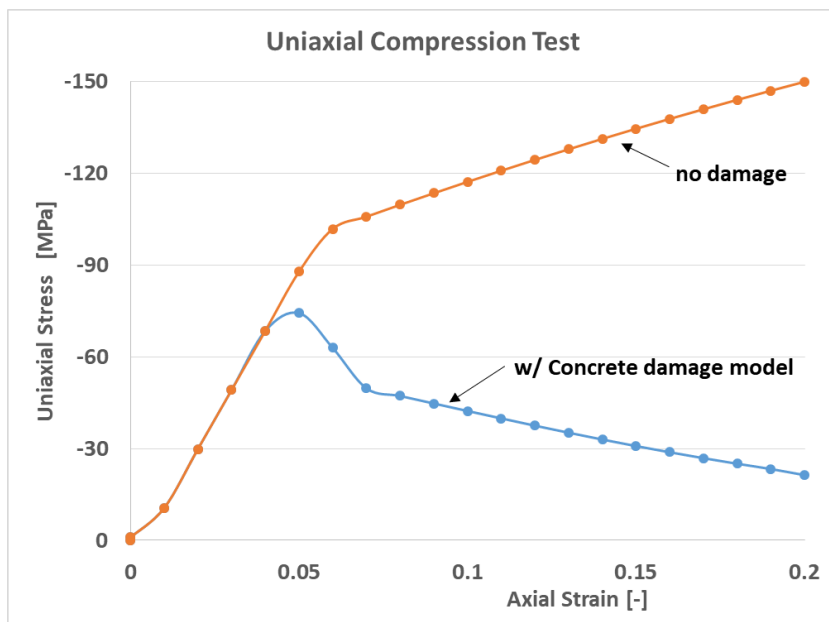
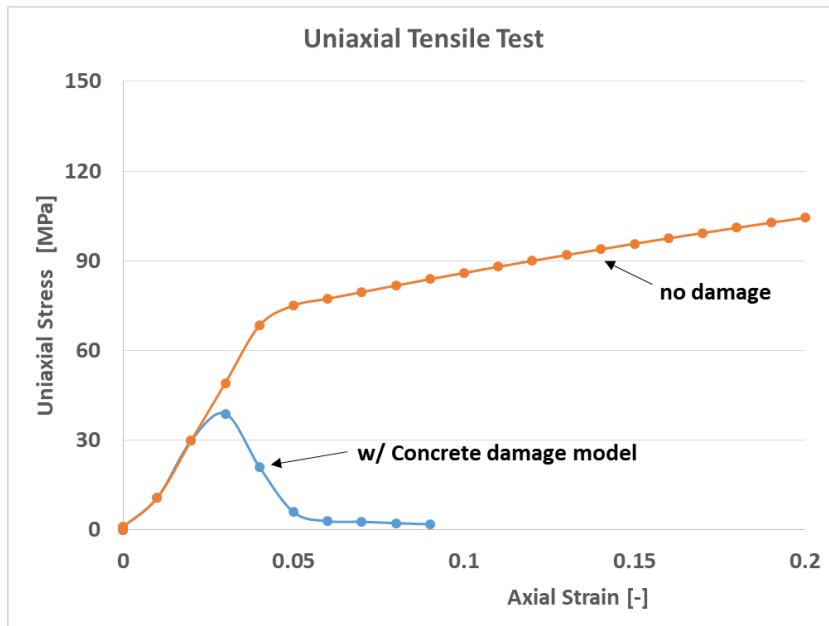
The expression

$$\sigma_{ij}^* = \left(1 - \left\langle \frac{\sigma_m}{|\sigma_m|} \right\rangle D_H\right) \sigma_m I_{ij} + (1 - D) \sigma'_{ij}$$

Is adopted, i.e., the contribution of D_H , hydrostatic damage, only takes place if we have hydrostatic tension, otherwise the material retains the ability of supporting compaction resistance, i.e. the unilateral effects (opening and closure of the micro cracks) of the damage.

Behavior of the model under Uniaxial Compression and Uniaxial Tension

In the following figures is shown the behavior of the model when simulating the classical uniaxial tension and compression tests, with the evolution of damage variables activated.

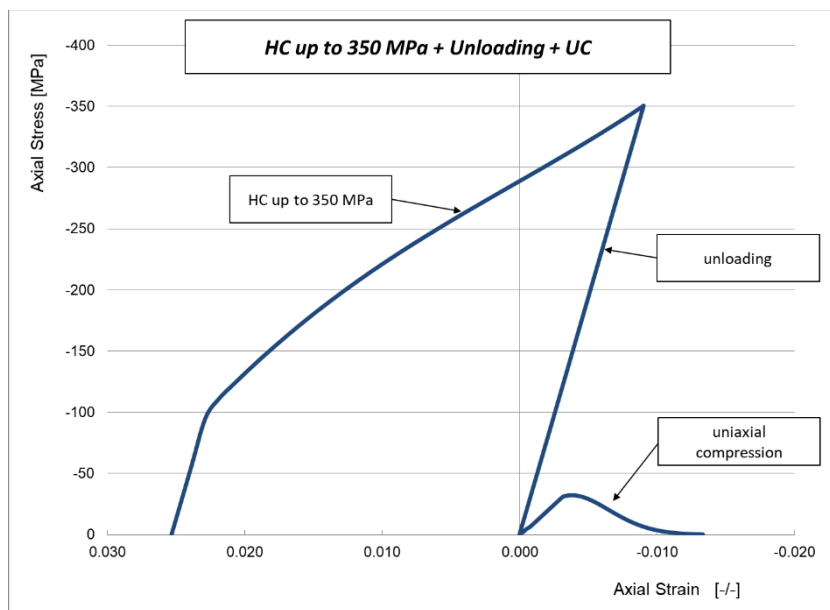


Behavior of the model under multiple loadings (HC followed by UC)

In what follows it will be shown a few results about the behavior of the model under two sequential loadings, namely:

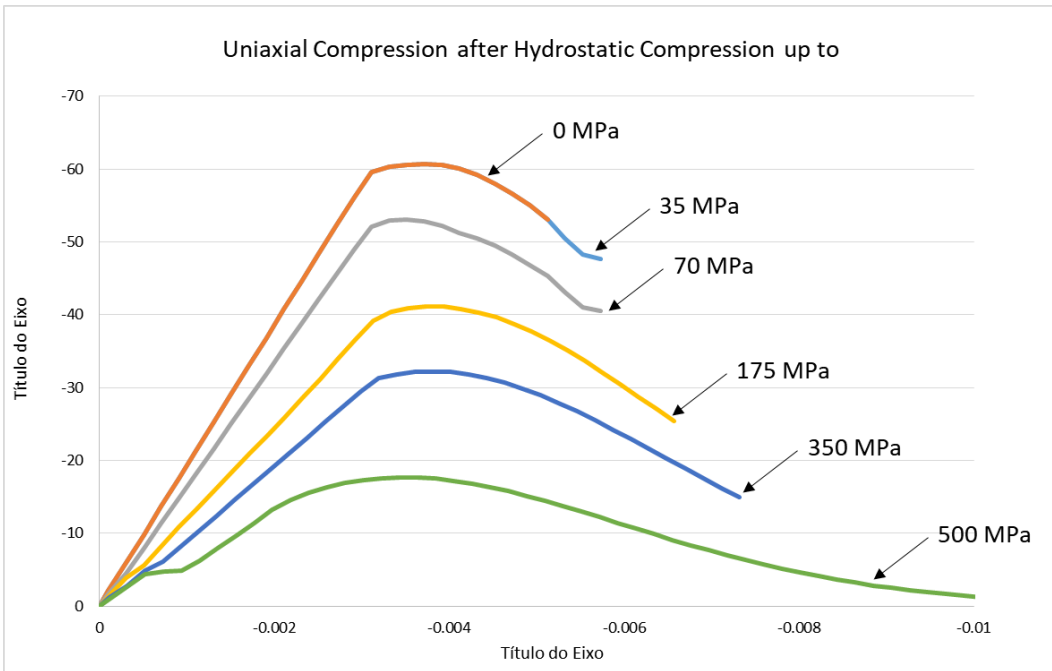
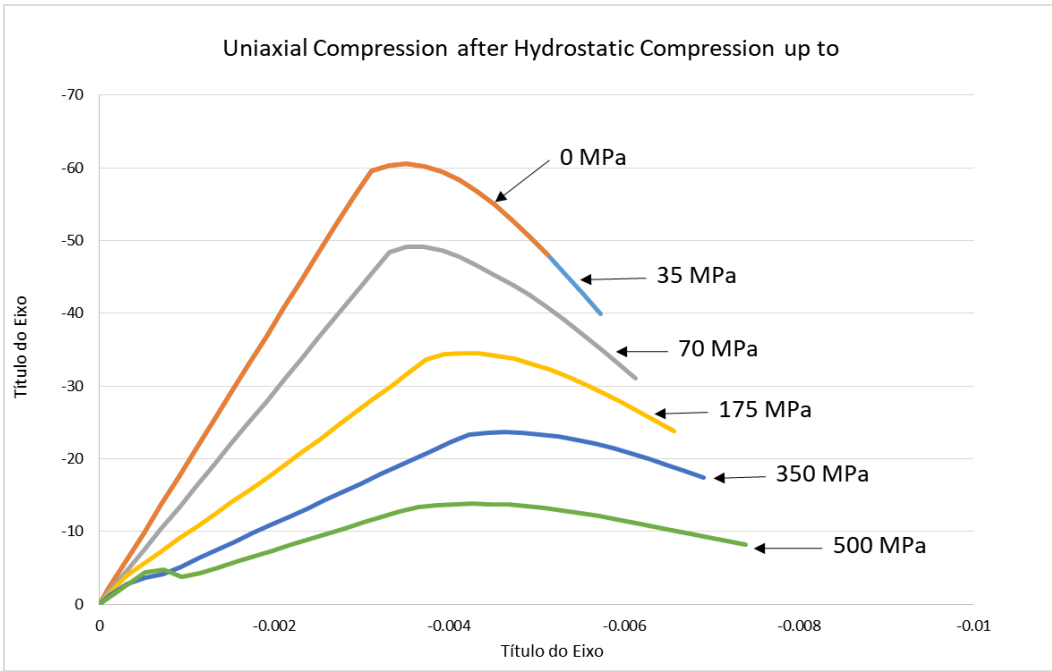
- HC – hydrostatic compression up to a predefined value of hydrostatic pressure
- Unloading of the hydrostatic pressure up to zero stress
- UC – reloading under uniaxial compression conditions.

Next figure shows the results of the axial stress strain versus axial strain for all tests, considering a hydrostatic compression of 350 MPa



Between loadings, the material preserves the memory and history in terms of either plasticity or damage variables. Other multiple loadings paths are possible, but the model must be calibrated with more accurate parameters.

As shown in the paper of Cui et al. 2018, next figure shows the comparison between the axial stress versus axial strain curves corresponding to only the uniaxial compression phase after several preconditioning hydrostatic pressures, namely 0, 35, 70, 175, 350 and 500 MPa.



Chapter 4

In this chapter are shown some results concerning the comparison between experimental and numerical results.

The question is “Which is the mechanical response of the porous concrete?”

Several hypotheses are hereafter considered and simulated using the RVE:

- elastic
- elasto-plastic
- elasto-plastic with a matrix displaying microporosity
- elasto-plastic, with the concrete obeying to the new MACROSCOPIC model briefly introduced in chapter3.

Information concerning the behavior of concrete / constituents is needed:

- matrix
- “aggregates”

However,

which is the correct amount of porosity to be considered in the simulation?

In fact, **a cementitious material must have more porosity than it apparently shows, or can be measurable from macro voids.**

And why such conclusion? Because taken into consideration Heard’s data on “Total Porosity”, we were not able to reproduce the HC test using a FE cell.

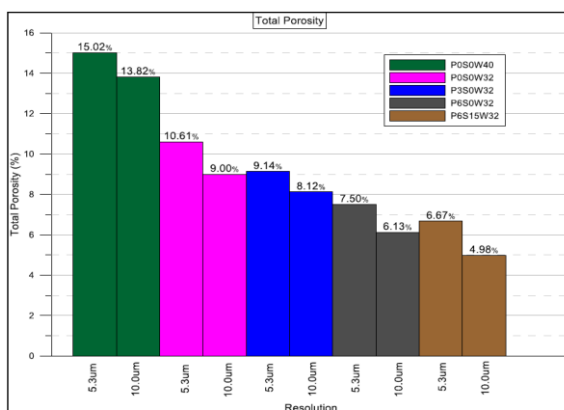
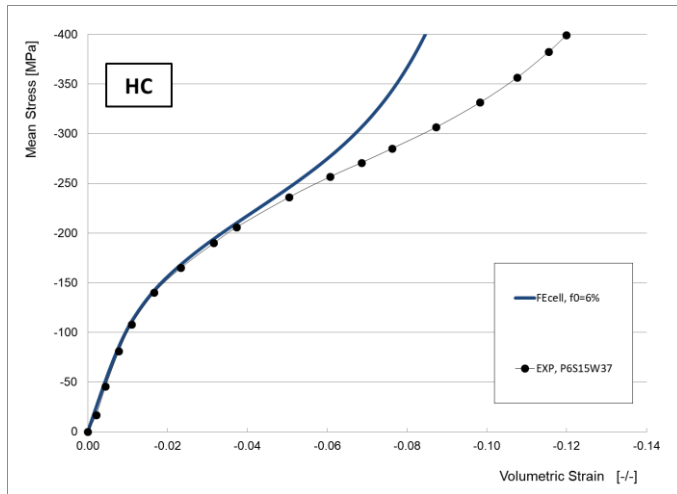


Figure 3.15 Total porosity for mix PxS0W32, P0S0W40 and P6SW32

(See title of the chart, “Total Porosity”)

The so-called P6S15W37 concrete display about 4% to 5% of initial porosity. Considering an initial porosity of ca. 6%, the following results were obtained:

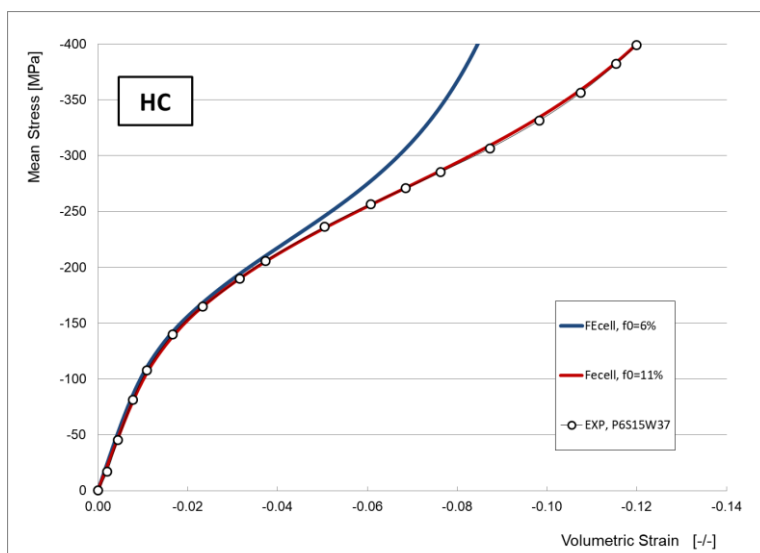


i.e., the volumetric strain is not compatible with the initially measured porosity of ca. 6%, what means that the total porosity that the material indeed has must be higher than the macroscopically observable and measurable.

By inverse analysis and using the HC test, we can obtain a good estimate of the total effect porosity.

The total porosity is given by the sum of two components,

- a) The macroporosity
- b) The microporosity



Main conclusion:

an initial porosity of 11%, i.e. 6% macro + 5% microporosity can fit very well the experimental results!

Mechanical response of the concrete

Which is the mechanical response of the porous concrete?

Several hypothesis are hereafter considered and simulated using the RVE:

1. **elastic**
2. **elasto-plastic**
3. elasto-plastic with a matrix displaying **microporosity**
4. elasto-plastic, with the concrete obeying to a **new MACROSCOPIC model** proposed

Information concerning the behavior of concrete / constituents is needed:

- matrix
- “aggregates”

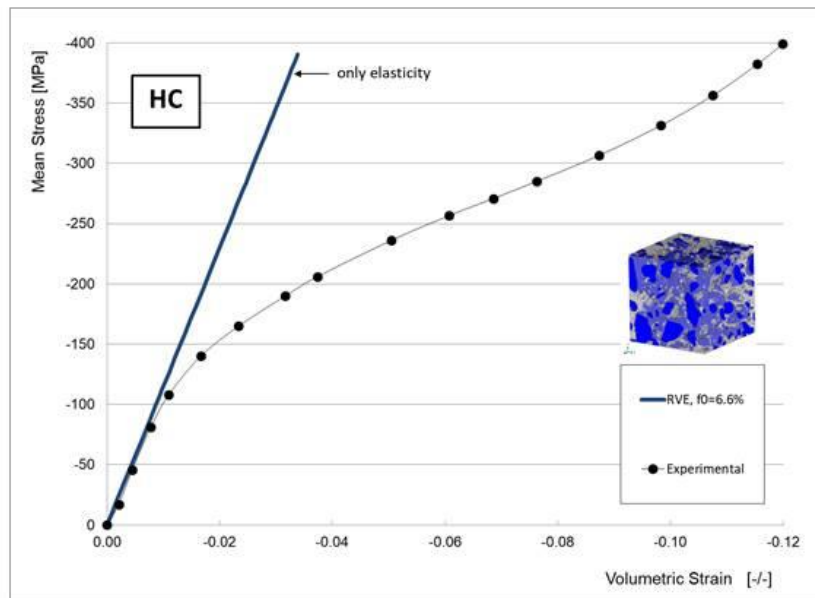
FE simulation of the overall response (1)

To obtain the response of the concrete,
we need to have information concerning the behavior of constituents:

- matrix
- “aggregates”

if elastic behavior

Such information is not available !



If the matrix is elastic:

Matrix:

- Young modulus = 16.5 GPa
- Poisson ratio = 0.18

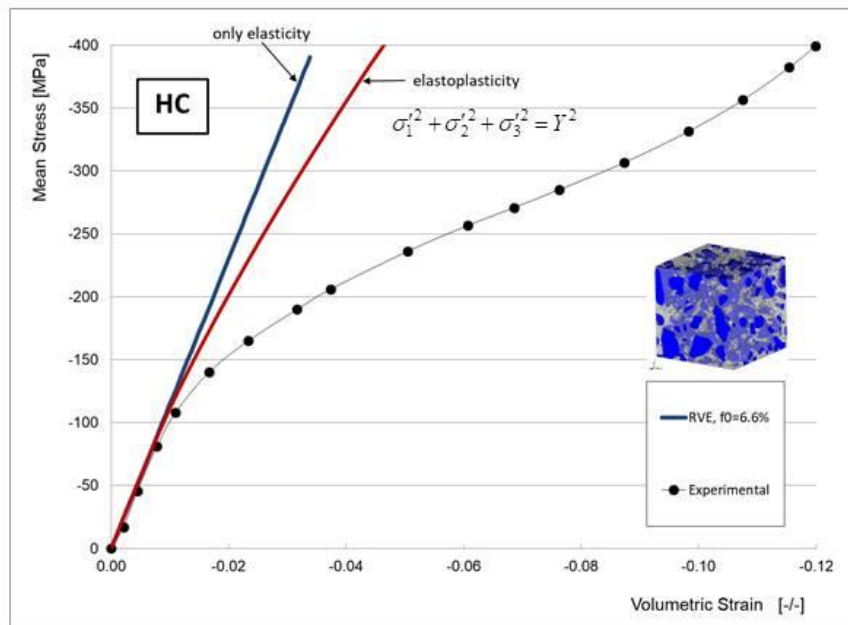
Aggregates: (\approx almost rigid)

- Young modulus = 33.0 GPa
- Poisson ratio = 0.33

FE simulation of the concrete response (2)

Constituents have **elasto-plastic behavior**:
Matrix: von Mises yield criterion

if elasto-plastic behavior



Plastic Properties

Matrix:

- $Y_0 = 65$ MPa
- $Y_{sat} = 160$ MPa

Aggregates:

- $Y_0 = 265$ MPa
- $Y_{sat} = 360$ MPa

- Yielding: yield surface

Remark: matrix and aggregates are assumed as fully dense materials, thus $f_0=6.6\%$.

→ *New model for the matrix:
energy-type criterion
key idea: to account for difference in dissipated energy
between compression and tension*

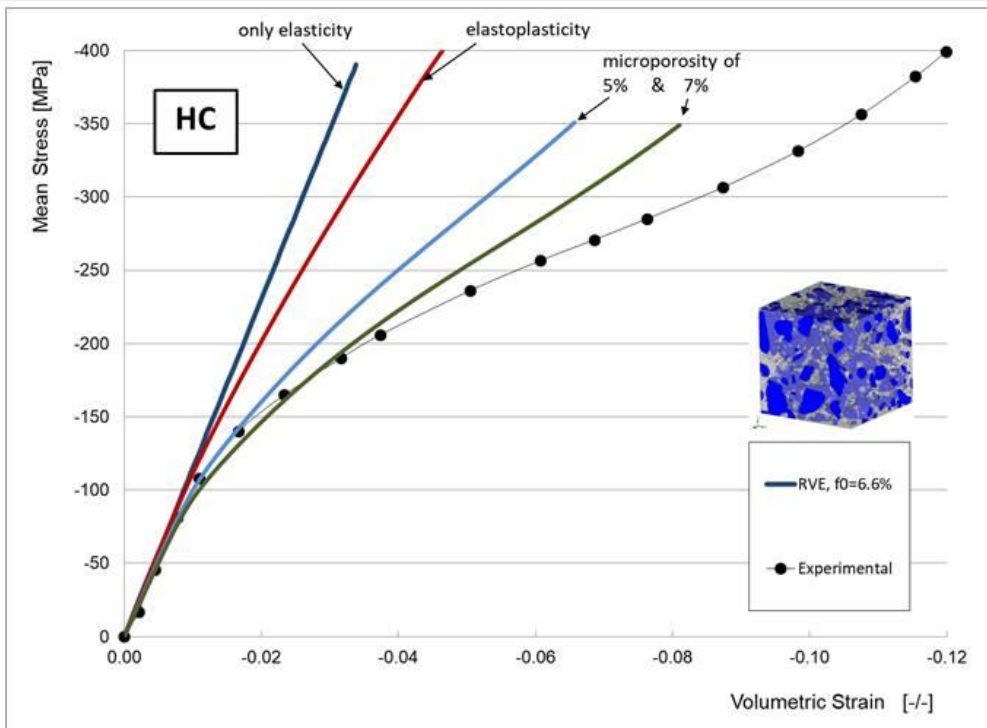
Proposed model for the matrix:

- (1) Isotropic
- (2) Dissipation: in compression completely different than in tension,
⇒ Need to modify von Mises criterion $\sigma_1'^2 + \sigma_2'^2 + \sigma_3'^2 = Y^2$



New criterion for concretes to be implemented and calibrated !!!

→ Perform new multi-scale simulations, including micro-porosity, macro-porosity and energy-based criterion for matrix



if elasto-plastic behavior with micro-porosity

Matrix (*new model*):

- $f_0 = 5\% \text{ \& } 7\%$

Aggregates:

- $f_0 = 0.1\%$

- Overall porosities of **10.2% and 11.6%**

Amount of porosity "required" taking into account the experimental results. Macroporosity is not enough.

→ *New criterion for the concrete*

If micro-porosity is “hidden” in the matrix => effect of pressure on the onset of plastic deformation of the matrix

Elasto-plastic behavior depends on both stress deviator σ' and mean stress σ_m , and the state of initial damage (or porosity) f in the material:

New *MACROSCOPIC* Model for the Matrix:

$$\longrightarrow \boxed{\varphi = \varphi(\sigma', p, f)}$$

$$p(\sigma) = -\sigma_m = -\frac{1}{3}\sigma : \mathbf{I}$$

α, m, A – model parameters

→ *Application of new model*

Heard's PhD experimental data on HC, UXC and TXC loadings

New porous yield surface developed to model the behavior of homogeneous porous and isotropic cementitious materials

Total porosity of 11%

Elastic properties (taken from Heard's thesis) of

- Young modulus = 23.6 Gpa
- Poisson ratio = 0.25

Plastic properties

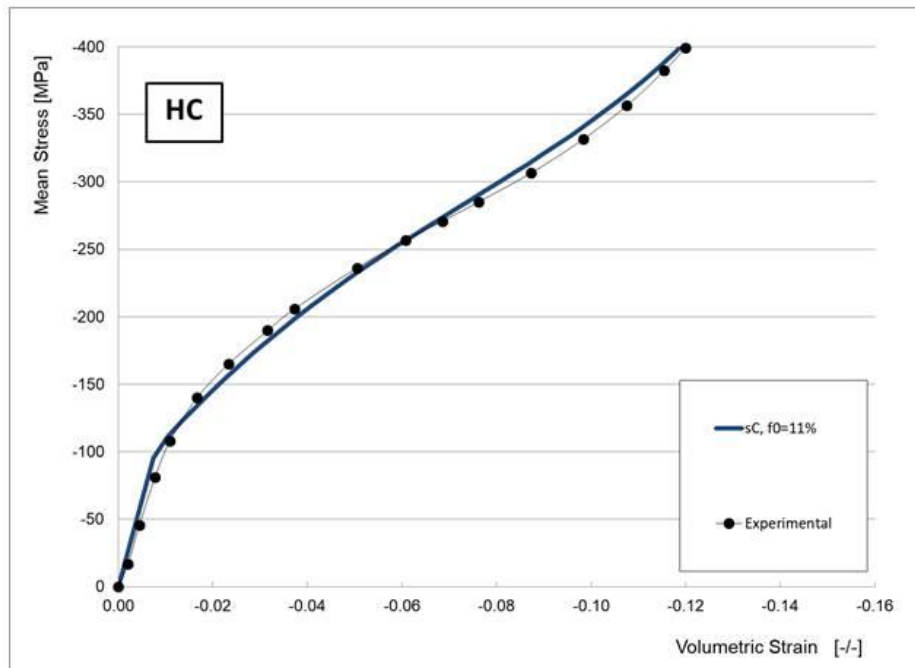
- $Y_0=85$ Mpa
- $Y_{sat}=200$ MPa

Yielding:

- **New model**
- $m=1.0$
- $a=$

→ example of application of sC model

HC loading

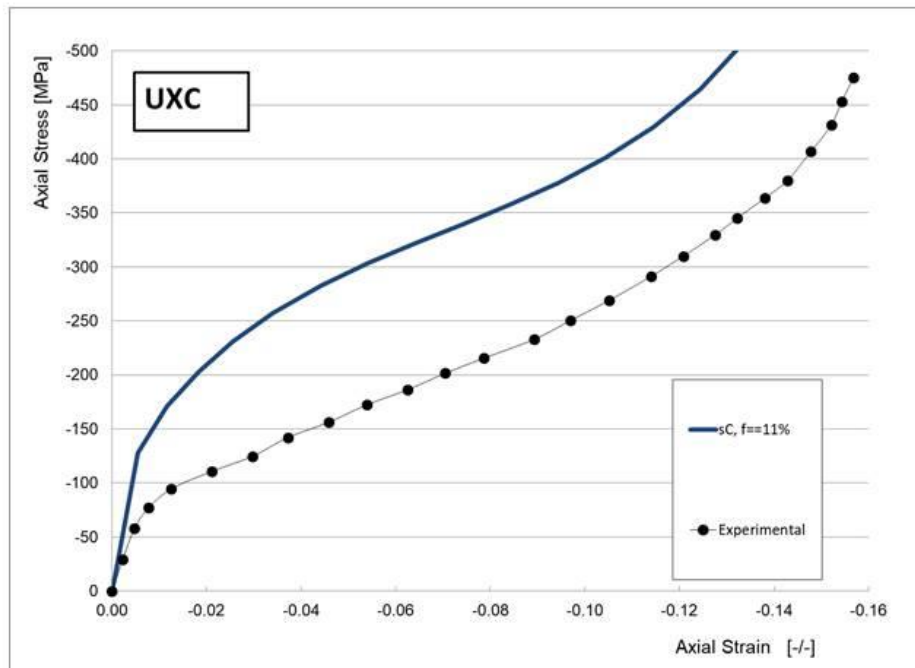


Example of application of the new model, coupling *micro* and *macro* porosity. Mechanical properties of the phases where determined by inverse analysis from the TXC400 loading.

← Evolution of the volumetric strain with the hydrostatic stress very well captured, no need of the Equation Of State (EOS)

→ example of application of sC model

UXC loading

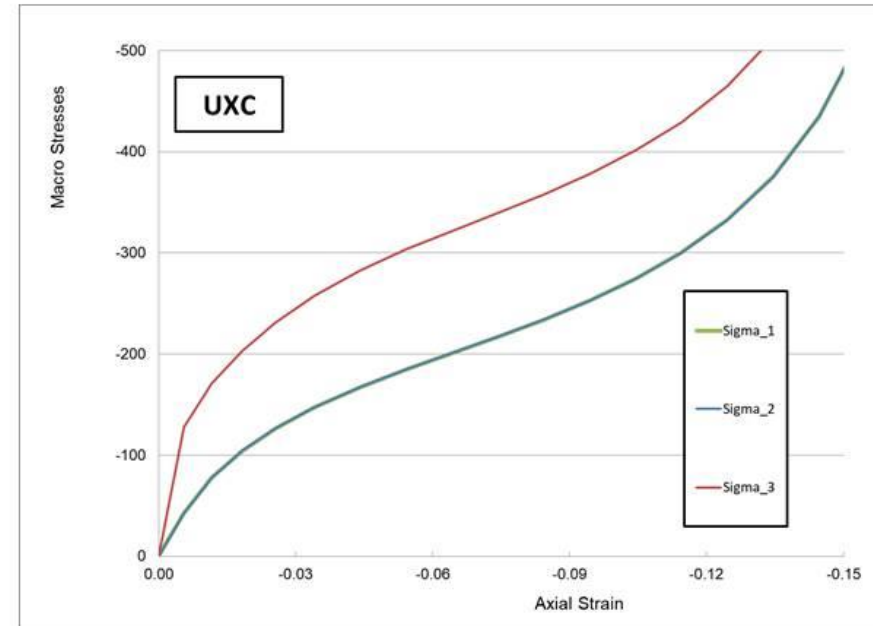
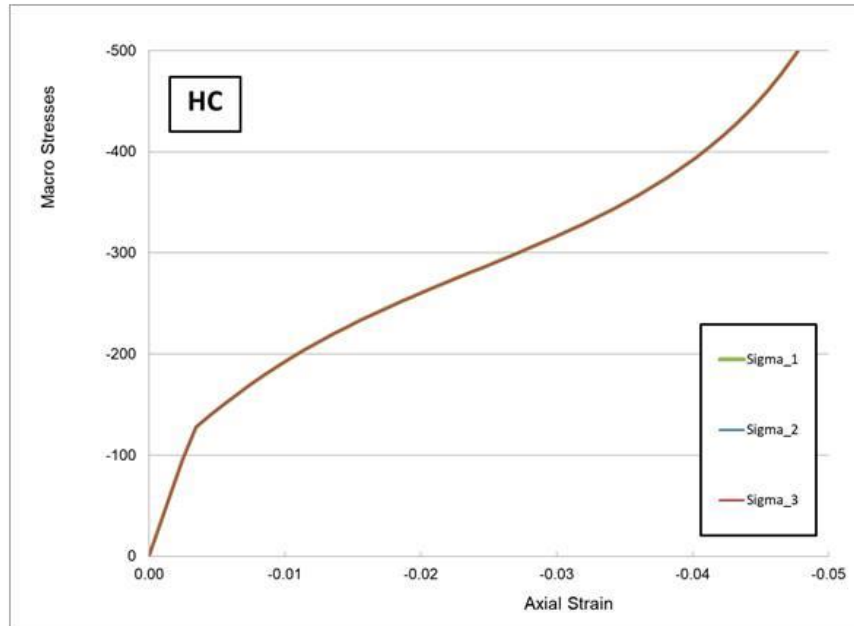


UXC result added.

I am not sure about the experimental results, because experimentally we can see a big difference between HC and UXC loading, but numerically not. In fact, in terms of stress states, they are very similar. The interpretation of these results deserves some more attention in the future...

→ example of application of *sC* model

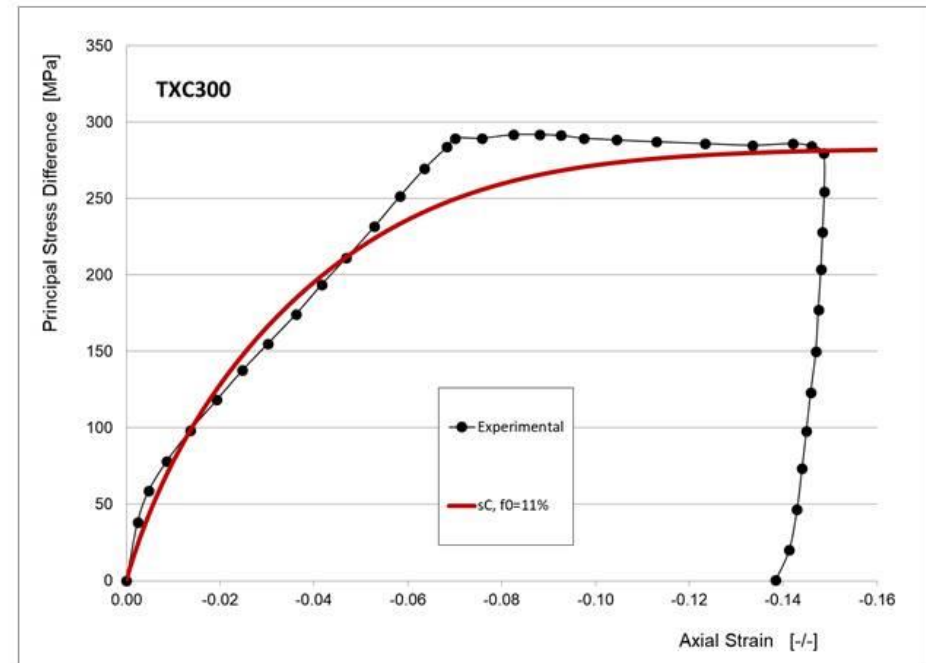
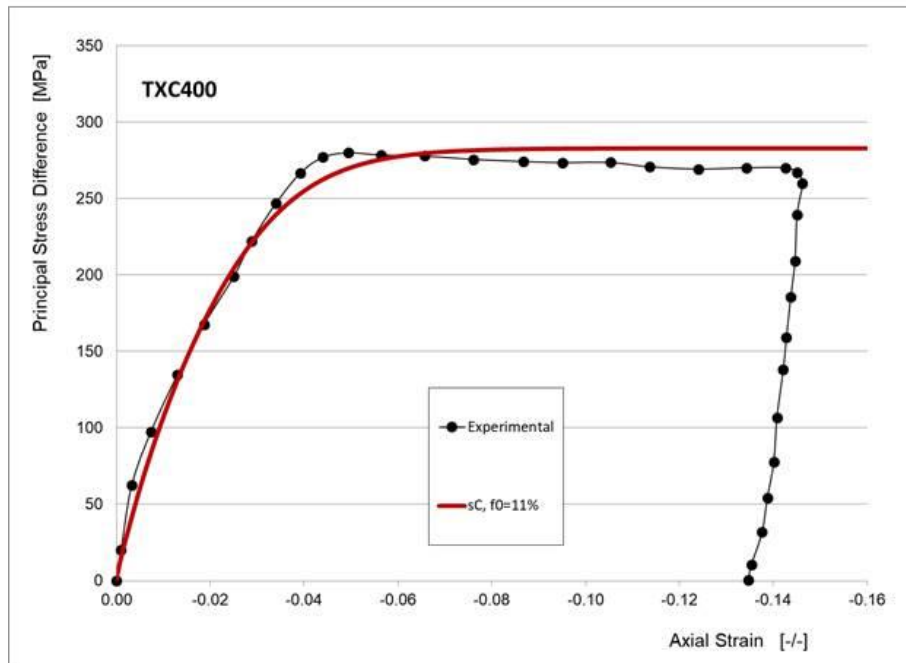
HC vs UXC stress states



Comment: the behavior is mainly being determined by the volumetric part. The role of the volumetric one remains to be understood...

→ *example of application of sC model*

TXC loadings



→ *example of application of sC model*

Preliminary conclusions:

Excellent behavior of the new model for high confining pressures

What about lower pressures ?

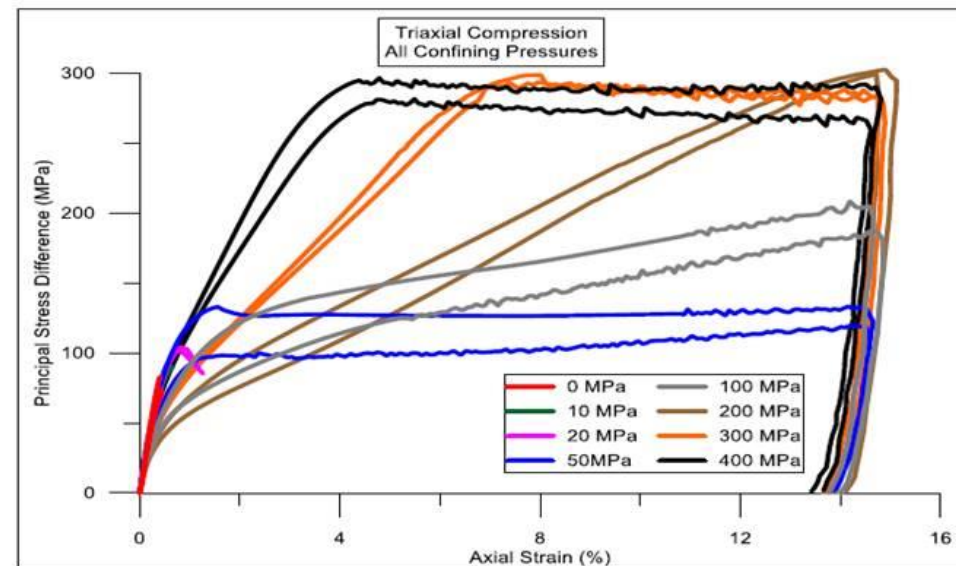
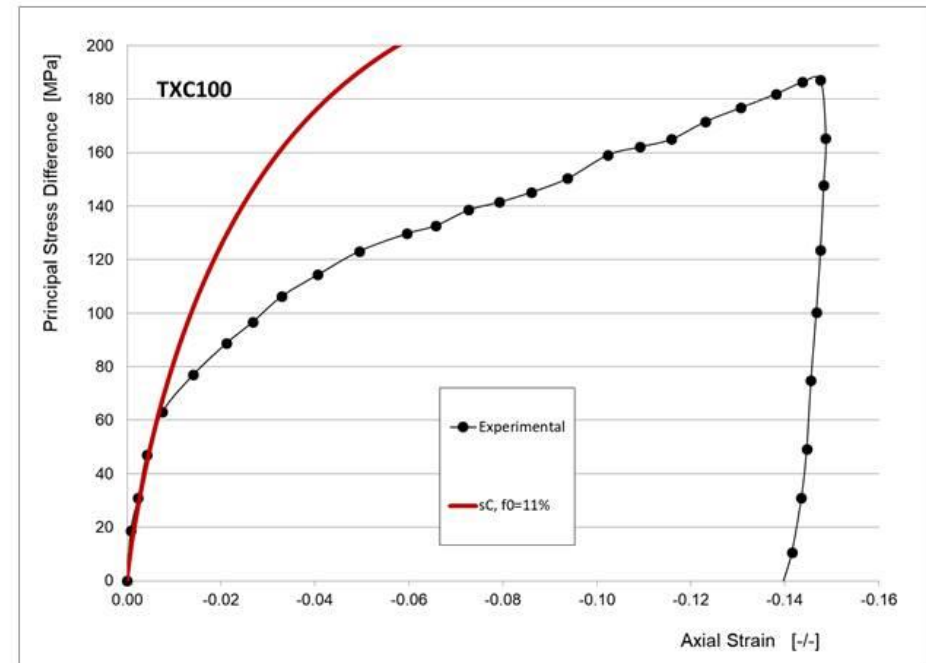
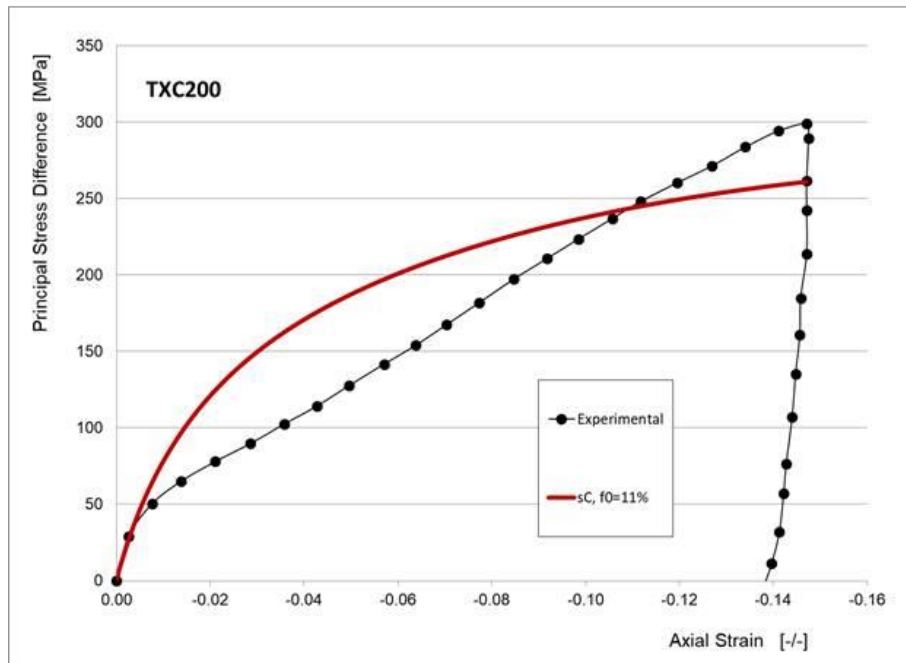


Figure 4.22 TXC: PSD vs axial strain for all confining pressures 0 MPa to 400 MPa

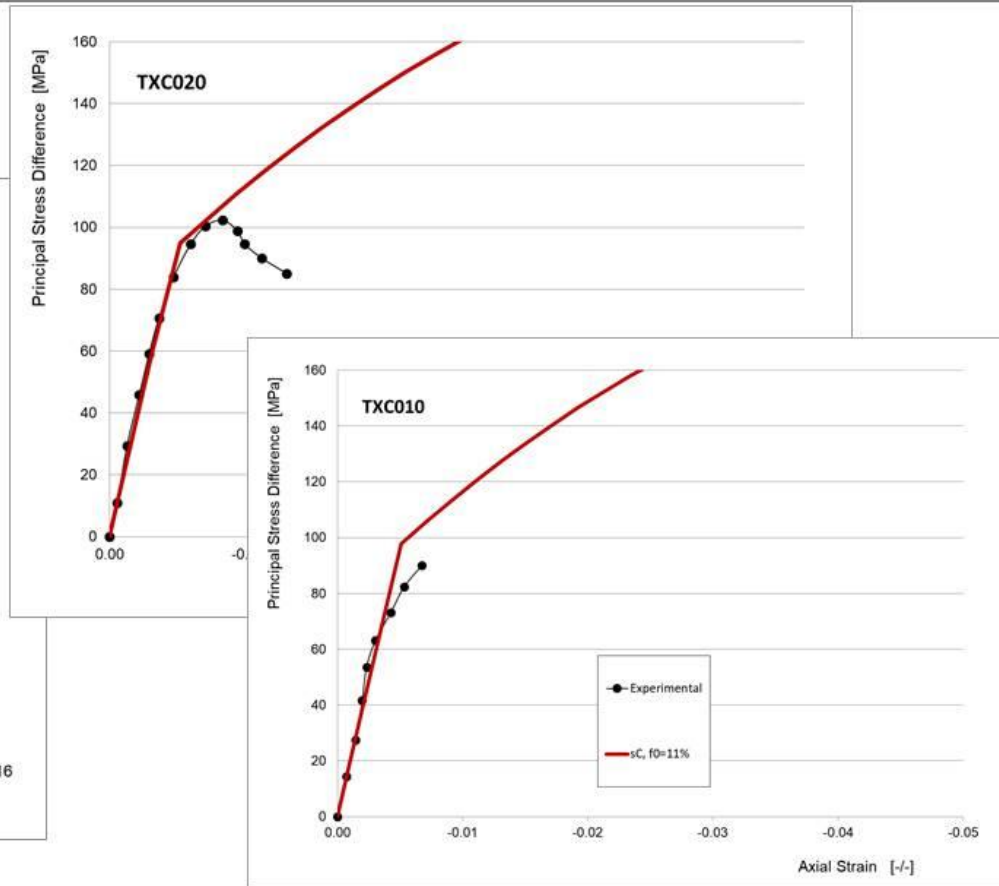
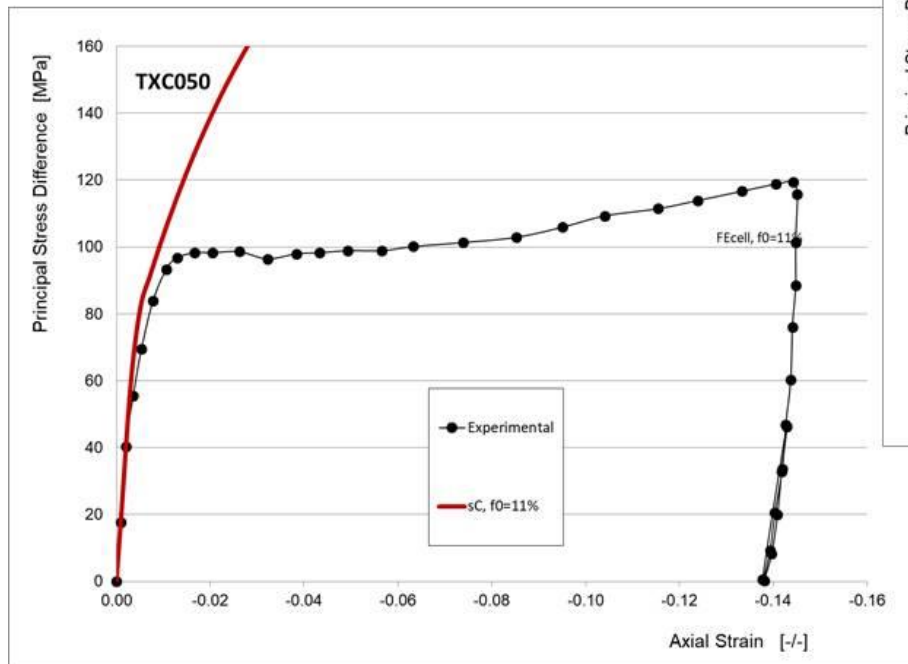
→ *example of application of sC model*

TXC loadings



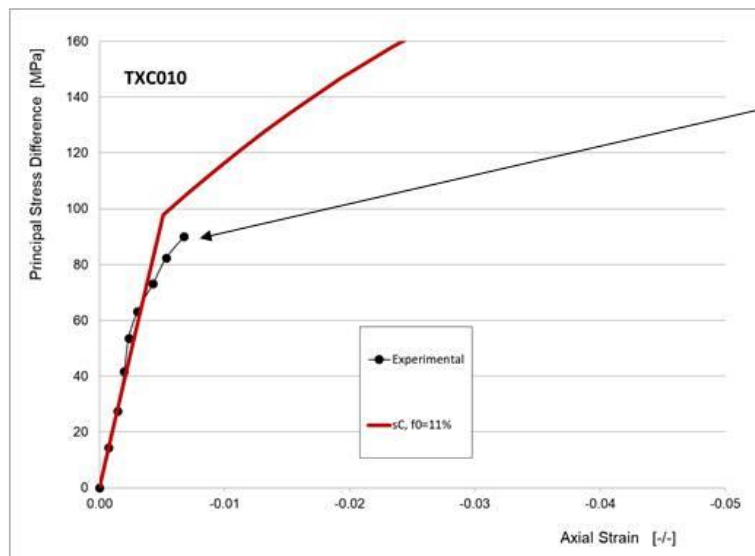
→ example of application of sC model

TXC loadings



→ damage modelling

Example of TXC010 loading:



Fracture !!!

Only a damage model can improve the numerical results obtained by a homogeneous isotropic porous elasto-plastic behavior

Need to include internal variables associated with damage/fracture:

⇒ *elasto-plastic behavior +*

⇒ *damage dependent on loading path and history*

→ ideas for damage modelling

Develop a coupled damage-plasticity model

How to model damage of the constituents?

-Fracture of cementitious materials is basically due to **positive strains** and **volumetric crushing**

Damage model (DM) should be able to describe sequential loadings:

take into account damage and plasticity history

However,

most damage models proposed in literature:

- are based on positive elastic strains;
ok, but we believe that it must be based on different measures of the density of elastic energy
- are based on only elastic strains (plasticity is not taken into account);
- are based on the total elastic strain tensor;
- evolution of the volumetric strain with the hydrostatic pressure is described by an Equation Of State (EOS)

Main ideas:

- **Brittle fracture occurs due to positive magnitudes of the principal strains, and**
- **Crushing-damage is introduced by the volumetric compression of the porous concrete.**

→ *damage modelling*

1st, no need of the **EOS**:

- Shear and volumetric effects are coupled;
- As previously shown, a porous model, setting the initial total porosity to a value close to the one of the real material, and tuning the hardening parameters, can describe very accurately the volumetric behavior of the concrete under hydrostatic compression.

2nd, the mechanical behavior of concretes seems to be coupled by three simultaneous phenomena:

- the **onset of plastic deformation** driven by the internal friction between particles, sensitive to the state of porosity, **DONE**
- the **damage by crushing**; and
- the **damage by tensile elastic strains** (opening of cracks).

The new coupled plasticity-damage constitutive model must address all the above-mentioned phenomena / damage mechanisms, preserving the history of both plasticity (permanent deformations) and damage.

Ultimate goal: to be able to describe/model sequential strikes...

→ damage modelling

elastic strain tensor determined incrementally,

$$\boldsymbol{\varepsilon}^e = \int_t \dot{\boldsymbol{\varepsilon}}^e dt, \text{ with } \dot{\boldsymbol{\varepsilon}}^e = \dot{\boldsymbol{\varepsilon}} - \dot{\boldsymbol{\varepsilon}}^p$$

$$\boldsymbol{\varepsilon}^e = \varepsilon_V^e \mathbf{I} + \boldsymbol{\varepsilon}^{e'}$$

Density of elastic energy measures,

$$U = \frac{1}{2} \boldsymbol{\varepsilon}^e : \mathbf{C}^e : \boldsymbol{\varepsilon}^e$$

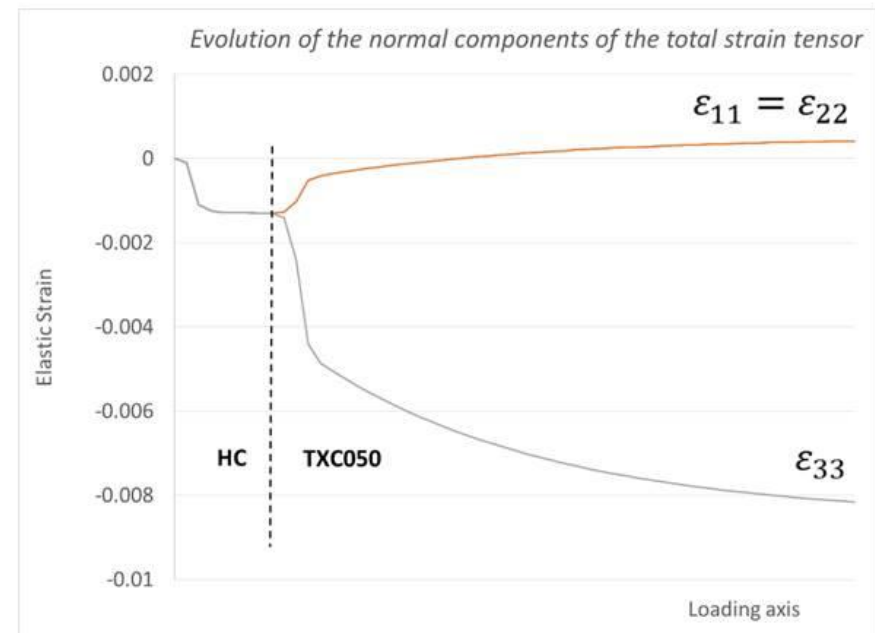
$$U^V = \frac{1}{2} \varepsilon_V^e \mathbf{I} : \mathbf{C}^e : \varepsilon_V^e \mathbf{I}$$

$$U^D = \frac{1}{2} \boldsymbol{\varepsilon}^{e'} : \mathbf{C}^e : \boldsymbol{\varepsilon}^{e'}$$

$$U^+ = \frac{1}{2} \langle \boldsymbol{\varepsilon}^e \rangle_+ : \mathbf{C}^e : \langle \boldsymbol{\varepsilon}^e \rangle_+$$

isotropic damage variables,

- D_H – Hydrostatic damage variable
- D_t – Tensile damage variable
- D – Total damage



→ damage modelling

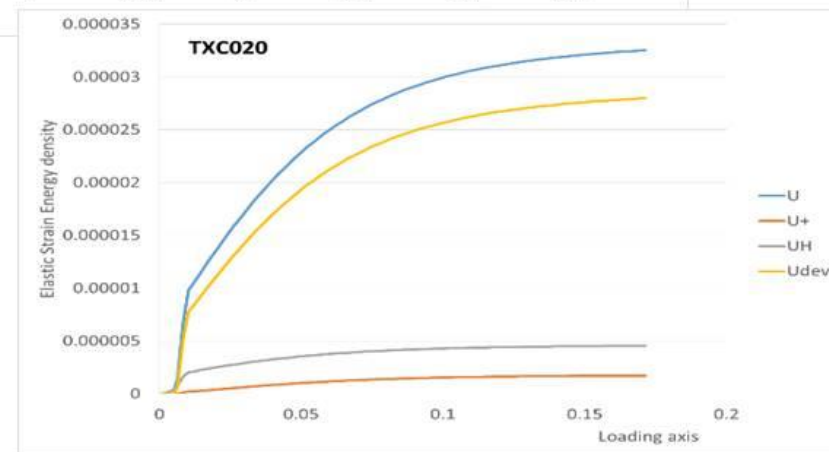
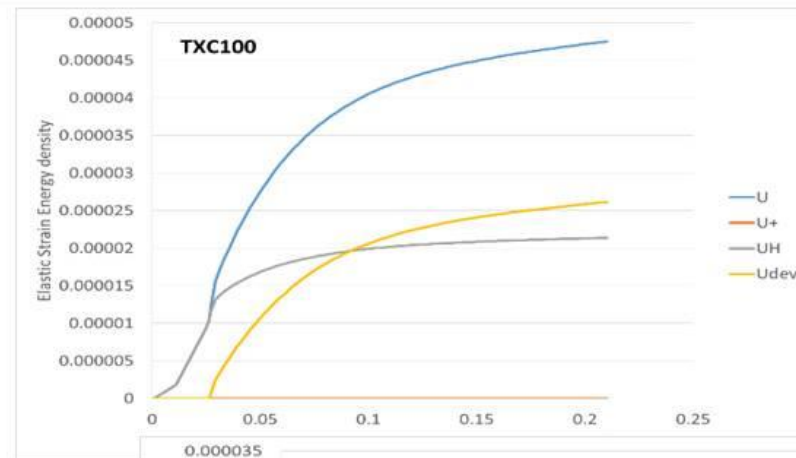
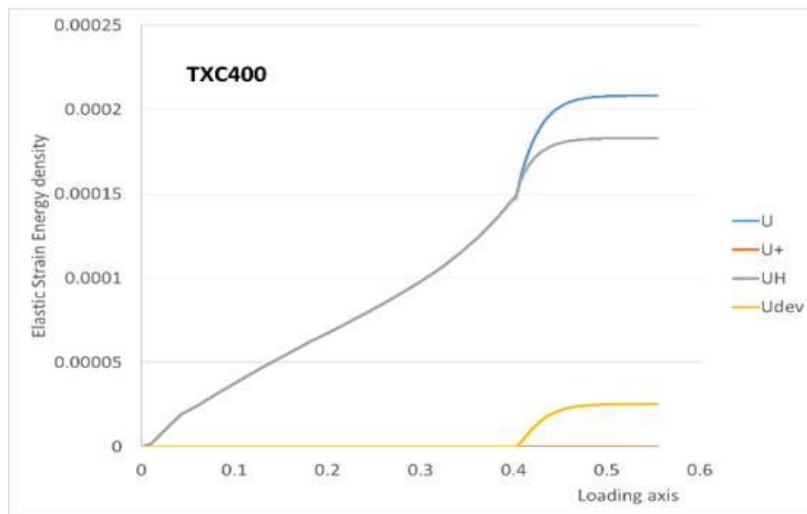
Density of elastic energy measures

$$U = \frac{1}{2} \boldsymbol{\varepsilon}^e : \mathbf{C}^e : \boldsymbol{\varepsilon}^e$$

$$U^V = \frac{1}{2} \varepsilon_V^e \mathbf{I} : \mathbf{C}^e : \varepsilon_V^e \mathbf{I}$$

$$U^D = \frac{1}{2} \boldsymbol{\varepsilon}^{e'} : \mathbf{C}^e : \boldsymbol{\varepsilon}^{e'}$$

$$U^+ = \frac{1}{2} \langle \boldsymbol{\varepsilon}^e \rangle_+ : \mathbf{C}^e : \langle \boldsymbol{\varepsilon}^e \rangle_+$$



→ damage modelling

D_H – Hydrostatic damage variable

Evolution of D_H is based on the following damage potential,

$$\Psi_H = \varepsilon_V - \varepsilon_V^c,$$

with

$$\Psi_H < 0 \Rightarrow \dot{D}_H = 0$$

$$\Psi_H = 0 \Rightarrow \dot{D}_H > 0$$

$\Psi_H = 0$ is the limit of the non-growing damage domain, ε_V^c is the present current value for ε_V , i.e.

$$\varepsilon_V^c = \max(\varepsilon_V, \varepsilon_V^{c0}).$$

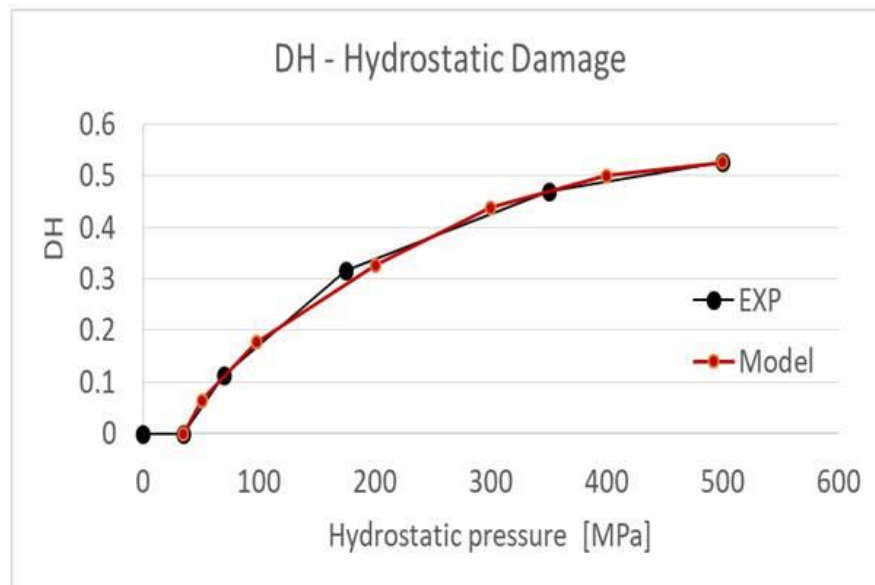
The proposed evolution law of damage variable D_H is

$$D_H = f(\varepsilon_V), \quad \text{such that} \quad D_H = C_1 \cdot \left(\frac{|\varepsilon_V| - \varepsilon_V^c}{2 \cdot f_0} \right)^{C_2}.$$

→ damage modelling

D_H – Hydrostatic damage variable

Example of the evolution law of D_H :



→ damage modelling

D_t – Tensile damage variable

The tensile damage variable is associated with tensile elastic strains.

Defined as

$$\Psi_t = U^+ - U_c^+,$$

where U^+ represents the density of elastic energy associated to the positive components of the total elastic strain tensor, and U_c^+ is a critical threshold value

$$U_c^+ = \max(U^+, U_{c0}^+).$$

Tensile damage evolution law is

$$\begin{aligned}\Psi_t < 0 &\Rightarrow \dot{D}_t = 0 \\ \Psi_t = 0 &\Rightarrow \dot{D}_t > 0,\end{aligned}$$

with the total tensile damage given by the expression, after integration,

$$D_t(U^+) = 1 - \frac{U_{c0}^+(1-A_1)}{U^+} - \frac{A_1}{\exp[B_1(U^+ - U_{c0}^+)]}$$

→ damage modelling

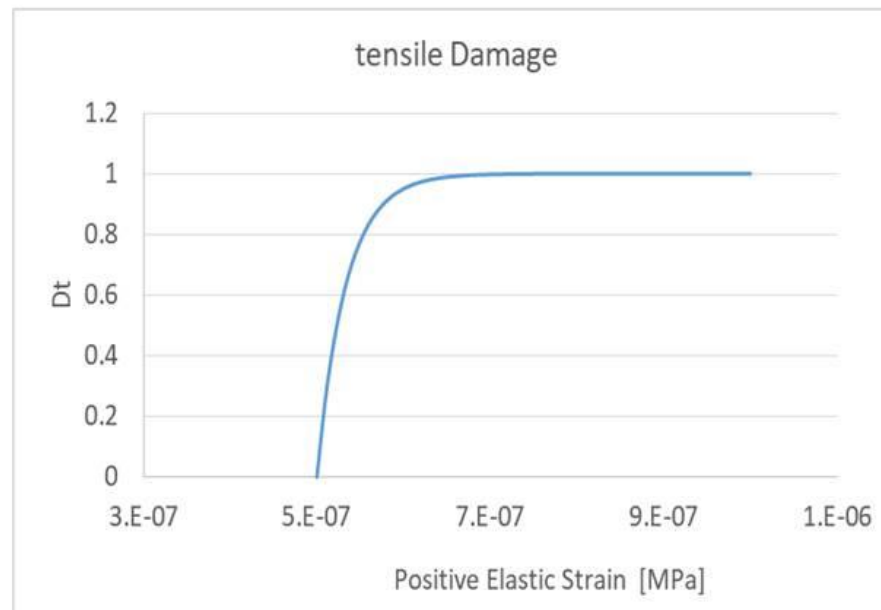
D_t – Tensile damage variable

As an example, the following parameters are chosen,

$$U_{c0}^+ = 5 \times 10^{-7} \text{ MPa},$$

$$A_1 = 3 \times 10^7,$$

$$B_1 = 1.$$



→ damage modelling

D – Total damage

$$D = 1 - \left(1 - \left\langle \frac{U^D - U^V}{U^T} \right\rangle_+ D_H\right) (1 - D_t)$$

Experimental observations show that under a purely compaction loading the material stiffens, with an observable increase of the bulk modulus.

So, if the loading path is predominately of the compaction type, the hydrostatic damage shall not be activated.

A loading path is considered **predominately of the compaction type** if the volumetric part of the elastic energy is larger than the deviatoric one, i.e. if $U^V > U^D$.

The hydrostatic damage is progressively considered as a function of the following ratio:

$$D_H = D_H \left\langle \frac{U^D - U^V}{U^T} \right\rangle_+$$

Some preliminary examples are given:

→ *damage modelling*

Weakening of the mechanical properties due to damage

After damage accumulation, the (*elastic*) mechanical properties of the material must be decreased.

The expression

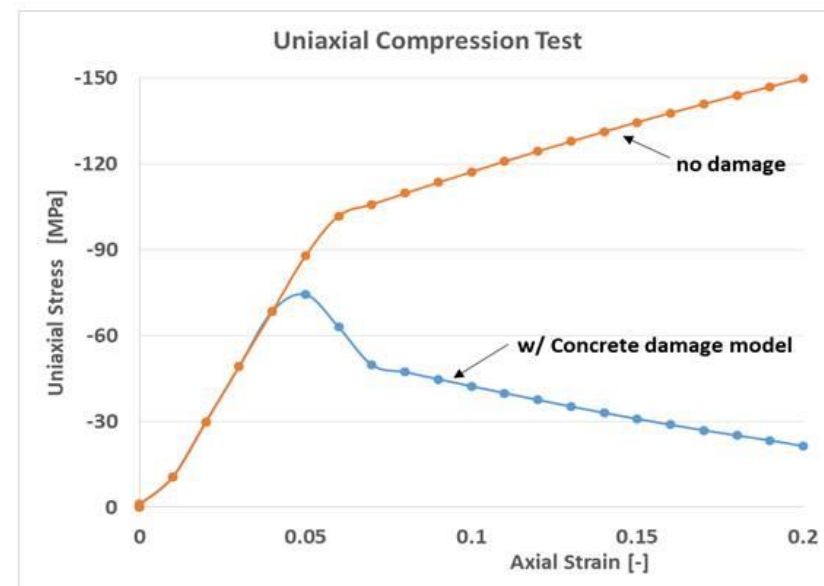
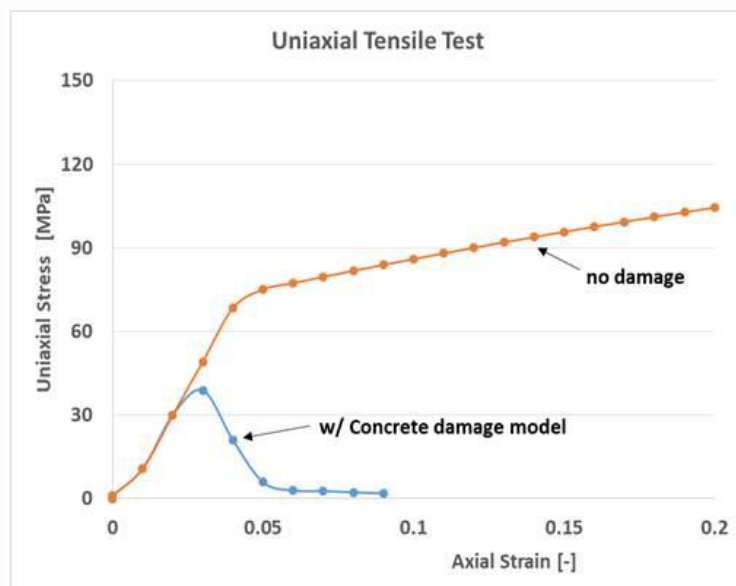
$$\sigma_{ij}^* = \left(1 - \left\langle \frac{\sigma_m}{|\sigma_m|} \right\rangle D_H\right) \sigma_m I_{ij} + (1 - D) \sigma'_{ij}$$

is adopted, i.e., the contribution of D_H , hydrostatic damage, only takes place if we have hydrostatic tension, otherwise the material retains the ability of supporting compaction resistance, i.e. the unilateral effects (opening and closure of the micro cracks) of the damage.

→ *damage modelling*

Behavior of the model under Uniaxial Compression and Uniaxial Tension

In the following figures it is shown the behavior of the model when simulating the classical uniaxial tension and compression tests, with the evolution of damage variables activated.

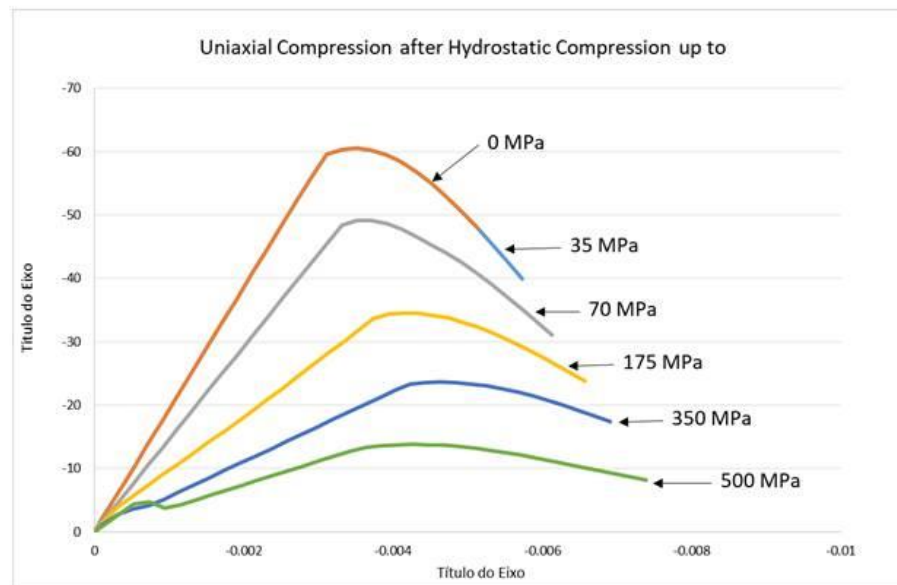


→ *damage modelling*

Sequential loading:

1. HC – hydrostatic compression up to a predefined value of hydrostatic pressure
2. Unloading of the hydrostatic pressure up to zero stress
3. UC – reloading under uniaxial compression conditions.

Results:

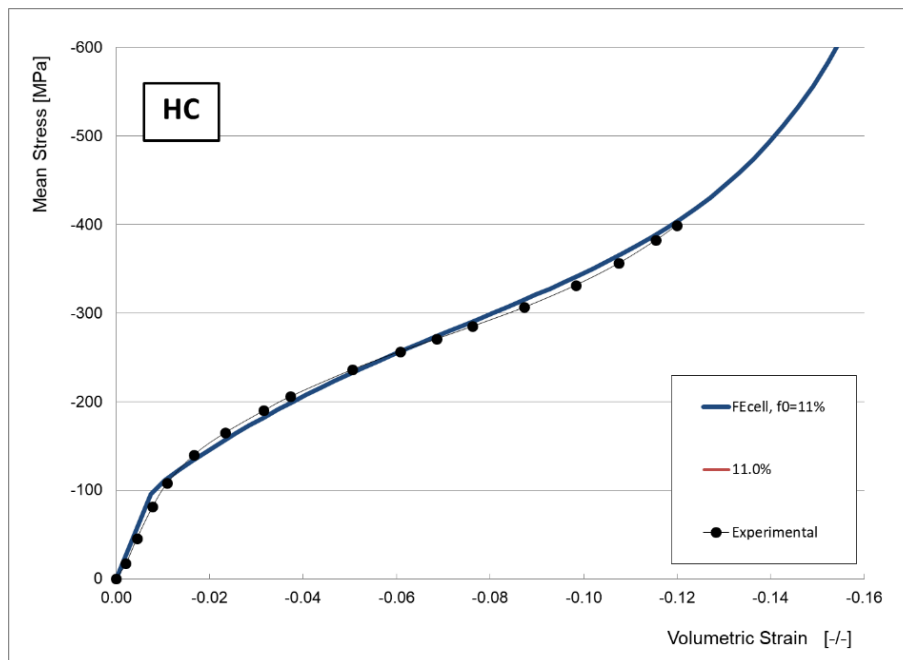


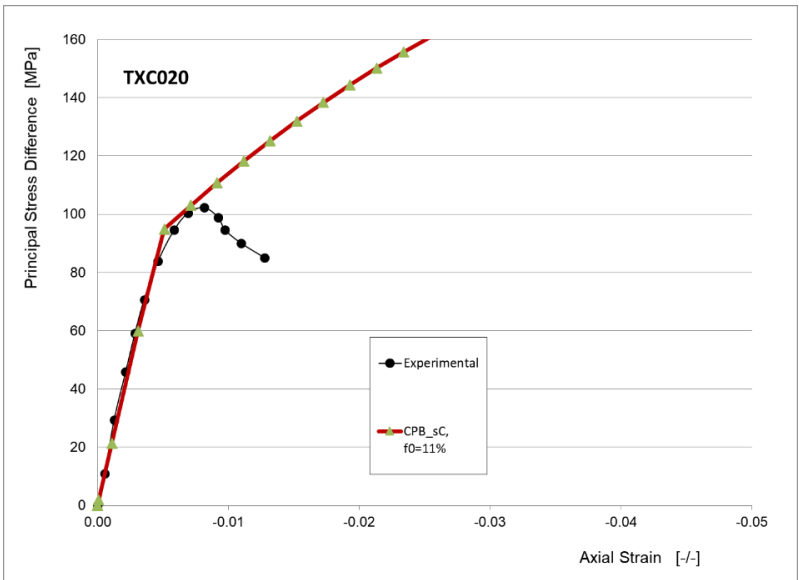
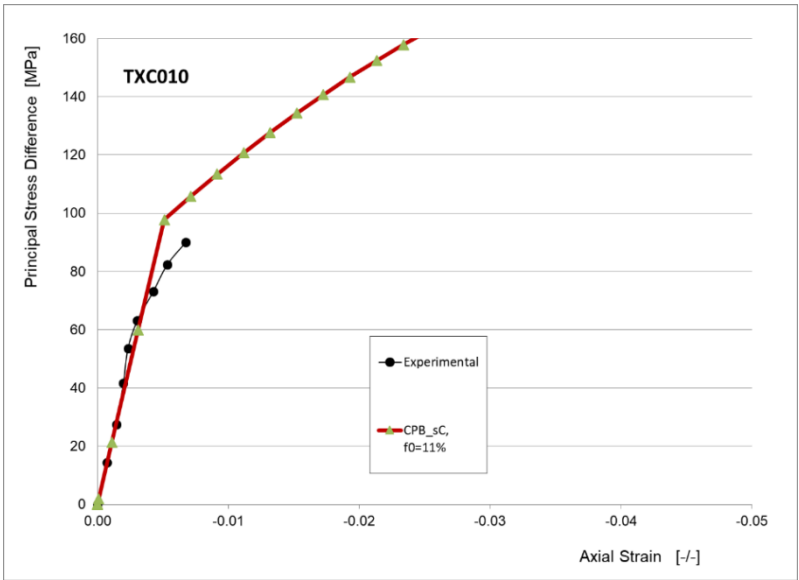
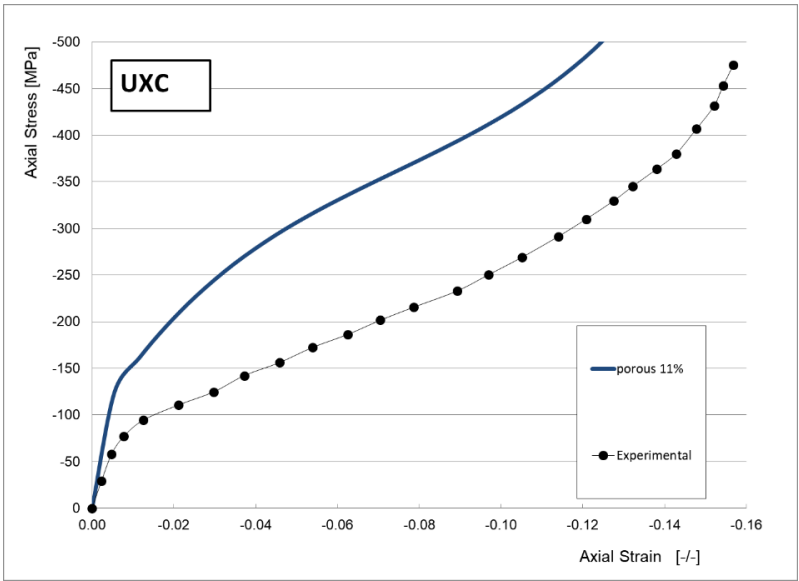
Final comparison between numerical and experimental results for all loading cases (HC, UXC, TXC)

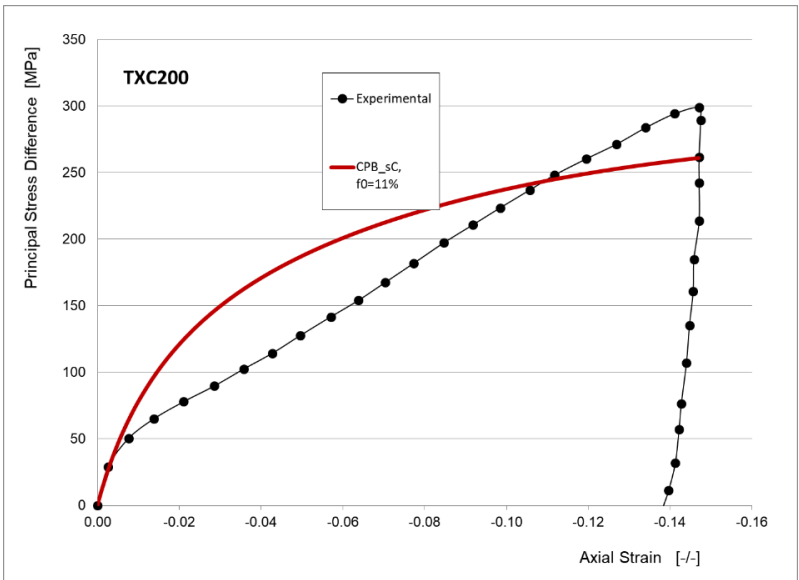
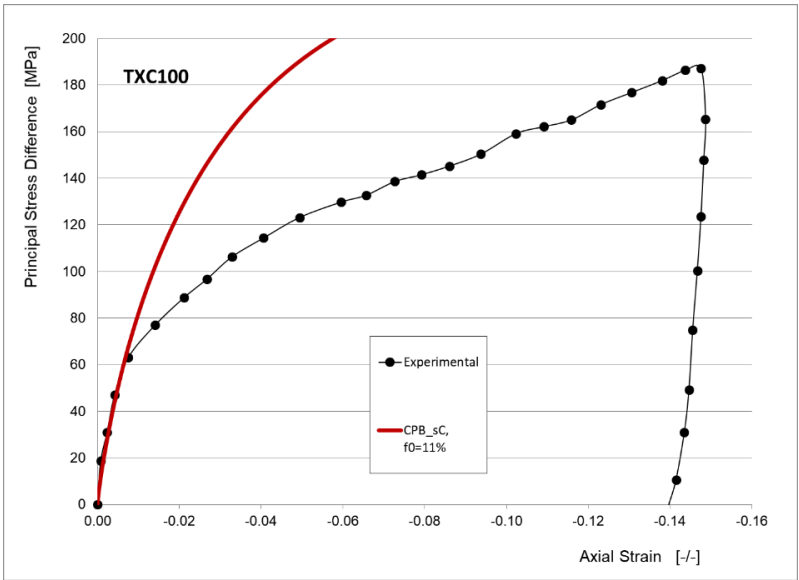
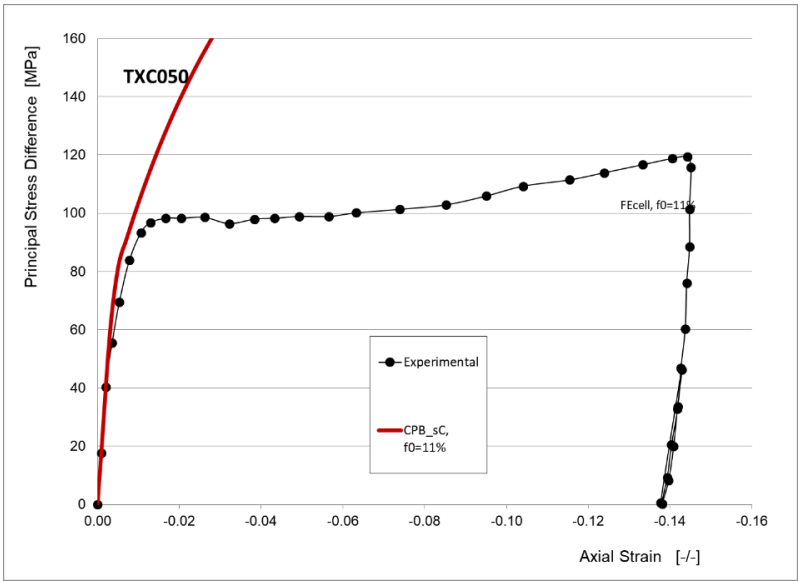
The final results concerning the comparison between experimental and numerical results using the newly proposed and coupled plasticity-damage model are shown hereafter:

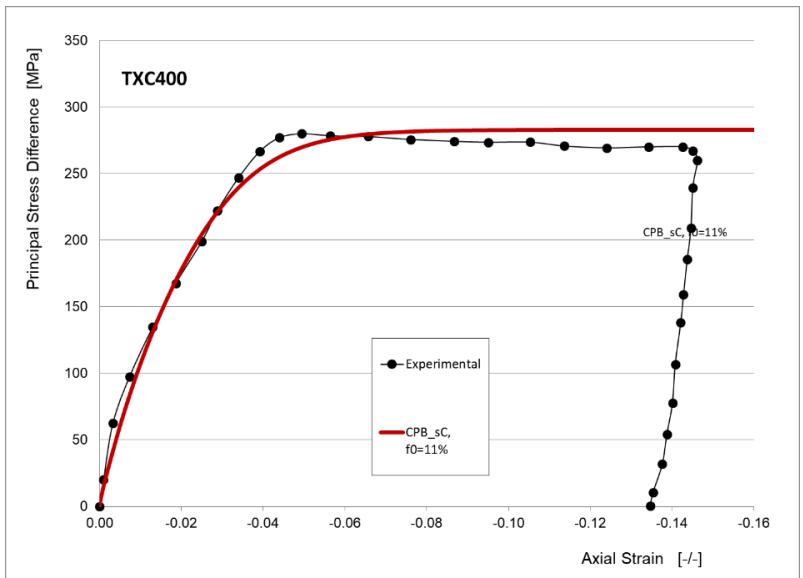
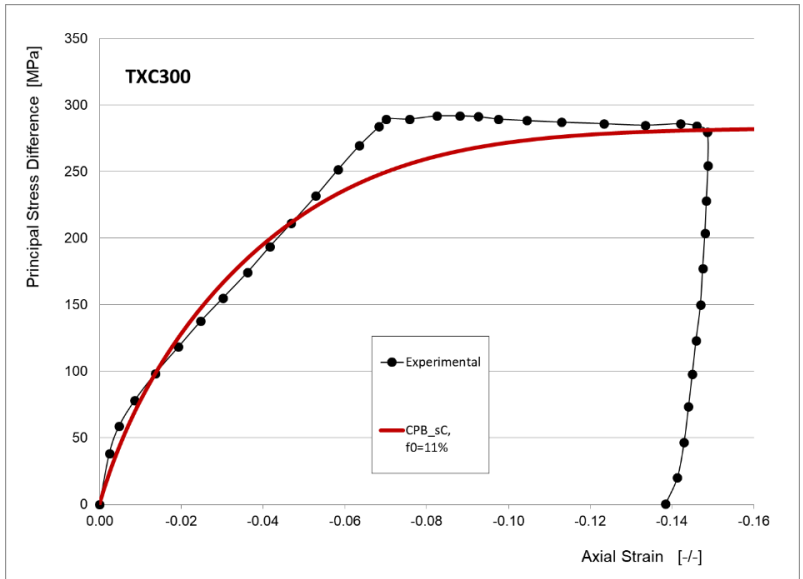
Constitutive and damage parameters:

Y0=85	
CY=28	
Ysat=200	
K=-1	
Alpha=0.0	
q1= q1=1.15	









In conclusion,
 for almost all loadings cases one can see a good agreement between
 experimental and numerical results. A fracture criterion (or final failure criterion)
 seems to be needed to determine the end of the tests.